Politecnico di Torino

Politecnico di Torino

Master of Science in Civil Engineering
A.Y. 2021/2022
Graduation Session March/April 2023

Assessment of 2D hydro-morphological processes to support river restoration at Isola Serafini in the Po River (Italy).

Topic as part of the twinning activity between the Po River's Renaturation Project (Italy) and the Room for the River approach along the Rhine Branches (the Netherlands) within the EU H2020 Green Deal Innovation Project MERLIN.

Supervisors:
Prof. Carlo Camporeale
Dr. Ir. Erik Mosselman
Ph.D. Melissa Latella

Candidate:
Francesco Bossini

Acknowledgments

The present thesis was undertaken in the framework of the MERLIN project (https://projectmerlin.eu), which has received funding from the European Union's Horizon 2020 research and innovation programme under grant agreement No. 101036337. And therefore, I would like to express my deepest gratitude to the *MERLIN Consortium* and to *Politecnico di Torino* for their assistance in financing this study and my stay in the Netherlands. Furthermore, this initiative would not have been possible without facilities and technical tools provided by *Deltares* and the data sharing from *ADBPO* and *AIPO.*

I am deeply indebted to Erik Mosselman and Ellis Penning for their extreme kindness and ability to motivate me and to make me aware of the multidisciplinary character of the subject. Thanks to their continuing encouragement, wise direction, and professionalism, I could complete this project and engage in additional activities that gave me with meaningful personal experiences. I must also thank Carlo Camporeale and Melissa Latella for agreeing to supervise the project and for their assistance throughout the process. I would like to extend my sincere thanks to Victor Chavarrias and Willem Ottevanger for their willingness to support the research and for their invaluable modelling guidance.

Many thanks to *Deltares* and *Rijkswaterstaat* for organising the field trip to the Rhine Branches and to all the participants; it was a great opportunity to interact and engage in dialogue with major river managers and experts in an inspiring European environment. Special thanks to Marta Martinengo and Paolo Piovani for sharing materials and perspectives, as well as to *WWF Italy* for participating in meetings that were beneficial to the progress of the project. I am also grateful to Elena Marsiglia and Laura Marsiglia for guiding me down the Po River and sharing a wealth of knowledge about Isola Serafini and its wonderful surroundings. I would also want to thank everyone who helped study the Po River at Isola Serafini prior to this research, and for providing vital information for the present investigation.

Lastly, I would like to recognize members of *Deltares*' departments of *Freshwater Ecology and Water Quality* and *River Dynamics and Inland Shipping* that gave me advice and suggestions throughout my time in the Netherlands.

Francesco Bossini

Torino, April 2023

Abstract

River restoration is anticipated to become a common basis for future river management in Europe. Dialogue and knowledge sharing coming from river restoration initiatives performed or still in progress may be essential for future implementations success. To that end, the EU H2020 Green Deal Innovation Project MERLIN envisages twinning activities as a means of exchanging best-practices expertise. The emerging "*Rinaturazione dell'Area Po*" project along the Po River in Italy has been designated as a twin case of one of the case studies that inspire the MERLIN Project, namely the Room-for-the-River programme implemented along the Rhine Branches in the Netherlands. As part of this twinning activity, *Politecnico di Torino* and *Deltares* collaborated to undertake the present study. River restoration should primarily strive to rehabilitate river functionalities that guarantee the provision of ecosystem services. These directly depend on river ecological integrity, strongly related to habitats diversity. Habitat distribution is created and maintained especially by hydro-morphological processes, that establish flow velocity and shear stress distributions and define bed topography patterns. The primary goal of the present study was to assess 2D hydro-morphological processes relevant for river restoration, with special reference to the Isola Serafini meander in the Po River in Italy.

It was first questioned what the Po River restoration could benefit from the Room-for-the-River programme's expertise. This was accomplished through critical literature review also based on field visits to both fluvial systems. Secondly, a 2D hydro-morphological model of the Isola Serafini meander was developed aiming at assessing hydro-morphological effects responsible for the formation of channel bedforms. This was performed by simulating the morphological development of the meander starting from a transversely flat topography and by parameterizing crucial hydro-morphological processes, namely the spiral motion and the gravity pull along transverse bed slopes on sediment transport. Finally, given that flows through the meander correspond to the barrage releases of the hydropower plant at the upstream end of the meander, the morphological influence of asymmetrical inflows imposed as inflow open boundary conditions for the model was tested.

It was found that the Po River restoration programme acknowledges the importance of giving "more space to the river". However, it still requires definition and quantification of ecosystem services that should be provided by this additional space and thus of expected hydro-morphological processes. The 2D modelling permitted to gain knowledge into the characteristic spatial distribution of bed topographies and to get useful insights for river restoration. It was also found that alternative operation rules could be implemented to influence the morphological development of the channel up to 6 km from the barrage by generating flatter or more heterogenous bed topographies, depending on the inflow distribution at the barrage.

Definition and quantification of expected ecosystem services rehabilitations for the Po River may be improved. The case study of the present Thesis, namely the 2D Isola Serafini model, highlights that hydro-morphological modelling might support decision making, yet it stresses the need for more data to increase the accuracy and reliability of the modelling results.

Contents

List of Figures

List of Tables

Chapter 1

Introduction

1.1 Context

Restoration measures on artificial and natural rivers have been implemented throughout Europe over the past decades as part of the EU Water Framework Directive's goal of ensuring good ecological status of water bodies (Schirmer et al., 2014). According to the 1st River Basin Managements Plans (2015) anthropogenic pressures such as navigation, hydropower and flood protection are responsible together for the hydro-morphological alteration of 40% of the European rivers (REFORM, 2015). In response to the European requirements for good ecological status two main tools were developed: the Water Framework Directive (WFD) 2000/60/EC and the Floods Directive (FD) 2007/60/EC. Their simultaneous implementation, in conjunction with the Natura 2000 European network (listed under the Birds Directive 2009/147/EC and the Habitats Directive 92/43/EEC), provides the essential basis for the development of innovative approaches to river management, named Integrated River Basin Management (IRBM). The programme Room-for-the-River, that has been carried out in the last two decades in the Netherlands, represents a good example of application of such approach. Interventions for developing nature and improving ecosystems, that have been boosted by the necessity to guarantee hydraulic safety, have resulted in a win-win strategy for the Rhine Branches. The programme has been recognized as a best-practice case study of restoration interventions and it is now one of the 17 case studies that inspire the EU H2020 Green Deal Innovation Project MERLIN, aiming at support in the optimization of river restoration measures around Europe. One of the strategies adopted within the MERLIN project is to define twin cases that can help in exchanging experiences and ideas. The Room for the River programme has been designated to be a twin case of the ongoing "*Rinaturazione dell'Area Po*" project along the Po River (hereafter Po Renaturation Plan) being the Rhine and the Po the two largest Rivers of the Netherlands and Italy, respectively. The present study was conducted as a part of these twinning activities.

Currently, basin-scale measures may be implemented along the Po River course, largely because of the European financing programme Next Generation EU (NGEU) and its uptake in the National Recovery and Resilience Plan (PNRR). PNRR aims at speeding up the ecological transition process, which is where the Renaturation Plan for the Po River is inserted (in line with Agenda 2030 and the European Green Deal), ultimate goal of which is to reduce the artificiality of the Po River by large-scale implementation of river restoration actions (ADBPO, 2022).

The Po River experienced considerable modifications during the 20th century, mainly due to human pressure exerted through various imposed constraints. As the river course shortened, the channel narrowed and gradually deepened. This was followed by a gradual transition from a multi-channel to a single-channel configuration followed by the reduction of longitudinal and lateral connectivity. As a result, several fluvial environments, such as relict landforms and side channels, are nowadays disconnected from the fluvial dynamics that previously were determining active hydro-morphological processes, key aspect for conservation of the fluvial ecosystem and its biodiversity. Several alteration factors can be identified: mining activity, river training, bank stabilization, water regulation by dams and barrages, intensive agriculture, and intensified land use. Among all these, sand mining has been recognized as the predominant one in past years, bringing several negative impacts to the fluvial environment and its ecosystem services (ADBPO, 2008a; Schippa et al., 2006). One of the greatest modifications induced by mining activity is the resulting unbalanced sediment transport, that in conjunction with the construction of hydropower dams, reforestation activities and hydraulic-forestry set up (causes of the long-term sediment supply shortage), led to the incision of the channel bottom (ADBPO, 2008a). River training resulted in additional alterations in the topography of the river course determining the transition from multi-channel to single-channel morphology and boosting the degradation process (Filippi et al., 2013). River training and intensified land use have deprived the river system of natural flooding areas, resulting in fragmentation of habitats and loss of biodiversity while exacerbating consequences of catastrophic natural events (Agapito et al., 2020). Bank stabilization works and dikes, with the main embankments usually too close to natural banks, are fixing the planimetric configurations of the channel and leading to singular arrangement of the course (ADBPO, 2008a). Flow modifications by barrages and water derivations has altered formative discharges while reducing flow dynamics (peak and base flows), harming the ecological functioning of the river.

Between the Trebbia River and the Arda River mouths, the Po River shows the effects induced by all the factors mentioned above (Figure 1). Aside from the deepening process, the hydro-morphological status of the river in this section is impaired by other two main factors of alteration: river training and the construction of the Isola Serafini hydroelectric plant. The operation rules of the hydropower plant have been modifying the hydrological regime of the meander loop as well as the sediment transport capacity on the upstream stretch (Maselli et al., 2018) and led to the hydro-morphological alteration of the downstream stretch (Filippi et al., 2013; Provincia di Mantova, 2005).

Along the meander loop, the bar volume and height are disproportionate compared to the channel width and the low-flow channel is deep and no longer connected with floodplains for ordinary flow so that lateral continuity between the main channel and bars is strongly reduced (Filippi et al., 2013). The set-up of bank defences and bars fix the low-flow channel in space with its thalweg too close to the strengthened banks that protect the main embankments from direct hydrodynamic pressures (Provincia di Piacenza, 2011). The meander is therefore an altered segment of the Po River, in which natural morphological processes are widely halted with consequences that directly impact the natural environment and its biodiversity. Nature conservation should be ensured especially because this area was designated as Site of Community Importance (SCIs) and as Special Areas of Conservation (SACs) in the context of the Natura 2000 network sites. Moreover, the Po River officially entered the World Network of Biosphere Reserves (WNBR) in 2019 with

the name "*Riserva della Biosfera Po Grande (RB Po Grande)"* as part of the UNESCO MAB Program (Man and Biosphere). This international research programme seeks to establish a scientifically based method for the development of sustainable use of natural environment and its resources throughout biodiversity conservation and protection.

In this context, significant efforts have been made in recent years to investigate the potentials for restoring the ecological state of the Po River system and reducing human stresses on it, and Isola Serafini is one of the sites where restoration measures have been proposed. In order to approach restoration effectively and implement appropriate and efficient measures, a comprehensive understanding of the system is crucial.

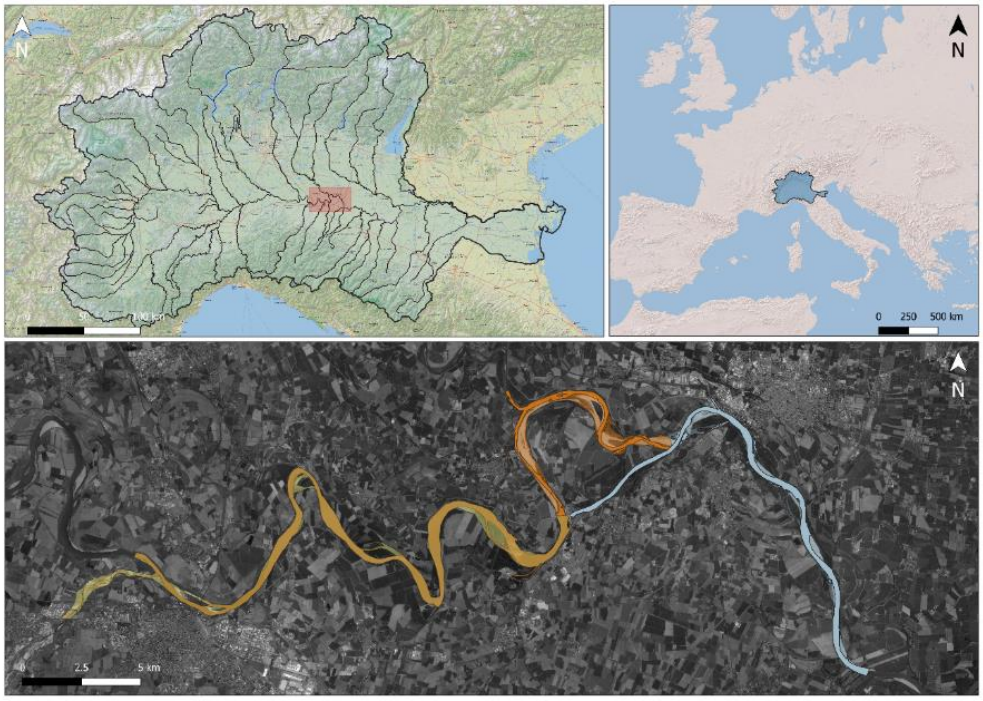

Figure 1. Territorial framework. Top right: Po catchment area in the European continent; Top left: Po Basin extent in Northern Italy and location of the Isola Serafini's area in red box; Bottom: Three segments of the Po River affected by the operation rules of the Isola Serafini hydropower plant as estimated by ADBPO (sources: GIS features provided by ADBPO; Topographical bases by ESRI and Google).

1.2 Problem statement

River restoration should strive to safeguard biodiversity by rehabilitating the many natural functionalities of a river system while preserving ecosystem services such as navigability, energy production, and water supply (Schirmer et al., 2014). These services are often ensured by adjusting river complexity and controlling dynamics through reduced flow variability in time and space, as well as suppression of hydro-morphological processes that would compromise their provision. As a result, such altered river systems are dominated by essentially one-dimensional processes that occur in the longitudinal direction. Since biodiversity is commonly linked with the degree of environmental heterogeneity (Noss, 1990), and thus with ecological and hydro-morphological

processes that result in high-quality habitats (Bandrowsky et al., 2015), the natural multi-dimensional character of river systems cannot be overlooked. The lateral direction is especially crucial SINCE 2D flow velocity distribution and resulting bed shear stresses establish the sediment transport regime (Vesipa et al., 2017), which shapes the spatial distribution of bed topography and defines the habitat patterns within the riverine area. Therefore, complex hydraulic and morphological systems with wet and dry regions (low-flow channel and side or point bars), shallower and deeper areas (pools and bars pattern) with variable flow conditions are produced, providing habitats for multiple species. The degree of environmental heterogeneity and diversity determined by the level of connectivity within the river environment itself is defined by this shifting mosaic of fluvial habitats (Tockner et al., 2000).

The overview of the previous studies carried out at Isola Serafini showed a deep knowledge of the overall morphodynamic behaviour of this stretch of the Po River. At the same time habitats have been mapped in the context of Natura 2000 and may be sufficient base of knowledge from an ecological and biological point of view. On the contrary, too little seems to be known about the influence that hydro-morphological processes have in habitat development and ecosystem conservation. Especially, there is a lack of insights in how 2D hydro-morphological effects need to be considered when approaching river restoration as modelling approaches adopted to date are exclusively 1D.

Many restoration measures, such as sediment mobilisation, reopening and reactivation of secondary channels, and structural adjustment to training works, are outlined in the Po Renaturation Plan. Since these actions alter the sediment transport regime, they will have an impact on river morphology and hence habitat distribution. Understanding both present and potential hydro-morphological processes is essential for guaranteeing not only the effectiveness of interventions but also the fulfilment of ecosystem integrity objectives.

1.3 Research objective

This research aims at assessing 2D hydro-morphological effects that are relevant for river restoration, with special reference to the Isola Serafini meander in the Po River in Italy by creating a new two-dimensional morphodynamic model using Delft3D-4. Moreover, comparison with the Room-for-the-River programme in the Netherlands and the modelling approach developed for the Rhine Branches will guide the discussion and the modelling phase. The main research questions can be listed as follows:

1) Which 2D modelling approach can be developed with existing knowledge to support river restoration of the Isola Serafini meander?
2) How and to what extent can alternative operation rules of the barrage influence the morphological development of the meander?
3) What can the Po River restoration benefit from the Room-for-the-River programme's expertise?

1.4 Approach

As part of the MERLIN project's twinning activities, an attempt was made to give useful insights for the Po River restoration employing the Room-for-the-River case study as the primary source of inspiration.

Starting with a literature review, the analogies and differences in river alterations and constraints between the Po River and the Rhine Branches were examined. Afterwards, the applicability of Room-for-the-River's restoration approach to the Po River was critically analysed also referring to concepts of naturalness and spatial quality based on field visits to both fluvial systems.

Moreover, 2D hydro-morphological models were used along the Rhine Branches to support in river management interventions and restoration projects based on a specific modelling strategy. Nonetheless, data scarcity and the demand to investigate the morphological functioning of the Isola Serafini's meander guided the research through the development of a specific modelling strategy. By performing simulations of constant discharge (formative discharge) flowing over a constructed initially transversely flat topography, the 2D hydro-morphological effects responsible for bar formation were addressed. The degree of non-linearity of sediment transport, as well as different values for variables that parameterized 3D effects on the 2D hydro-morphological model (spiral flow and transverse bed slope effects on sediment transport), were tested aiming to reproduce the known topography of the channel.

Finally, the potentials for river restoration measures involving the barrage operation scheme have been analysed. Based on the results of the previous phase of the study, the impact of asymmetrical inflows from the barrage was assessed through running simulations starting from the previously generated transversely flat topography. The adaptation length of perturbations in the transverse profile of depth-averaged streamwise flow velocity was employed to assess short-term effect taking as reference condition the modelling result obtained with the simulation that best fit the known topography during the preceding step of analysis. Medium-term effects were qualitatively evaluated again by comparing topographical modelling results.

Chapter 2

Literature review and theoretical background

2.1 River restoration

2.1.1 What is river restoration?

The numerous definitions developed throughout the years demonstrate how difficult it is to precisely define what river restoration is and what its ultimate goals are. There are several new idioms related to freshwater ecosystems (Freshwater glossary - Freshwater Information Platform) and river restoration approaches (CIRF, 2006).

According to the European Centre for River Restoration, River Restoration is an umbrella term used to identify different ecological, physical, spatial and management measures and practices aiming at restoring functionalities of river systems while moving toward more natural states. Restoration of a river demands not only the rehabilitation of its ecological status or the mitigation of unfavourable impacts. It indeed involves the assessment of induced modifications to other river functionalities, especially those linked to human-related services such as navigability, water supply for industrial and agricultural sectors, economic and cultural resources (e.g., hydropower and recreational activities). Lastly, the necessity to guarantee hydraulic safety of the areas adjacent to the river system.

Other functionalities of rivers are related to the so-called ecosystem services that rivers provide. Natural riparian systems especially play a variety of roles, ranging from flood and drought mitigation to the formation of biological corridors crucial to biota survival (Camporeale et al., 2013). These are categorized as provisioning (supply of matter), regulating, and maintaining (development of a healthy and safe environment) or cultural (spiritual or recreational function) as reported by the European Environmental Agency (2019). Ecosystem services provided by natural systems are related to benefits that human can get form the environment beyond than the ones strictly connected to nature itself (Penning, 2022, personal communication). Therefore river restoration success should be assessed even with respect of beneficials gained by humans (Schirmer et al., 2014) in addition to the degree of improvement achieved in the degraded hydro-morphological and ecological processes that support the natural ecosystem (Wohl et al., 2005). However, when addressing river restoration, ecosystem services rehabilitation should be the driving factor, suggesting protection or enhancement of environmental biodiversity.

2.1.2 Fluvial system dynamics and heterogeneity

According to Noss (1990) biodiversity translates into heterogeneity of structure, function and composition and it is therefore related to ecological concepts such as succession, ecotones and connectivity (Ward et al., 1999). Nevertheless, due to the fragile nature of biodiversity, even a slight alteration to the river system can cause a disruption in the associated fluvial environment, resulting in notable changes to the abiotic compartment and its biotic populations (Wohl et al., 2005). It follows that when greater modifications are introduced, implications for the loss of ecosystem heterogeneity and integrity are substantial.

River regulation may be among the most impacting human measures, altering the natural dynamics of rivers as in the case of the construction of dams and barrages for energy production. Dams' construction induces modifications on sediment supply and flow regime, influencing transport capacity. Sediment supply and transport capacity are, together with vegetation coverage, the three main factors that determine the channel morphology of rivers (Montgomery & Buffington, 1998). Consequently, modifications such as channel incision and width reduction are expected to occur, impacting the hydro-morphological quality of rivers. Bandrowski et al. (2015) explain how morphological heterogeneity, maintained by processes linked to sediment transport, translates in high-quality habitats. Especially scour and fill process, bank erosion or lateral channel migration contribute to create a complex arrangement of different channel units (pools, bars, shallow areas) that provide niches for fluvial fauna. This process of morphological reworking and self-adjustment is fundamental even for the substrate replacement and the riparian vegetation rejuvenation and it results strongly reduced in regulated rivers (Fryirs & Brierley, 2009; Vesipa et al., 2017).

Riparian zone has been defined as the area immediately adjacent to the river that influences and is influenced by the river in terms of environmental matrix and condition through quality elements related to hydro-morphology, biology, and physio-chemical composition (EC, 2003a). Internal to the riparian zone, dynamic mechanisms are maintained by the simultaneous hydro-morphological and ecological processes that create diversity in time and space (Camporeale et al., 2013). Natural fluvial ecosystems are made up of several ecotones of various orders, each of which is distinguished by relatively steep gradients, that compete and interact together to shape patterns of species richness. This shifting-mosaic of fluvial habitats generated by floods variability establishes the degree of environmental heterogeneity and diversity according to the level of connectivity within the river environment itself (Tockner et al., 2000).

As reported by Camporeale et al. (2013) ecological dynamics has been characterized trough five different hydrological parameters, whose three main ones are flood magnitude, return interval and flood duration. While annual flow variations affect the annual plants behaviour, forest communities are susceptible only to annual flood and drought events with complete resets to earlier successional stages that can occur consequently to extreme floods. This demonstrates how river communities result from a mixing of short, medium and long term effects as a function of the flood pulse (Junk et al., 1989). Tockner et al. (2000) distinguish between overbank inundation (associated to the flood pulse concept) and flow pulses that occur in floodplains although when streams do not reach bankfull conditions. The first type, even called erosive flooding, acts at the annual or higher time scale and it is responsible for the periodic disruption of habitat patches. Its occurrence can lead to the increase of the overall connectivity and the decrease of system's

heterogeneity demonstrating that the highest biodiversity is not always linked to the higher degree of connectivity (Tockner et al., 2000). Flow pulses, then, occurs at shorter timescale and determine the fluctuation of water stages that which in turn concurs in defining the hydrological connectivity of the present fluvial environment that structures its biodiversity and successional patterns.

Connectivity can be defined as the ease with which fluxes of water-related matters (organisms, nutrients, sediments and energy) occur within the fluvial systems (Ward et al., 1999) and thus not only as water exchanges (hydrological connectivity). Several definitions of connectivity are reported by Wohl (2017). The European Commission (2021) identifies four dimensions of connectivity that define a free-flowing river, namely longitudinal, lateral, vertical and temporal one. This means that apart from streamwise and lateral flows, hyporheic flows within the channel as well as groundwater flows that can occurs at the wet-dry boundaries are encompassed in the definition. Lateral river dynamics, exerted trough migration of the main channel via bank erosion-deposition process, defines lateral sediment connectivity, key aspect for the erodible corridor concept (EC, 2021). Also, time-dependence connectivity characteristics of flows are crucial such as its intensity (rare, intermitted or permanent submerged conditions), strictly linked to the geomorphological characteristics of channels (Bornette et al., 1998).

Wohl (2017) stresses about the circumstance for which too often recent river managements set the prior goal to be the increase of connectivity, reputing it a favourable solution for the ecosystem, no matter the specific river's nature. The true objective should be to assess which is the natural or the desired level of connectivity of the river (based on the current state and considering past conditions) that can enhance heterogeneity and biodiversity. Indeed, as reported by Fryirs & Brierley (2009) the belief that dysconnectivity is always bad is fallacious, as can be perceived observing the degree of connectivity of unimpaired rivers. Certain level of isolation and disconnection could enhance species richness or even improving the filtering capacity of the river, determining a gain on its resilience and ability to isolate degrading processes (Fryirs & Brierley, 2009). For that reason, Wohl (2017) introduced the concept of gradational connectivity (from fully connected to fully disconnected) to describe the degree of connectivity of river in time and space. Restoration of lateral continuity can be obtained implementing measures such as barrier removal (bank defences), enhancement of sediment dynamics (nourishment or mobilization of sediments) or by restoring natural flow (e.g., increasing the variability of flows by modifying the operation rule of dams).

2.1.3 The approach to river restoration

Afterwards, restoring a river entails the assessment of its fluvial system status to be recover because it has been degraded due to natural or anthropic driving forces. That implies the existence of a past, unaltered condition and a current modified one that no longer meets the natural or human-related functionalities it was used to absolve. It is important to understand that the former condition cannot be selected to be the final target to reach through river restoration.

Given the dynamic nature of rivers systems and their resilience characteristic - meant as their ability to adapt to external disturbance and to withstand climate and human pressures (Fryirs &

Brierley, 2009) - it is misleading to talk about well-defined and static natural configurations. It would be appropriate instead to thinking about the current functionality the river is providing and its evolutionary trajectory (in past and in future) driven by the current constrains. The target should be the one of understanding if these constrains represent or will represent a possible obstacle for its dynamic equilibrium and for human-related interests. Wohl et al. (2005) expressed the ecological integrity concept that refers to the condition for which natural rates of hydrological, geomorphic and ecological processes are intact and depend on a certain level of disturbance. Long-term evolution of the river, however, is the prerequisite for assessing which are the modifications occurred in the past, the causes of these changes and the eventually still in process ones and therefore defying the rehabilitation measures to be implemented (Fryirs & Brierley, 2009).

It was thought very useful to report here the definition of naturalness given by Fryirs & Brierley (2009). It is based on a geomorphic perspective view for which a natural river is the *"one that is appropriate for the given landscape or environmental setting, with a character and behaviour that is expected given the boundary conditions under which the river operates. In this way, naturalness is not embedded in the past. Rather, it is a functional state that adjusts its character and behaviour in response to flow, sediment, and vegetation fluxes. Unless perceptions of naturalness allow for evolution and change (in its broadest sense), it could be argued that rehabilitation activities are managing for historical relicts rather than river futures".*

Aside of the temporal analysis of the river system, the spatial scale of investigation represents the other key aspect of river restoration. Indeed, ecosystem processes that characterized fluvial environment are strictly interconnected not only in time but also in space, such that it would be incorrect more than limiting to study a specific reach of the river only. Wohl et al. (2005) suggest that the spatial entity of analysis should be that at the watershed scale and that is confirmed by the IRBM concept. The Multi-scale Hierarchical Framework, developed by REFORM for the hydro-morphological assessment works exactly in that direction.

In conclusion, given that the timescale for which morphological and vegetational response to interventions is long (decades or centuries), it emerges how river restoration objectives are fundamentally long-term targets. Thus short-term objectives should be based on re-establishing functional integrity of rivers (Ward et al., 1999), with the adaptive management approach (systematic campaign of observations, interrogation, interpretation and monitoring) being the key to success (Fryirs & Brierley, 2009).

2.1.4 Implementation of river restoration in Europe

The MERLIN project

In response to the loss of habitats and biodiversity that freshwater ecosystems are experiencing around the European continent, the European Union recently funded the newly formed EU H2020 Green Deal Innovation Project MERLIN. MERLIN relates to the *Mainstreaming Ecological Restoration of freshwater-related ecosystems in a Landscape context: by Innovation, upscaling,*

and transformation. The project aims at speeding up restoration measures in the European context by assisting in overcoming the main obstacles to restoration implementation identified as:

- Inadequate founding on restoration initiatives;
- Stakeholders' conflict of interests;
- Not sufficient inclusion of restoration measures on political agendas.

MERLIN 's objective is to stress on the potential of nature-based solutions strategies on counteracting the socio-environmental challenges posed by environmental degradation and climate change. To that scope, MERLIN is built on a best-practices knowledge base of 17 existing freshwater restoration projects that can be seen as interventions in different locations on a hypothetical catchment area (Figure 2).

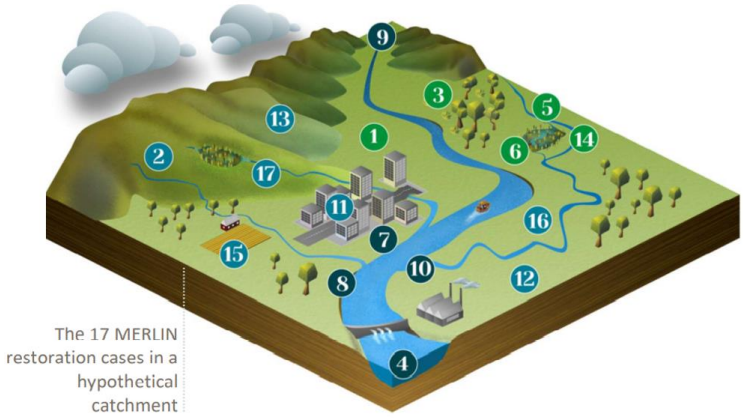

Figure 2. Learning from best practices, location of types of restoration measures within the hypothetical catchment area (provided by Penning, E.)

The same case studies are grouped in projects related to:

- Peatlands and wetlands;
- Small streams and basins;
- Large transboundary rivers.

Projects constituting the knowledge base will serve as blueprint for possible upscaling of in-progress restoration initiatives around the Europe. To that scope, so-called twining case studies are selected to promote exchanges, dialogs, and inspiration.

Internal to the Large transboundary rivers group, one can find the Room-for-the-River programme that has been implemented along the Rhine in the Netherlands during the last two decades. It has been proposed to be a twinning case for the on-going river restoration initiatives along the Po River in Italy. The approach adopted in Room-for-the-River programme will be introduced and briefly described in the next paragraph.

The Room-for-the-River programme in the Netherlands

The Rhine and the Meuse are the two largest rivers in the Netherlands. The Meuse River originates in France and flows through Belgium before of entering the Netherlands and drains into the North Sea for a total length of about 925 km. Its catchment area accounts for around 34,500 km^2 and its average discharge is 230 m^3/s.

The Rhine River is a 1,230 km long river that rises in the Swiss Alps and flows over three countries (Switzerland, Germany, and the Netherlands) but its catchment area (around 185,000 km^2) encompasses a total of nine European countries. The river course changes name frequently moving towards the sea and when entering The Netherlands it splits in its three main branches, the Waal, the Nederrijn – Lek and the Ijssel. When entering the country, the annual average discharge is about 2,200 m^3/s with flow rates along the branches completely controlled by a designed system of bifurcations and weirs.

Figure 3. The Meuse and the Rhine Branches in the Netherlands (source: from Klijn et al. (2018)).

For centuries, the Dutch had cope with nature by embracing the strategy of adapting it to their needs. In fact, the Dutch territory is largely below sea level (about 2/3 of the total surface), and repetitive flooding and storm surges have made life here difficult and hostile, forcing people to search for solutions. Therefore, over the centuries, landscape has been modified by man through the construction of embankments and dikes, followed then by the combined use of windmills and dams, that prompted the design of polders, artificially constructed low-lying tract of land for optimal territorial and water management (Mosselman, 2007). However, even in previous ages, when dikes were already been constructed, rivers in the Netherland were moving freely and large areas were regularly flooded and channel shifting occurred every few hundred years.

Damming of rivers started form the 12th century but it was during the second half of the 19th century that major structural interventions along the river courses were conducted to meet river trading requirements (Brinke & Zetten, 2021). Normalization works consisted of meander cut-offs, bifurcation modifications and groyne constructions aiming at enhancing navigability conditions

and controlling bar formation (Mosselman, 2020). These measures also helped improving the water drainage system as well as fresh water supply distribution meanwhile resulting in strong modifications to the morphodynamic behaviour of rivers. River degradation was also fuelled by sand mining and land reclamation (particularly intense in the last 150 years, see Figure 4) that altered natural river dynamics and sediment balance, inducing noticeable problems with desiccation and biodiversity loss (Brinke, 2019). The reduction of natural hydro-morphological processes, not allowable along highly regulated rivers such as the Rhine, interrupts natural vegetation succession (Baptist et al., 2004) leading to its excessive growth that is responsible for the lowering of conveyance capacity and the overall biodiversity loss over time.

Consequently, river managers in the Netherland must nowadays deal with different critical aspects. One of those is clearly given by the fact that being the Rhine considered the backbone of the Northwest European waterways network, navigability should be ensured for as long as possible during the year. Other requirements are connected, among others, to flood safety, fresh water supply and nature conservation. Anyway, typically required measures for specific objectives can conflict with the achievement of other kind of goals. The greatest challenge precisely is to integrate nature conservation, which presupposes ensuring spatial and temporal variability, with hydraulic protection measures (Brinke & Zetten, 2021). Especially when dealing with nature and ecosystem, things get tougher because the space for nature dynamic is truly limited here.

Typically, dikes were always raised following major flood events. After the devastating flood of 1953, the level of dikes was revalued all along the Rhine Branches guided by a new scientific-economic approach based on the probability of flooding (probability of overflow equal to 1/1250). However, it was soon realized that these estimates would soon have to be revised, also in view of the exacerbation of climatic effects - increasing of 15% and 50% for high and low discharges respectively (Brinke & Zetten, 2021) - in parallel with the increase in assets exposed to flood risk. The 1993 and 1995 flood events especially influenced statistic, leading to the definition of a new design discharge for which a new round of dikes' raising, or a lowering of flood levels was required to ensure flood safety (Silva et al., 2001). The idea of a new rise in embankments levels clashes with public opinion and forced politics to consider a new approach on river management that was been proposed in earlier years by Dutch ecologists first and finally followed by engineers and policy makers too (Mosselman, 2022).

Room-for-the-River was the name of this innovative approach mainly based on the following concept: implementing methods for river widening and deepening without requiring further dikes strengthening as a new management strategy to regulate the existing degree of safety (Silva et. al, 2001). The real added value of this strategy would have been to integrate hydraulic protection measures with interventions to increase ecological status of river systems, in the context of landscape planning projects (Mosselman, 2007). This entailed, for example, the ecological rehabilitation of floodplains thanks to dismission of agricultural fields and house removal in favour of more natural areas in which to develop semi-artificial mechanism of rejuvenation (Baptist et al., 2004) and preserve biotic and abiotic natural components. Enhancing the spatial quality of landscapes was considered as a key objective to be reached in parallel with the development of a sustainable flood risk management. The first one, merely a qualitative attribute, necessitated a deep analysis of natural and cultural heritage of landscapes (Klijn et al., 2013) whereas the second

one was based on the quantitative estimation of the hydraulic effectiveness of site-specific measures, i.e., reduction of flood levels (hydraulic efficiency, mm/km) and increase of conveyance capacity.

The process of identification and definition of feasible interventions was based on a wide multi-stakeholder participatory, supported by initiatives for population participation - i.e., planning kit (Mosselman, 2009b) - with the aim of avoiding top-down decision-making processes. The program was meant to be an interactive planning process (Silva et al., 2001) participated by all relevant local and regional administrative bodies. The projects proposals were also supervised and guided by a team of experts (landscape architect, urban planner, river engineer, ecologist, physical geographer) called Q-team that critically helped in the selection of the final 39 project to be implemented out of the approximately 700 proposals of interventions (Klijn et al., 2013). The proposed measures (Figure 4) were mainly based on storing water along the Rhine Branches in polders and storage areas and increasing the discharge capacity of the river by: lowering of floodplains and groynes, deepening of the summer bed, removing hydraulic bottleneck and obstacles from the floodplains, excavation of side channels and floodways, relocation of embankments (setting back dikes), de-poldering and water storage.

The executive phase ended in 2015 with a total of 2.3 billion € of economic investment for a total of 39 individual measures resulting in the immediate reduction of the flood levels over the entire length of the Rhine Branches within the design water levels (Klijn et al., 2013). One of the biggest results of the program was the return of floodplains to the fluvial dynamics that accounted for 4,400 ha of extra floodplain areas over a total of 28,800 ha (Klijn et al., 2018).

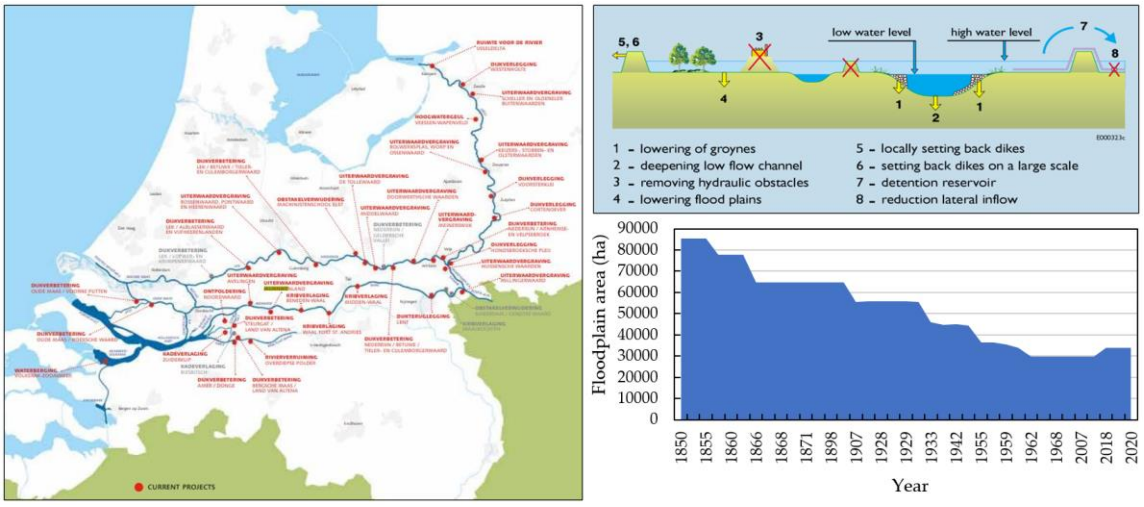

Figure 4. One the left: **t**he 39 measures constituting the Room for the river program along the Rhine Branches (source: Infographics English 2015 by ruimtevoorderivier Stack - Issuu); Top right: interventions studied within the Room for the River program (source: from Silva et al. (2001)); Bottom right: loss of area available for drainage and water storage along the Rhine Branches since 1850 (adapted from Brinke & Zetten (2021)).

But as the problem of high-water levels was overtaken by increasing the conveyance capacity, the current problem of hydraulic safety shifted to the one of dikes stability. Indeed, since 2017 new standards are based on the probability of defence failure (Mosselman, 2002) and it is reasonable that strengthening of embankments will be necessary within the next years.

2.2 The Po River course and the Isola Serafini case study

2.2.1 Legislative framework

In accordance with the requirements of the Water Framework Directive (WFD) 2000/60/EC, the Italian territory has been divided into eight River Basin Districts (Figure 5), the largest of which is the Padan one (ITB) that coincides with the Po River's catchment area. The Po Basin Authority (hereinafter ADBPO) is the main body responsible for planning functions and tasks related to the hydrogeological safety of the hydrological network and the safeguarding of water quality and quantity. Another agency acting along the Po River System is *AIPO* that implements measures meanly related to hydraulic safety, water's state property and navigation. The law L. n. 183 of 1989, which resulted in the adoption of the *PAI Basin Plans* (DPCM 24/5/2001), is the key piece of legislation in the Italian context relating to territorial planning and management. These plans seek to ensure mitigation of hydraulic and hydrogeological disruption phenomena through imposing restrictions on land use and sand mining, while restoring riparian zones and improving the defence work system of rivers.

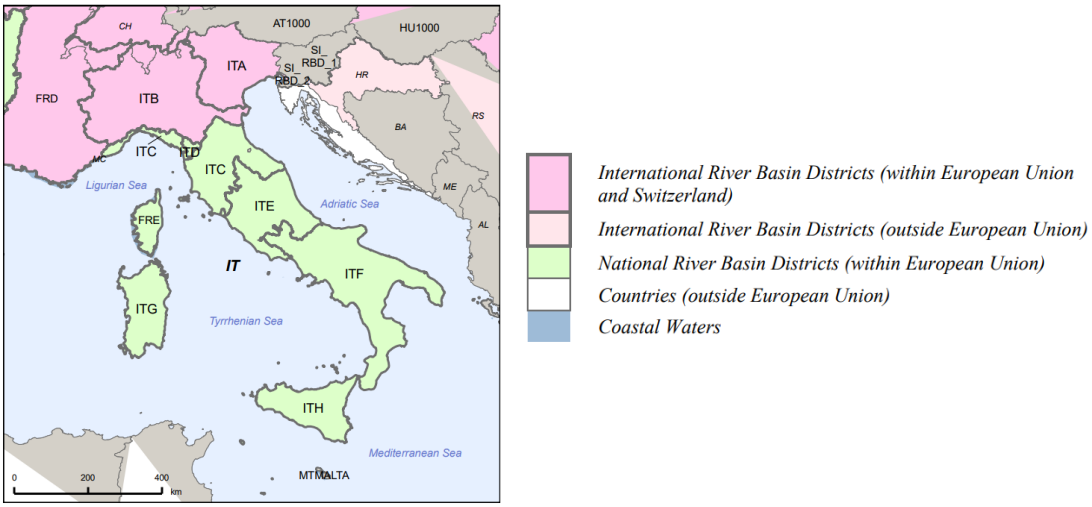

Figure 5. River Basin Districts (RBDs) of Italy (source: from European Commission (2019)).

One of the outcomes of PAI's implementation was the so-called Sediment Directive (CI n° 9/2006), which consist of a cognitive analysis of the hydromorphology of Italian major rivers. The latter followed the Renaturation Directive (CI n° 8/2006), its target being the rehabilitation of natural functionalities of river systems. Both directives aimed at improving the hydro-morphological quality and the ecological status of rivers, respectively. The first directive led to the creation of the Sediment Management Program (adopted in three successive excerpts for the Po River) as an operational tool for river management whereas the second directive called for the predisposition of a plan based on the understanding of the ecological status of the river.

The first excerpt of the Sediment Management Plan (ADBPO, 2005b) does in fact provide the most insight into the general morphological state of the Po River, related to the intermediate segment of the course. This was preceded by a feasibility study (ADBPO, 2005a), which described

the state of the current river's course based on an assessment of the river's changing dynamics through key activities among which the estimate of the sediment transport budget. The Sediment Management Plan and the feasibility study assess morphological dynamics and indicators of solid transport by quantifying planimetric, and volumetric changes occurred to banks, bed forms and riverbed during the reference period 1982-2002. The studies consisted of the analysis of geomorphological topographical information integrated with the implementation of a 1D hydrodynamic model of the river course with fixed bed. The model permitted to quantify characteristic hydraulic parameters of the incised channel (bars submerged and bankfull capacity discharges and associated average flow velocities) and draw longitudinal free surface profiles for characteristic discharges. Modelling investigations of effects induced by sediment management interventions (i.e., opening of side channels, removal of stabilized bars) were also conducted, but only in terms of the already mentioned characteristic hydraulic parameters (ADBPO, 2005a).

More recently, based on the WFD and the FD, two distinct operational legislative tools were designated for the Padan River Basin District, *Piano di Gestione (PdGPo)* and *Piano Alluvioni (PGRA)*, respectively. The PdGPo (first and latest adoptions in 2010 and 2021) aims at safeguarding the qualitative and quantitative status of water resources while conserving ecosystems and biodiversity. The PGRA (first and latest adoptions in 2015 and 2021) addresses the management of floods protection in areas with high risk of damage. To create what is known as Integrating River Basin Management (IRBM), the European Commission envisions the two European directives being integrated. Therefore, it is expected that integration and coordination processes between the different plans would take place. In light of this, the PGRA and PAI have been integrated, leading to the creation of the cartographic tool, *Atlante delle fasce di mobilità morfologica* (ADBPO, 2008c). These maps distinguish two zones:

- *Fascia di mobilità di progetto (FMP):* this zone, which is also referred as the "project mobility band," defines the sections of the river where the Sediment Management Program will be implemented in order to restore and preserve the natural morphological dynamics;
- *Fascia di tutela morfologica ed ambientale (FTMA):* literally "morphological and environmental protection band", it delimits the territory occupied by relict landforms. Although no longer active in ordinary hydro-morphological dynamics, these areas should be preserved for their landscape and environmental value related to the presence of riparian and aquatic habitats.

IDRAIM, developed by the Italian Institute ISPRA, is a further geomorphological tool to support river management within the IRBM concept. It provides an operating approach for the assessment and monitoring of the morphological quality of rivers and for the identification of heavily modified water bodies. Two applications of the IDRAIM approach have been made so far on the Po River one of which (Filippi et al., 2013) investigates the segment analysed in the present study.

A Registry of Protected Sites was created as part of the PdGPo, and it includes several typologies of areas subject to different conservation legislation, such Natura 2000 network areas. Natura 2000 is the European Union's framework (92/43/EEC) aiming at the conservation of biodiversity. Both Natura 2000 and the EU Directive on the conservation of wild birds (79/409/EEC) have been transformed in the Italian context in national law of the protection of biodiversity.

2.2.2 The Po River: general context

The Po River is Italy's longest water course (total length of about 652 km). It originates in Piedmont (Monviso mountain) and flows into the Adriatic Sea. The catchment area of the Po includes nine distinct regions as well as small areas of France and Switzerland. It is the largest basin in Italy (approximately 71,000 km^2) and it is enclosed by Alpes and Apennine to the North, West and South and by the Adriatic Sea to the Est. The river course is typically divided into four sections (Lanzoni, 2012): the upper Po (from its sources to the confluence with the Ticino River), the middle Po (from the confluence with the Ticino River to that with the Mincio River), the lower Po (from the confluence with the Mincio River to the junction with the Po di Goro, at Serravalle) and the Delta (from Serravalle to the outlet into the sea).

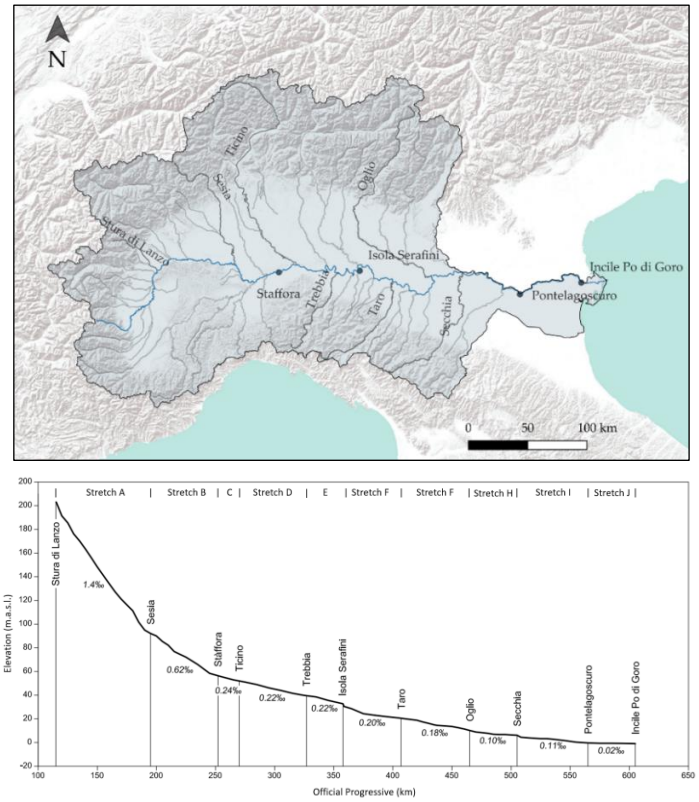

Figure 6. Top: Hydrographic network of Po River Catchment Area (sources: Geoportal ADBPO and ESRI base map); Bottom: Longitudinal profile of the mean elevation of the bottom of the Po River main course from the confluence with Stura di Lanzo to Incile Po di Goro (adapted from Lanzoni (2012)).

For much of its course the river flows over the Po Valley, the area of greatest industrial development in Italy. Its basin, however, is extremely heterogeneous and diverse since up to 12 distinct river regimes have been identified within it and it accounts for a total of 141 tributaries. Despite being one of the most anthropized area of Italy, the riparian zone and its geomorphological and dynamics are partially preserved (Agapito et al., 2020).

The annual hydrograph is distinguished by two low-flow periods (winter and summer) and two flood periods (late autumn and spring) connected with peak rainfall events and melting processes in the basin's mountain areas respectively (Montanari, 2012). Around 60% of the annual total precipitation is estimated to be converted in runoff while the annual sediment transport account

for 13 x 10^9 kg (Maselli et al., 2018) in the face of a mean annual water discharge of about 1,500 m^3/s measured at Potelagoscuro station (Montanari, 2012).

The Po River is part of the "Padano-Veneto" commercial waterway system (section of the Mediterranean corridor of the Core network (Sistema idroviario Padano Veneto - AIPO)). The same waterway system has been identified by European Union as a key facility for the development of the trans-European transportation network.

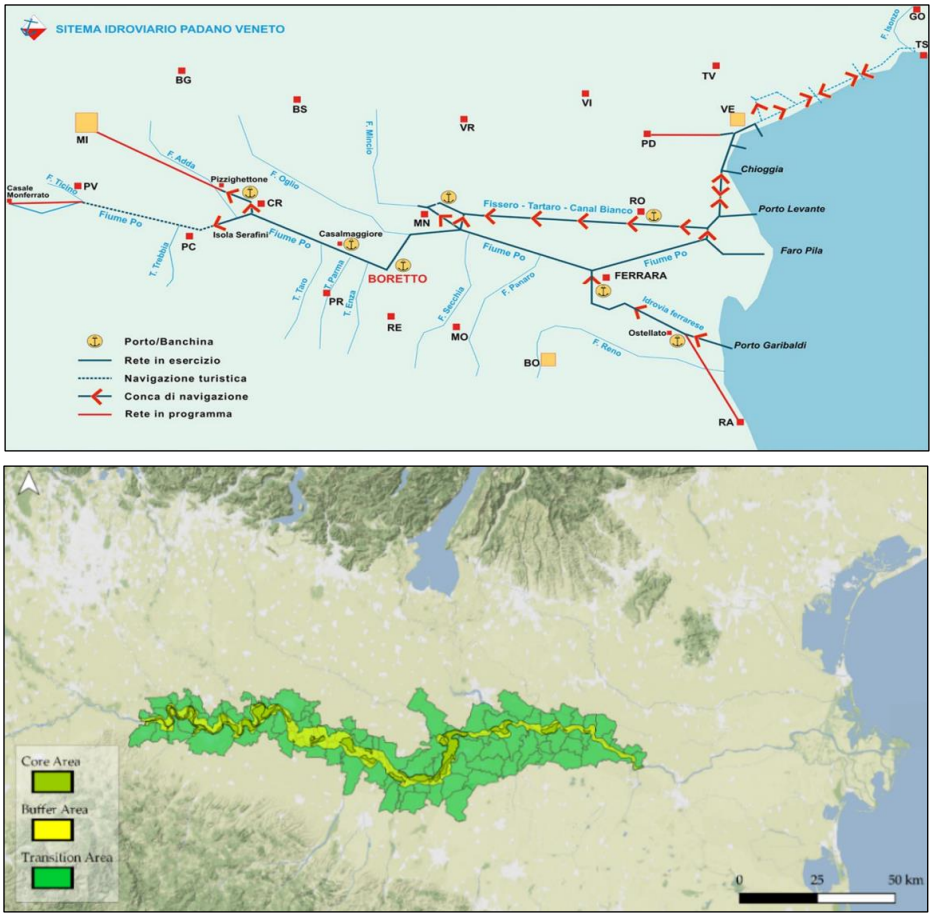

Figure 7. Top: Padano Veneto Waterway System of the Po River; Bottom: The Biosphere Reserve MAB "Po Grande" (sources: Geoportal ADBPO and ESRI base map).

The Po River catchment area accounts for a total of 687 Natura 2000 sites of which 587 are Sites of Community Importance (SCIs) (ADBPO, 2022) including 20 habitats of community interest along the river course, such as natural eutrophic lakes and alluvial forests, constituting its important ecological network. These areas are of paramount importance for the presence of habitats and protected species and their conservation.

The Po River catchment area also accounts for three of the 738 sites constituting the World Network of Biosphere Reserves within the MAB UNESCO Programme ("Riserva MAB Delta Po", "Riserva MAB Collina Po", "Riserva MAB Po Grande"). The MAB program is an intergovernmental scientific program aiming at developing a scientific basis for enhancing the relationship between people and their environments. The program's ultimate scopes are conservation of biodiversity, sustainable development and logistic support. Along the intermediate segment of the Po River, the Biosphere Reserve MAB Po Grande has been designated. Such

reserves are designated as areas where to promote scientific cooperation, interdisciplinary research, and environmental sustainability throughout the involvement of local communities. Each reserve is zoned into areas of differing importance (Figure 7) as:

- Core Areas: areas well conserved in which ecosystems and species must be protected and preserved and natural ecological processes remain mostly unharmed.
- Buffer Areas: zones that surround the former ones and constitute ecological corridors between the various core areas. Sustainable use of natural resources should be planned within these areas aiming at managing and rehabilitating the ecosystem (i.e., sustainable forms of agriculture and tourism).
- Transition Areas: territories free of legislative limits where local authorities are encouraged to promote and adopt sustainable economic growth methods that benefit the core areas.

2.2.3 Past modifications and current constrain.

During the last century the Po River was subjected to a deep process of artificialization to which the river responded by manifesting several changes. The main modifications occurred to the river system are:

- Width and length reduction of the river bed;
- General incision of the bed level;
- Morphological transition from multi-channel to single-channel course.

These modifications affected the river system contemporarily so that it is quite complex ascribing specific cause-effect relationships for individual modifications. Among all of these, sand mining has been recognized by multiple authors as the predominant factor in past years (ADBPO, 2008a; Schippa et al., 2006).

Table 1: Estimates of the total amount of sediments extracted from the Po River between 1982 and 2002. (source: from ADBPO (2008a)).

Operational Office	Extracted m^3 (1982-2002)	Operational Office	Extracted m^3 (1982-2002)
Alessandria	638,550	**Reggio Emilia**	291,700
Pavia	3,778,560	**Mantova**	2,543,266
Piacenza	3,694,609	**Ferrara**	991,784
Cremona	1,184,931	**Rovigo**	2,268,215
Parma	810,300	**Total**	16,201,915

Mining activity brought several negative impacts to the river system both to fluvial and morphological and to natural processes and ecosystem services. Mining modified sediment budget and forced the river to erode sediments from its channel bed (ADBPO, 2005b). Since the 1980s mining activity has been progressively reduced. According to ADBPO (2008a) the number of sediments extracted starting from the 1950s progressively increased up to an estimated value of 12,000,000 m^3/year in the period between 1960 and 1980. Since 1982 there was a turnaround

because of the new imposed environmental restrictions. In the period between 1982 and 2005 the extractions accounted for 700,000 m^3/year (ADBPO, 2008a).

The construction of hydropower dams in the Alpine tributaries, in parallel with reforestation activities and hydraulic – forestry set up, have contributed to the overall reduction of sediment supply to the downstream sections of the river. Guerrero et al. (2013) estimate halving of the sediment transport during the last century to values of 5 x 10^6 m^3/year. Anyway, to meet its sediment transport capacity, the river was forced to erode its alluvial bed, inducing a great erosion trend along the entire course (Figure 8). Indeed, the general deepening of the riverbed begun at the start of 20th century and sped up around the period 1950 – 1960 (Provincia di Mantova, 2005).

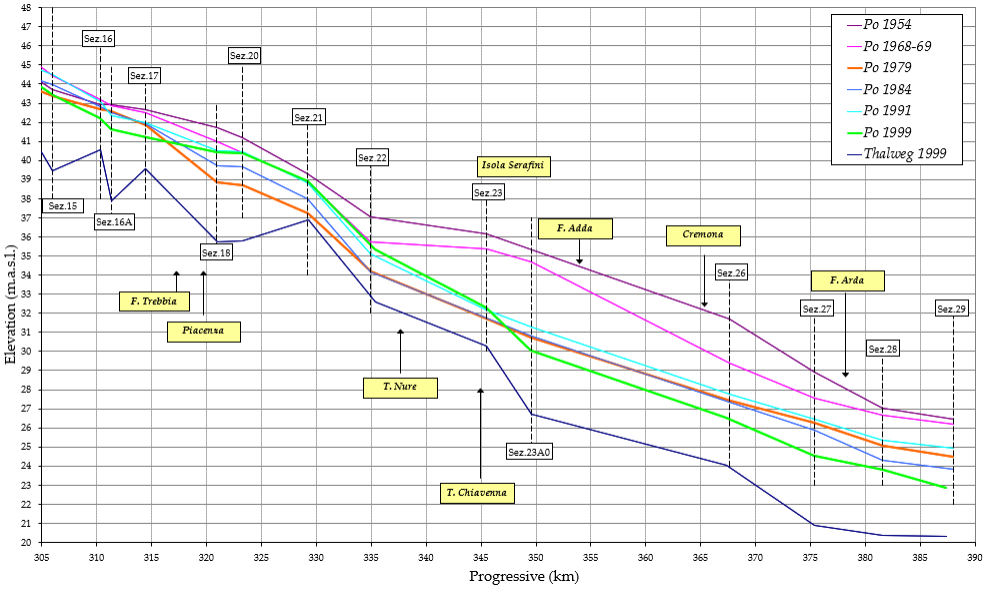

Figure 8. Evolution of the longitudinal profile of the mean elevation of the bottom of the Po River (from section 15 to section 29), (adapted from ADBPO (2005b)).

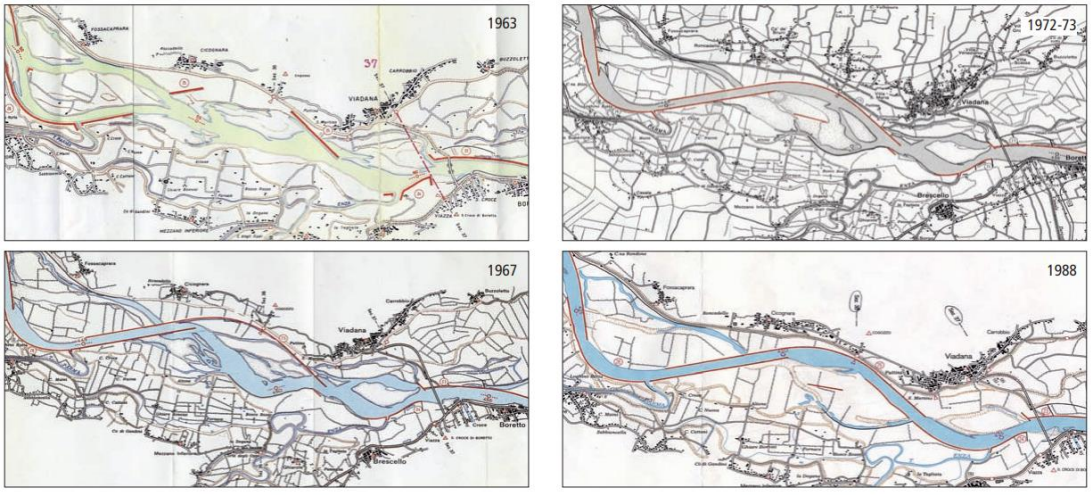

Figure 9. Illustration of the sequence (from 1963 to 1988) of navigation works that transformed the morphological pattern of the Po River (source: from ADBPO (2008a)).

The works for ensuring navigability conditions, had fixed the planimetric configuration of the river, changing its morphological patterns, moving from multi-channel to single channel

morphology (ADBPO, 2008a). These works have bounded the ordinary flow to the main channel, accelerating the ongoing bed level erosion process (Schippa et al., 2006) while depriving floodplains of periodic inundations. Drastic reduction of the channel width occurred especially along the stretch between the Adda River mouth and the Mincio River mouth where the low flow channel width passed from 450 m to 250 m on average (Provincia di Mantova, 2005). The low flow channel was stabilized between 1919 and 1970 (strong development between 1955 and 1964). The navigation channel (Figure 9), designed to convey the low flow discharge of 400 m^3/s (ADBPO, 2008a) can nowadays convey 5,000 m^3/s corresponding to the ordinary peak discharge with a return period of 2 years (ADBPO, 2005b) because of incision. This is leading to a self-feeding process of erosion of the bottom channel. Provincia di Mantova (2005) states that the remarkable height of the longitudinal training walls seems to be the original cause of deepening.

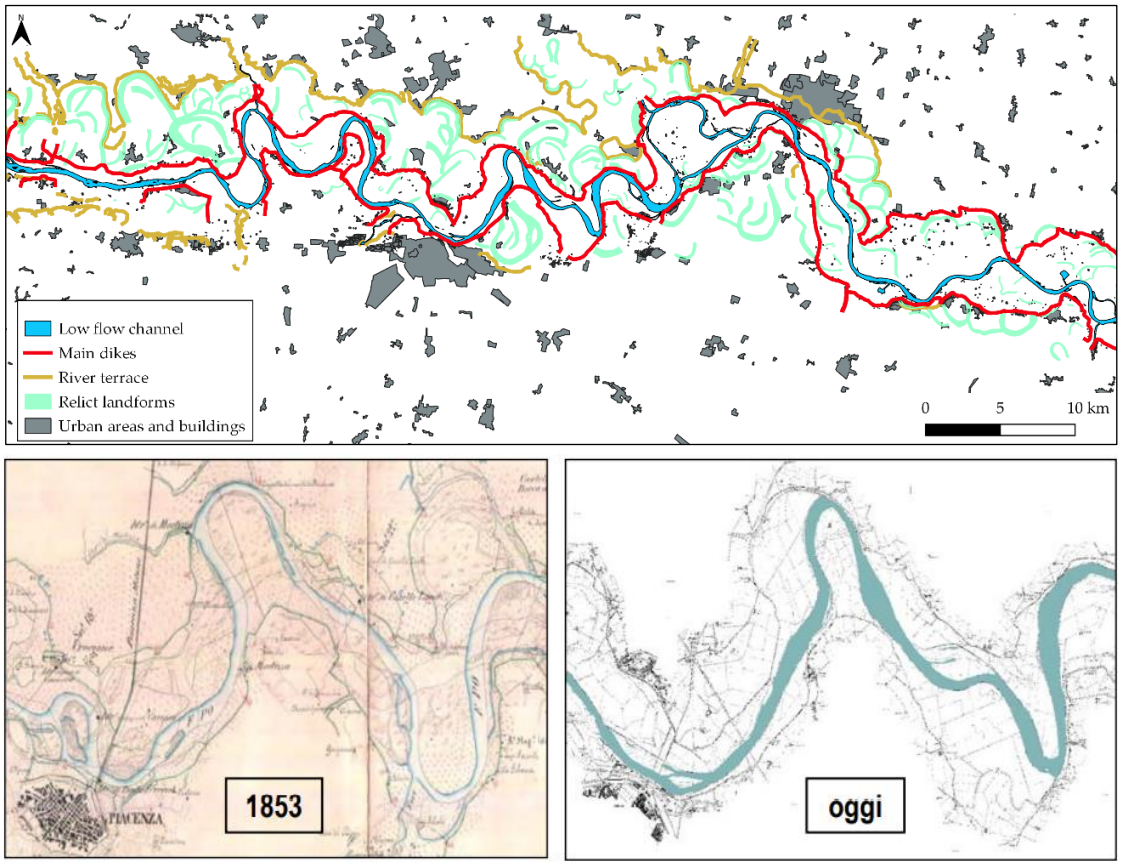

Figure 10. Top: Map showing main dikes between fluvial terraces and main course that strongly reduce areas of possible river migration and flooding, halting the dynamics of the course. Past morphological dynamic of the river is testified by the large presence of relict landforms outwards of the system of main dikes (adapted from ADBPO (2005b)); Bottom: Time comparison (1853 and 2005) of the section of the Po River downstream of Piacenza in which main dikes arrested the lateral migration of river meanders (source: ADBPO (2005b)).

The Po River predominantly flows nowadays on a restricted and fixed part of the entire alluvial channel. Consequently, lateral connectivity of water and solid between floodplains and the main channel drastically decreased, disrupting ecosystem services which floodplains should normally provide (Filippi et al., 2013).

An important role has been played even by banks stabilization works and dikes. The reclamation of land for agriculture purpose as well as dikes construction required to provide hydraulic safety

Theoretical framework to urban areas have increasingly deprived the river of areas in which it could exert its dynamic and reduced the space available for habitat development. The erodible corridor is predominantly forced inside the main embankments and bank defences limiting bank erosion processes and with it natural morphological functionality, sediment reload activity and riparian vegetation development (Filippi et al., 2013). The main embankments are usually too closed to natural banks thus they fix the planimetric configurations of the channel leading to singular arrangement of the course with very pronounced bends (Figure 10) that may results in hydraulic structures instability (ADBPO, 2008a).

As mentioned above, the growing demand for energy production had boosted dam's construction resulting in a further reduction of sediment supplies to valley regions (ADBPO, 2008a). Flow modifications induced by barrages and water derivations can also alter formative discharges and degrade habitats by reducing flow dynamics, like in the case of Isola Serafini hydropower plant.

2.2.4 The Po River at Isola Serafini

Isola Serafini is a fluvial island along the Po River, located between the Trebbia and the Arda River mouths. This part of the river is strongly modified and especially the deepening of the bed channel has been particularly marked, reaching peak values up to 8 meters (Filippi et al., 2013). Cremona has been recognized as the epicentre of the deepening process (Figure 11) with studies estimating the growing tendency of about 9 cm/year (Provincia di Mantova, 2005). River training has completely changed the low flow channel course and altered the sediment dynamics whereas the construction of the Isola Serafini hydroelectric plant appears to be having an impact on the natural morphological development of the entire stretch.

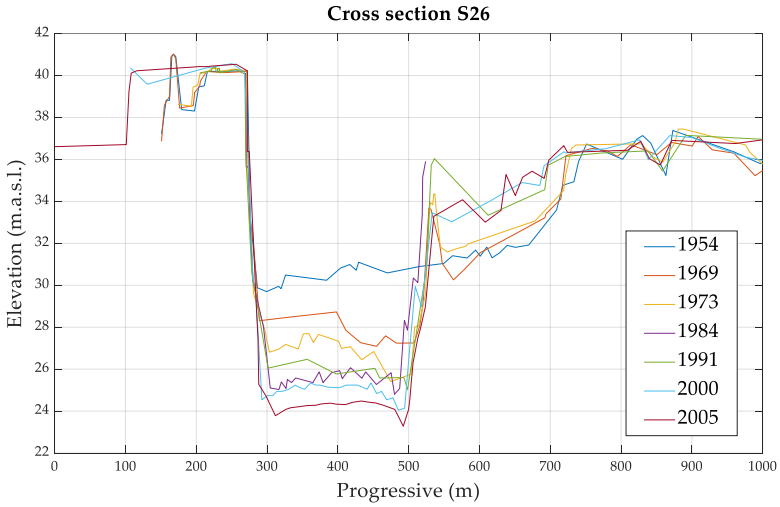

Figure 11. Cross section S26 (located approximately 4 km downstream of the conjunction between the meander of Isola Serafini and the tailrace of the hydropower plant) is the more powerful image that demonstrates the high degree of channel bed erosion that has been taking place along the Po River.

This segment of the river seems to have always been subjected to a high morphological dynamic that stopped after the construction of the barrage that create the hydraulic jump necessary for

energy production. The area was previously characterized by the presence of a set of fluvial islands (Figure 12) but major flood events occurred during the 19th century profoundly altered the river set-up (from 1828 map to 1889 map of Figure 12).

After the flood event of 1917 the river was flowing along a meander loop 12 km long which starting and ending points were speared only by 500 m long limb of land with an elevation gain of about 2 m (1921 map of Figure 12). The idea of building a waterworks to generate energy, originally arose around the beginning of the 20th century (Zorzoli, 2008). Eventually, in 1951, a natural meander cut-off occurred around 10 km downstream of the current barrage and consequently the river course was shortened of about 5 km. The relict fluvial bedform of the river can be clearly identified on satellite images (this old part of the river is called nowadays "Po Morto", literally the Dead Po).

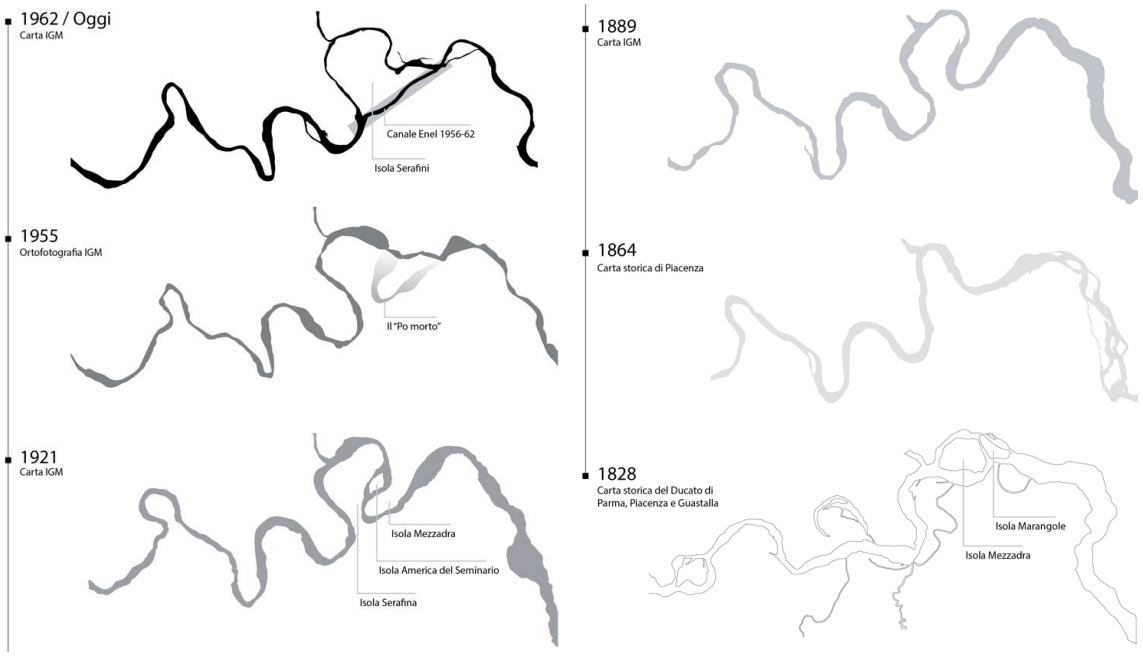

Figure 12. Top left: Historical map of Ducato di Parma (1828); Top right: Historical map Ducato di Piacenza (1864) (source: Geoportal Emilia-Romagna); Bottom: Sequence of morphological modification of the Po River at Isola Serafini (source: Master science thesis "Isola Serafini: Architettura per paesaggi labile" – Falcone, M., Santulli, F., Toma, G).

The alluvial plain surrounding Isola Serafini has a mean slope of about 0.5 ‰ in which the river course flows with a meandering morphology (sinuosity index ranging between 2.19 and 1.51 (Filippi et al., 2013) and a mean bed slope of about 0.2-0.3 ‰ (ADBPO, 2005b). The average width of the bankfull channel is 420 meters from the barrage to the Adda River mouth, and 565 meters between the latter and the confluence of the meander and the tailrace (Filippi F et al., 2013). Nevertheless, due to the deepening of the channel, even for higher flow rates, the stream is bounded in a small part of the incised channel not involving the adjacent floodplains (Comune di Monticelli d'Ongina, 2008).

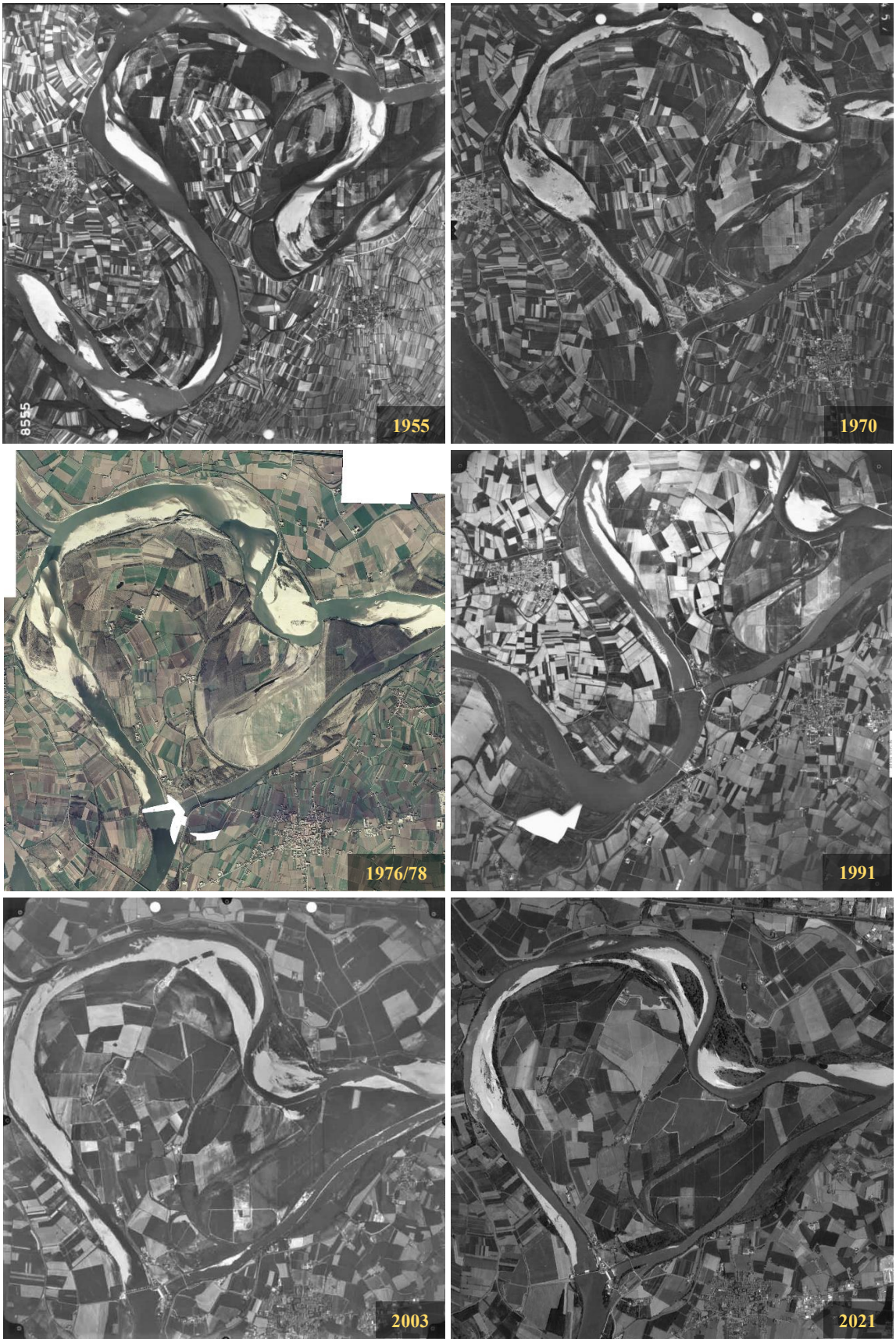

Figure 13. Series of orthophotos and satellite images of Isola Serafini since 1955 to the present (sources: https://www.adbpo.it/la-documentazione-conoscitiva-della-fascia-fluviale-del-po/ and Google Map).

The hydrological regime of the Po River at Isola Serafini will be described in Chapter 3. Table 2 shows water discharges estimated for characteristic return period together with the main historical flood events occurred. The operation rule of the hydropower plant alters the natural flows along the meander such that for most of the year the flow rates along the meander are mainly formed by the Adda River's contribution whereas along the stretch between the barrage and the Adda River mouth predominant discharge can be considered insignificant (ABDPO, 2005b).

Table 2: Discharges (m3/s) associated to return periods for the Po River (at Cremona and Piacenza) and for the Adda River (at Pizzighettone and at the Adda River mouth) ; Historical discharges measured at Cremona.

Q_{TR} (m^3/s)	Po Cremona (PAI)	Po Cremona (Arpa Simc E.R.)	Po Piacenza (PAI)	Adda Pizzighettone (SIDRO - ARPAL)	Adda confluenza Po (SIDRO - ARPAL)
$Q_{1.33}$	-	4140	-	605	608
Q_2	5475	5400	4664	-	-
Q_3	-	6370	-	-	-
Q_5	7310	7640	6290	1245	1250
Q_{10}	8525	8850	7366	1533	1539
Q_{20}	-	-	-	1825	1832
Q_{25}	10061	-	8725	-	-
Q_{50}	-	-	-	2227	2236
Q_{100}	12330	-	10735	2883	2557
Q_{200}	13456	-	11733	3355	2895
Q_{500}	14942	-	13049	3355	3369
Historical peak at Cremona hydrometric station (m^3/s)					
Event of 2000				11.800*	
Event 1994				11.300*	
Event 1951				13.750**	

* Values obtained from the discharge rating curve.
**Estimated values by Ufficio Idrografico.

There is not perfect correspondence in literature review about the operation rule of the barrage. It has been decided to refer to the latest study by Bizzi et al. (2015), integrating this information with the last available document made by the power plant operator (ENEL, 2021). The minimum discharge for energy production is 200 m^3/s and the minimum vital flux (MVF) on the meander is fixed at 100 m^3/s. Thus, for incoming discharges lower than 300 m^3/s, the flow is entirely conveyed in the meander (except for a MVF for the tailrace). Turbines can produce energy for a total flow of 1,000 m^3/s so when the incoming discharge is higher than 1,100 m^3/s the gates of the barrage are gradually opened. The opening succession is determined by the operator also in view of downstream bathymetric surveys (ENEL, 2012).

The barrage construction had hampered the natural regressive erosion induced by the natural meander cut-off, transferring, however, morphological instability on the downstream stretch (Provincia di Mantova, 2005). The operation rules of the hydropower plant have been also modifying the sediment transport capacity on the upstream stretch of the barrage and consequently sediment supply to the meander (Maselli et al., 2018). The level of the water in the reservoir is kept constantly at 41.5 m.a.s.l. and backwater effect extends for approximately 30 km upstream (Maselli et al., 2018).

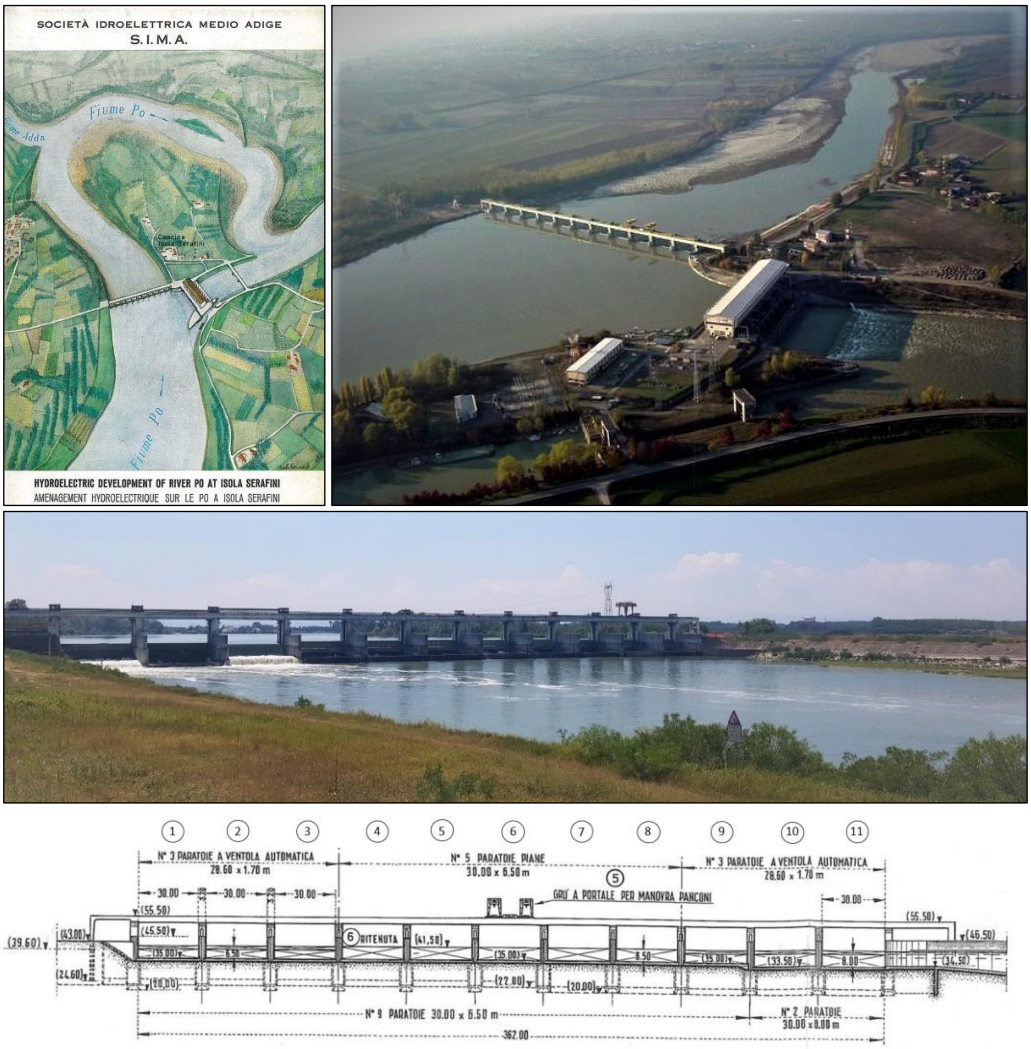

Figure 14. Top left: SIMA (1960) publication cover; Top right: Aerial picture of Isola Serafini hydropower plant with a particular view on the channel downstream of the barrage (source: http://www.ilgiornaledelpo.it); Centre: Photo of the barrage taken from valley section during the field visit; Bottom: Geometric representation of the barrage from upstream (adapted from SIMA (1960)).

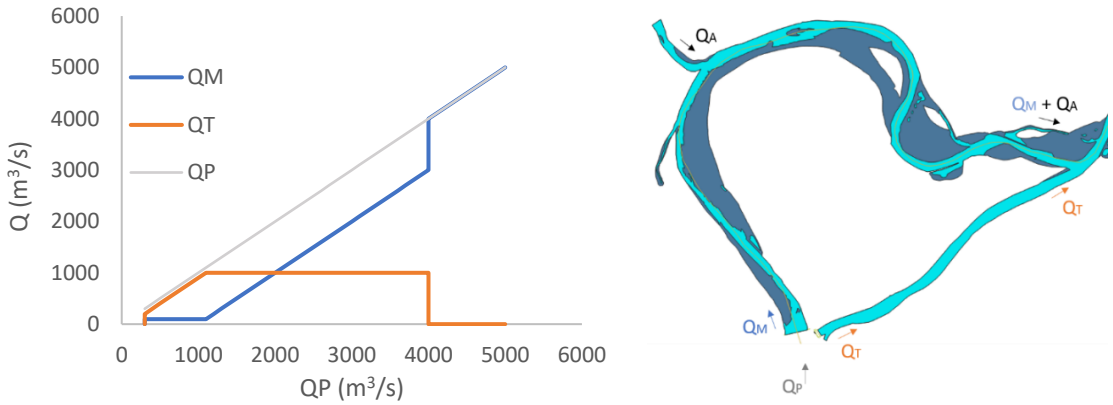

Figure 15. Schematic operation rule of the hydropower plant. QP: inflow Po discharge; QT: turbined discharge conveyed through the tailrace; QM: discharge passing through the gates of the barrage and flowing into the meander; QA: Adda discharge.

Different authors (Provincia di Mantova, 2005) show that the barrage influences the flow upstream leading to sedimentation on banks and bed channel whereas others argue that sediments are partially trapped by Isola Serafini's reservoir, so that dredging is necessary to restore conveyance capacity of sections (around 400,000 m^3/year). By contrary, according to Oldani et al. (2008), the balance between erosion and deposition on the reservoir of the barrage is approximately zero, as proven by bathymetric surveys repeated over time. The author concludes that apparently, the deepening of the bed occurred along the entire stretch, is controlled by drivers at a larger scale than the local one.

Also, ENEL (2012) assesses that the presence of the barrage is irrelevant for sediment transport mechanism because of the following remarks:

i. Given that sediment transport manifests through the migration of bedforms (i.e., ripples and dunes) as a function of flow velocity, this is relevant only for medium and high discharges, when the gates of the barrage are already opened.
ii. The bottom of the gates is positioned at the same level of the channel bed thus sediments are not stopped since the rising phase of the flood.

As proof of this ENEL (2012) notes how, subsequently to each flood event, new depositions areas emerge downstream of the barrage, whereas repeated topographic surveys (from 1971 to 2007) show no aggradation on the upstream stretch. The same study concluded that the operation rules of the barrage are fully compatible with the fluvial dynamics.

It is a matter of fact, however, that sediment transport is altered someway also because of the presence of the barrage. The sediment transport mechanism across Isola Serafini is well explained by Maselli et al. (2018). According to the authors, depending on the flood intensity, the river exhibits very different sediment transport behaviours on the upstream stretch of the barrage. For low flow conditions the floodgates are almost entirely closed (only the MEF of 100 m^3/s can pass through the gates), inducing an upstream M1 type backwater profile (Figure 16). Low energy conditions are therefore established, for which, resulting bed shear stress are sufficiently low that bedload transport is negligible (shear stress below the critical threshold for silt sediments). It leads to aggradation of the bottom channel as highlighted by (ADBPO, 2005b), especially between official progressive 320 and 340. By contrary, for higher discharges (2,100-4,800 m^3/s), when the floodgates are progressively opened, a M2 type backwater profile occurs (Figure 16), velocities increase and thus bed shear stresses, determining the removing of fine-grained sediments previously deposited (Maselli et al., 2018).

This mechanism confirms that sediments are only partially transferred through the barrage and specifically for high flow regime only (ADBPO, 2005b), establishing an impulsive-type solid transport mechanism. Upstream of the barrage, fine-grained sediments are especially deposited along the channel bed during low discharges, but these are removed currently with higher discharges, when coarser sediments can be mobilized too. Consequently, sediment composition is finer approaching the barrage with D_{50} passing from 0.6 mm (10 km far from the barrage) to 0.2-0.01 mm (Maselli et al., 2018). Along the meander loop, the same dynamic produces a mechanism of removal and deposition of fresh sand during the rising and falling phases of peak events

respectively that lead in the medium-term to progressive deepening of the low-flow channel (Figure 17) and uplift of bars (ADBPO, 2005b).

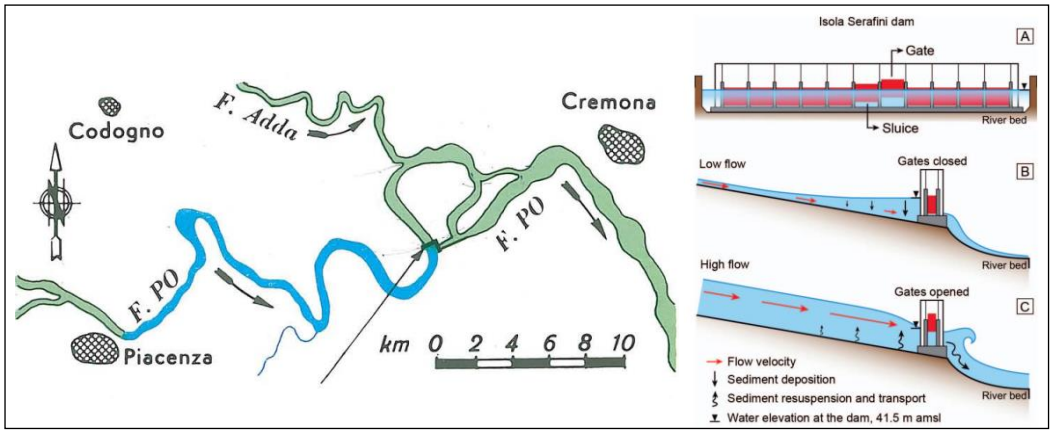

Figure 16. On the right: Representation of the longitudinal extent of backwater effect induced by the operational rule during low-flow conditions (source: from ENEL (2010)); On the left: Representation of free surface profiles upstream of the barrage for low and high-flow conditions (source: from Maselli et al. (2018)).

This is confirmed by results obtained (Figure 18) via the modelling-experimental approach by ADBPO (2005b) that analyse sediment budget on a time span of 20 years (1982 – 2002). A further confirmation is given by Filippi et al., (2013) that assessed how bars size is disproportionate with respect of the wet channel dimension because of the bad balancing between liquid and solid regime induced by the operation rules. Moreover, the operation rules determine a reduction of the discharge on the meander of about 1,000 m^3/s and therefore a reduction of the frequency of occurrence of formative discharges that have been estimated between 4,000 and 5,000 m^3/s by Filippi et al. (2013).

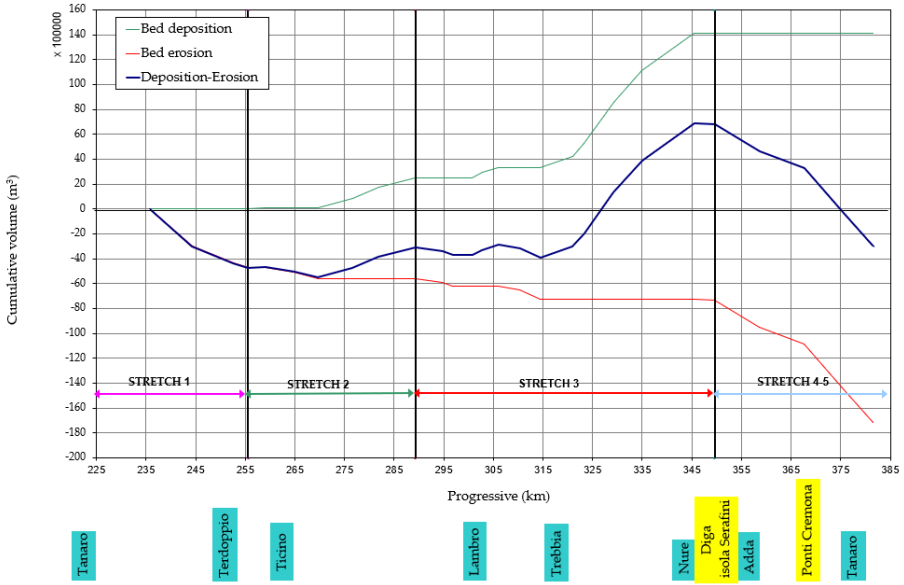

Figure 17. Cumulative deposition and erosion of the channel bed along the Po River between Tanaro River mouth and Adda River mouth in the period 1982-2002 (adapted from ADBPO (2005b).

The barrage also represents an obstacle for organic matter and fish migration and it has been recognized as the primary cause for extinction of two of the three sturgeon species that once

resided in the Po River (Regione Lombardia, 2018). The barrier stopped the ecological corridor and prevented migratory species to reach spawning sites on the upstream stretch, triggering their long-term conservation. With the *LIFE11NAT/IT/188 CON.FLU.PO project "Restoring connectivity in Po River basin opening migratory route for Acipenser naccarii"* a new migration route has been opened. A passage for fish was built located between the barrage and the power station of Isola Serafini connecting the upstream segment of the Po River with both the meander and the tailrace (Regione Lombardia, 2018). Additionally, the barrage represents an obstacle to woody debris as confirmed by the plant operator (Enel) that declares to remove from the barrage about 3,000 tons per year of floating woody material, which would represent organic supply for the downstream reach and would contribute to structuring habitat diversity (Filippi et al., 2013).

Aside from the longitudinal continuity, lateral connectivity between the main channel and the floodplains is hampered by bank protections, which are prominent throughout the meander loop and obstacle lateral movement of the main channel and bank retreat ADBPO (2005b). Alteration of sediment dynamics is induced even by navigation works constituted by longitudinal training walls that disconnect side channels from the active fluvial dynamics. According to Filippi et al. (2013) side channel's contribution to solid transport begins only when the training walls are topped by the water. This occurs, however, only for discharges between 5,000 and 9,000 m^3/s characterized by a very low frequency of occurrence to actively contribute to morphological dynamics. For lower discharges the side channels can be only flooded from downstream sections, determining conditions of low energy flow that lead to their progressive clogging.

ADBPO (2005b) concludes that between Tanaro and the Trebbia River mouths the Po River's annual sediment transport capacity can be estimated to be around 500,000-600,000 m^3/year and it progressively reduces up to Isola Serafini's barrage where the sediment transport is practically nil. It is gradually recovered moving downstream of the barrage, reaching values of about 250,000 – 300,000 m^3/year only close to the Arda River's mouth (around 30 km downstream of the barrage) with sediment load mainly aided by the bottom of the river, which is deepening, indeed.

Another typical evidence of morphological alteration is the absence of active floodplains (Filippi et al., 2013). The same applies for other characteristic lowland landforms such as abandoned meander channels, side channels, and oxbow lakes, which are locally common but completely disconnected from fluvial dynamics (Filippi et al., 2013). Fluvial wetlands are now restricted to a narrow and discontinuous zone especially because incision and intensive use of agricultural lands, with arable corps and poplar groves dominating the whole floodplain area.

Morphological problems not only affected the meander loop but even the tailrace that is experiencing a great deepening of the bed channel (apparently is not receiving any sediment input from upstream). The water levels along the tailrace had become too low in time making the old navigation lock inefficient so that a new one needed to be built.

Finally, the following navigability requirements must be guaranteed along the stretch:

- Commercial navigation downstream of Cremona: minimum water depths of 2 meters for 340 days per year (AIPO).
- Permanent tourist navigation from Adda River mouth to Cremona: minimum water depth of 0.5 meters (ADBPO, 2005b).

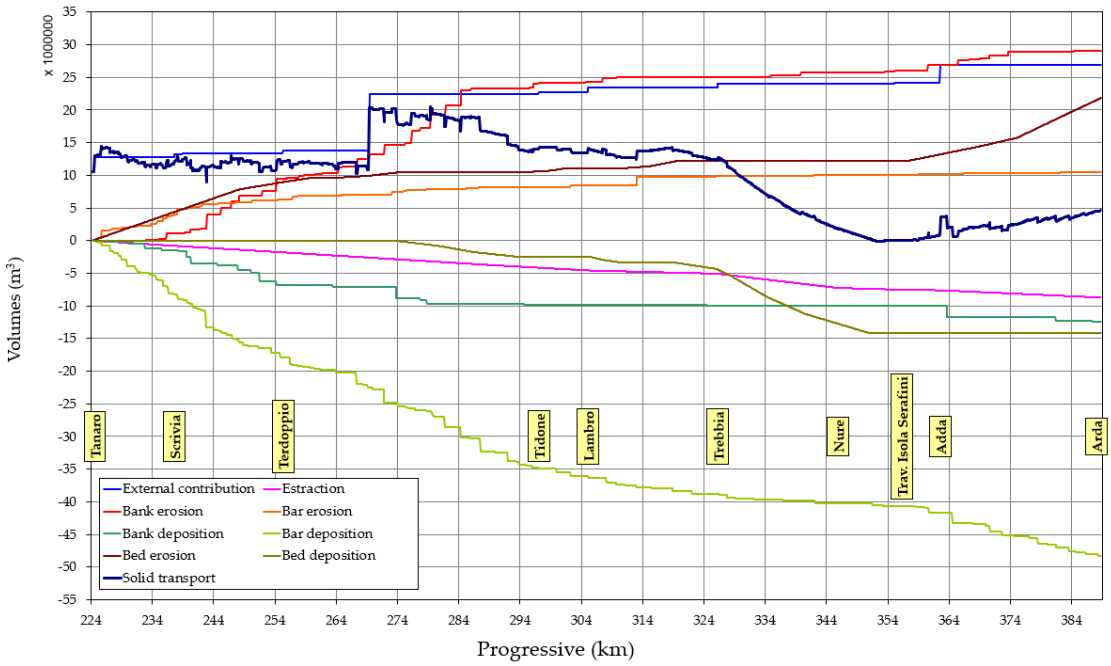

Figure 18. Sediment transport budget along the Po River between Tanaro River mouth and Adda River mouth in the period 1982-2002 (adapted from ADBPO (2005b).

Isola Serafini was established as part of the site (SIC) SIC ZPS IT4010018 "Fiume Po da Rio Boriacco a Bosco Ospizio" within the Natura 2000 network, for the large extensive wetlands and sandy regions that draw many permanent and migratory bird species including sea swallows, owls, falcons, and woodpeckers. Furthermore, the entire area has been marked as core area and buffer area within the Riserva MAB Po Grande, demonstrating the importance of this site for the Po River ecological corridor.

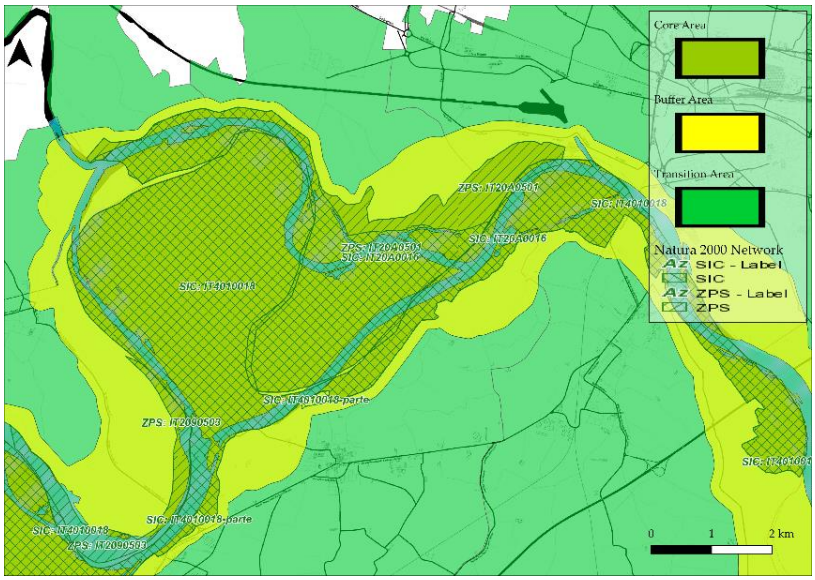

Figure 19. Biosphere Reserve MAB "Po Grande" and Natura 2000 sites at Isola Serafini. The whole area of Isola Serafini is a site of community interest (SIC) and constitutes an important part of Po River's core areas (sources: GIS features from Geoportal ADBPO).

2.3 Theoretical framework

2.3.1 Delft3D-4: 2D hydro-morphological model.

Delft3D is the integrated flow and transport modelling system developed by *Deltares*. Delft3D suite is composed by several modules that can interact with one another. Among theme, Delft3D-FLOW solves multi-dimensional hydrodynamic problems of steady and non-steady flow and transport phenomena by making use of a rectilinear or curvilinear, boundary fitted grid. It therefore provides the hydrodynamic basis for other modules such as water quality, ecology, and morphology. The program is coupled with basic features such as:

- RGFGRID: for the generation of curvilinear grids.
- QUICKIN: for creating and manipulating grid-oriented data such as bathymetry or initial conditions.
- Delft3D-QUICKPLOT: for visualizing and animate results of simulations.

The setting-up of a hydrodynamic model requires for the predisposition of an input ASCII file named Master Definition Flow file or MDF-file that contains all data required for defining a model and running the simulation program. The latter can be prepared on the graphical user interface (FLOW-GUI) consisting of several Data Group to set up. By enabling from Data Group sediment transport process and morphology based on the feedback of bottom changes is possible to simulate a comprehensive morphodynamic computation.

Given the objective of the present study, a two-dimensional (2DH, depth-averaged) model of the Isola Serafini meander was generated, integrated with sediment transport phenomena. The system of governing equations consists of the horizontal equation of motion, the continuity equation, and the transport equation for conservative constituents. A physical cartesian orthogonal curvilinear co-ordinates system (ξ- η) in the horizontal plan was adopted to create a computational space with grid lines composing the computational grid extended along the two curvilinear ξ- and η-direction.

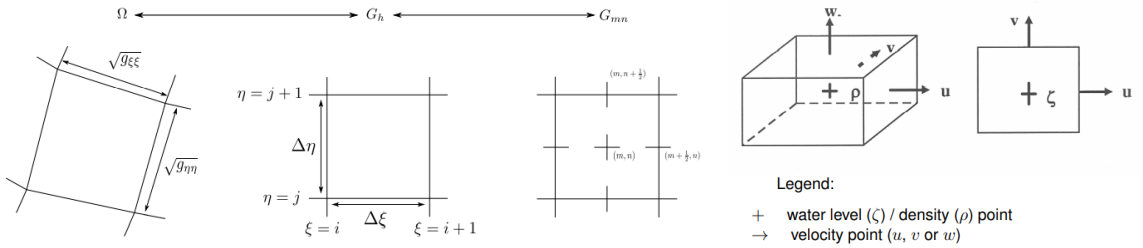

Figure 20. To the left: Mapping of physical space to computational space; To the right: Grid staggering, 3D view and top view (source: from Deltares (2018)).

The numerical method of Delft3D-FLOW is based on finite differences with discretization of the area to be modelled by means of a curvilinear grid. The latter is even called staggered grid because of the arrangement for which velocity components are perpendicular to the grid cell faces whereas the water level points are defined in the centre of the cells. The vertical reference system was based

on a horizontal flat plane for which only one layer above the entire horizontal computational area is enclosed between the two so called σ-planes that follow the bottom topography and the free surface respectively.

The σ co-ordinate system is defined as:

$$\sigma = \frac{z-\zeta}{d+\zeta} = \frac{z-\zeta}{H},$$

with:

z: the vertical co-ordinate in physical space.
ζ: the free surface above the reference plane (at $z = 0$).
d: the depth below the reference plane [m].
H: the total water depth, given by $d + \zeta$ [m].

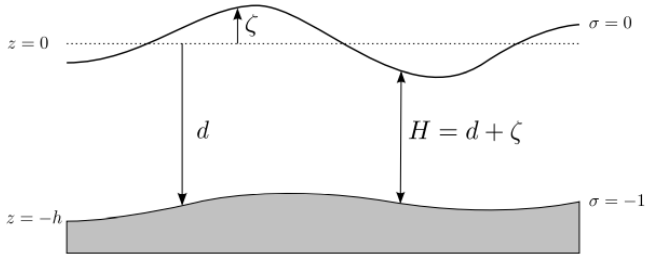

Figure 21. Definition of the water level (ζ), depth (h) and total depth (H), (source: from *Deltares* (2018)).

Under the 2D shallow water hypotheses, the integration for the continuity equation for incompressible fluid over the total depth (considering the kinematic boundary conditions at water surface and bed level and the geometrical quantities for the system transformation) leads to:

$$\frac{\partial \zeta}{\partial t} + \frac{1}{\sqrt{G_{\xi\xi}}\sqrt{G_{\eta\eta}}} \cdot \frac{\partial \left((d+\zeta)U\sqrt{G_{\eta\eta}}\right)}{\partial \xi} + \frac{1}{\sqrt{G_{\xi\xi}}\sqrt{G_{\eta\eta}}} \cdot \frac{\partial \left((d+\zeta)V\sqrt{G_{\xi\xi}}\right)}{\partial \eta} = (d+\zeta)Q,$$

whereas the momentum equations in the horizontal direction are given by:

$$\frac{\partial u}{\partial t} + \frac{u}{\sqrt{G_{\xi\xi}}} \cdot \frac{\partial u}{\partial \xi} + \frac{v}{\sqrt{G_{\xi\xi}}} \cdot \frac{\partial u}{\partial \eta} + \frac{w}{d+\zeta} \cdot \frac{\partial u}{\partial \sigma} - \frac{v^2}{\sqrt{G_{\xi\xi}}\sqrt{G_{\eta\eta}}} \cdot \frac{\partial \sqrt{G_{\eta\eta}}}{\partial \xi} + \frac{uv}{\sqrt{G_{\xi\xi}}\sqrt{G_{\eta\eta}}} \cdot \frac{\partial \sqrt{G_{\xi\xi}}}{\partial \eta} - fv$$
$$= -\frac{1}{\rho_0 \sqrt{G_{\xi\xi}}} P_\xi + F_\xi + \frac{1}{(d+\zeta)^2} \cdot \frac{\partial}{\partial \sigma}\left(\nu_V \frac{\partial u}{\partial \sigma}\right) + M_\xi,$$

and

$$\frac{\partial v}{\partial t} + \frac{u}{\sqrt{G_{\xi\xi}}} \cdot \frac{\partial v}{\partial \xi} + \frac{v}{\sqrt{G_{\eta\eta}}} \cdot \frac{\partial v}{\partial \eta} + \frac{\omega}{d+\zeta} \cdot \frac{\partial v}{\partial \sigma} - \frac{uv}{\sqrt{G_{\xi\xi}}\sqrt{G_{\eta\eta}}} \cdot \frac{\partial \sqrt{G_{\eta\eta}}}{\partial \xi} + \frac{u^2}{\sqrt{G_{\xi\xi}}\sqrt{G_{\eta\eta}}} \cdot \frac{\partial \sqrt{G_{\xi\xi}}}{\partial \eta} + fu$$
$$= -\frac{1}{\rho_0 \sqrt{G_{\eta\eta}}} P_\eta + F_\eta + \frac{1}{(d+\zeta)^2} \cdot \frac{\partial}{\partial \sigma}\left(\nu_V \frac{\partial v}{\partial \sigma}\right) + M_\eta.$$

where:

v, v and w: flow velocity in ξ, η and z-directions, respectively [m/s].
U and V: depth-averaged velocity in ξ, η-directions, respectively [m/s].
Q: global source or sink per unit area [m/s].
$\sqrt{G_{\eta\eta}}$ and $\sqrt{G_{\eta\eta}}$: coefficients used to transform curvilinear to rectangular co-ordinates.
fv and fu: Coriolis parameter in ξ, η-directions, respectively [1/s].
ν_V: vertical eddy viscosity coefficient [m^2/s]
P_ξ and P_η: gradients hydrostatic pressure in ξ, η-directions, respectively [$kg/(m^2s^2)$].
F_ξ and F_η: turbulent momentum fluxes in ξ, η-directions, respectively [m/s^2].
M_ξ and M_η: sources or sinks of momentum in ξ, η-directions, respectively [m/s^2].

Depth-averaged equations do not resolve vertical quantities thus neglecting the helical motion, flow pattern developing in curved channel and characterized by a combination of streamwise flow and cross-stream velocities, resulting in a downstream spiralling motion. This flow pattern is crucial to calculate riverbed modifications in morphological analyses, especially regarding the generation of lateral bed slopes. It is possible, however, to consider indirectly the effect of the spiral motion generated by the helical flow by means of a secondary flow model. The secondary flow is characterized by a velocity profile directs towards the outer bend at the water surface and towards the inner bend next to the channel bed, establishing a cross-stream rotational pattern. Associated to the mainstream, such flow conditions induce not only lateral transport of downstream momentum but even a downward one next to the outer bank, strongly impacting the sediment transport dynamics and bank erosion processes. A spiral motion intensity of the secondary flow I is introduced in the model to measure the magnitude of the velocity component v (σ) normal to the depth-averaged main flow along the vertical. It can be evaluated as follow:

$$I = \int_{-1}^{0} |v\ (\sigma)|\ d\sigma.$$

The actual local velocity distribution v (σ), is calculated by multiplying the spiral motion intensity I [m/s] by the vertical distribution of the secondary flow that is assumed to be a universal function of the vertical co-ordinate f (σ).

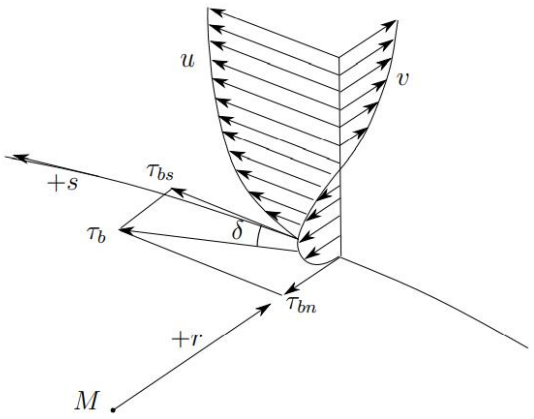

Figure 22. Vertical distribution of the secondary flow V in a curved channel and resulting sediment transport direction (source: from Deltares (2018)).

Consequently, the bed shear-stress is deviated from its undisturbed direction (parallel to the depth-averaged flow direction) by the new normal to the flow component τ_{bn} induced by the spiral motion, affecting the sediment transport direction. The shear stress normal to the depth-averaged flow direction is given by:

$$\tau_{bn} = -2\rho\alpha^2(1-\alpha)\left|\vec{U}\right| I,$$

in which

$$\alpha = \frac{\sqrt{g}}{\kappa C} < \frac{1}{2},$$

where:

κ: Von Kármán constant.
C: Chézy roughness [$m^{1/2}/s$].

Secondary flow effect on the depth-averaged flow is considered by extending the depth-averaged shallow water equations with additional terms in the momentum equations to account for the horizontal effective shear-stresses thus originated.

For sediment transport and morphology modules bedload for non-cohesive sediments were selected adopting the schematization "bedload" such that suspended load is neglected and the advection-diffusion equation for suspended not solved. The total transport corresponds then to the bedload component.

Computation of bedload is made by two steps. Firstly, the magnitude and direction of the bedload transport at the cell centre is computed based on the selected sediment transport formula. Secondly, the transport rates at the cell interfaces are evaluated corrected for bed-slope effect and upwind bed composition and sediment availability.

Some sediment transport formulae (such as the ones that was selected in this research) do not prescribe transport direction (only its magnitude) thus the latter is assumed to be equal to the depth-averaged flow direction next to the riverbed. But when effect of secondary flow is considered in the computation, the sediment transport direction φ_τ is deviated and it can be evaluated by:

$$tan(\varphi_\tau) = \frac{v - \alpha_I \frac{u}{U} I}{u + \alpha_I \frac{v}{U} I},$$

in which,

$$\alpha_I = \frac{2}{\kappa^2} E_s \left(1 - \frac{\sqrt{g}}{\kappa C}\right),$$

where:

E_s: coefficient to be specified by the user as *Espir* keyword in the morphology input file.

The bed level changes in each grid cell are computed by means of an input-output sediment transport mass balance at the control volume of each cell. At each computational time step the bed level of the single grid cell is therefore updated based on the mass balance.

The model was then integrated with the introduction of fixed layer in areas that were expected to not erode (i.e., defences works or longitudinal training walls). These layers are modelled to pose a halt to the sediment entrainment of areas with reduce sediment availability. Once a certain level of erosion in the computational cell is reached, no more sediment can be eroded from the cell. This is done by imposing a limited sediment thickness on cells. The bedload formulation compares this sediment layer availability with a user-defined threshold value and reduces the transport magnitude based on:

$$S_b'' = f_{FIXFAC} \cdot S_b'',$$

where:

S_b'': mass bedload transport rate [kg/(ms)].

f_{FIXFAC}: upwind fixed layer proximity factor: $f_{FIXFAC} = \frac{DPSED}{THRESH}$ limited to the range:

$0 \leq f_{FIXFAC} \leq 1$.

DPSED: depth of sediment available at the bed.

THRESH: user-defined erosion threshold.

Bedload transport at open boundaries can be prescribed as bedload transport rates (in case the model input is known) or as free or fixed bed level development for which the effective bedload transport rates can derived from the mass balance at the open boundary points. Sediment load entering through the boundaries will be thus near-perfectly adapted to the local flow conditions and very little accretion or erosion should be experienced near the model boundaries. Furthermore, sediment transport is affected by bed slopes (longitudinal and transverse bed slopes). If longitudinal bed slopes can affect the magnitude of the sediment transport by

$$\vec{S}''_b = \alpha_s \cdot \vec{S}''_b,$$

the transverse bed slope entails even a change of sediment transport direction. Several formulations are available in Delft3D-FlOW to consider this effect. For this case study the Koch and Flokstra (1980) formulation extended by Talmon et al. (1995) was selected. It gives α_s as:

$$\alpha_s = 1 - \alpha_{bs} \cdot \frac{\partial z}{\partial s},$$

where α_{bs} is a user-defined tuning parameter (default=1.0) and the bedload transport direction is modified as:

$$tan(\varphi_s) = \frac{\sin(\varphi_\tau) + \frac{1}{f(\theta)}\frac{\partial z_b}{\partial y}}{\cos(\varphi_\tau) + \frac{1}{f(\theta)}\frac{\partial z_b}{\partial x}},$$

in which φ_τ and φ_s are the original and final direction of sediment transport and $f(\theta)$ is equals to:

$$f(\theta) = A_{sh}\vartheta_i{}^{B_{sh}} \cdot \left(\frac{D_i}{H}\right)^{C_{sh}} \cdot \left(\frac{D_i}{D_m}\right)^{D_{sh}},$$

where:

$\frac{\partial z_b}{\partial x}$ and $\frac{\partial z_b}{\partial y}$: bed slope in the x and y-direction, respectively.

A_{sh}, B_{sh}, C_{sh} and D_{sh}: tuning coefficients to be specified in the morphology input file.

As it will be described in section 3.2., the sediment transport formulas selected in this case study are the Engelund-Hansen (1967), structured as a power law of the flow velocity, and the General formula. The latter was adopted to generate a sediment transport formula structured as the Engelund-Hansen one but characterized by a lower degree of nonlinearity in the dependence of sediment transport on the flow velocity for reasons that will be describe later.

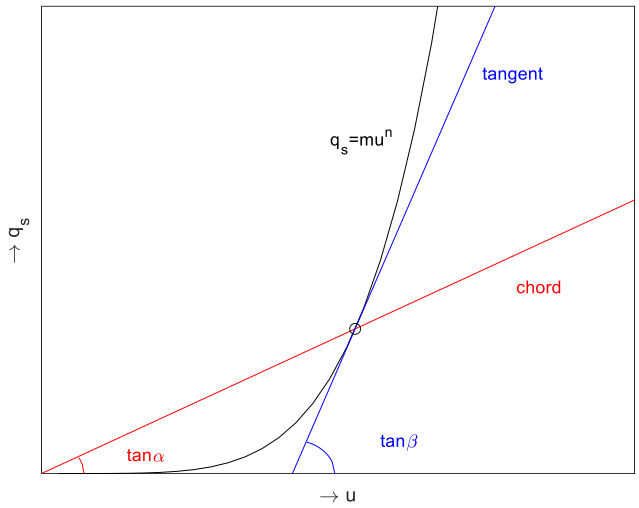

Figure 23. Graphical representation of the degree of nonlinearity in sediment transport predictor (adapted form material provided by *Deltares*).

Assuming bedload transport q_s depending on flow velocity u through the generic power law $q_s = m \cdot u^n$, the degree of nonlinearity of sediment transport b is defined as

$$b = \frac{\tan\beta}{\tan\alpha} = \frac{dq_s/du}{q_s/u} = \frac{u}{q_s} \cdot \frac{dq_s}{du} \quad \rightarrow \quad b = \frac{u}{m \cdot u^n} \cdot m \cdot n \cdot u^{n-1} = n.$$

The Engelud-Hansen formula is given by:

$$S = S_b + S_{s,eq} = \frac{0.05\alpha q^5}{\sqrt{g}C^3\Delta^2 D_{50}},$$

where:

S_b: bedload transport [kg/(ms)].

q: magnitude of flow velocity [m/s].

Δ: the relative density $(\rho_s - \rho_w)/\rho_w$.

D_{50}: median diameter of sediment [m].

α: calibration coefficient $\big(O(1)\big)$.

Two calibration coefficients must be specified in the sediment transport input file, namely α and the roughness height r_k (dummy parameter).

The General formula is based on Meyer-Peter-Muller formula's structure with coefficients and power that can be adjusted to fit specific requirements (α, b, c, μ, θ_{cr}).

$$S = \alpha D_{50}\sqrt{\Delta g D_{50}} \cdot \theta^b (\mu\vartheta - \xi\theta_{cr})^c,$$

in which,

$$\theta = \left(\frac{q}{C}\right)^2 \cdot \frac{1}{\Delta D_{50}},$$

where:

α: calibration coefficient.
b and c: powers.
μ: ripple factor or efficiency factor.
θ_{cr}: critical Shields' mobility parameter.
ξ: hiding and exposure factor for the sediment fraction considered.

2.3.2 Linear Bar Theories

Apart from numerical models, analytical solutions can be useful as a rapid and preliminary method for the assessment of specific conditions. These include the Linear Bar theories.

These theories are based on a fundamental assumption, the linearization. Linearization consists of defining a specific flow condition made up of a constant mean value (basic state) and a deviation term (perturbation), the latter assumed to be much smaller that the former one. Furthermore, it is assumed that the perturbation term is represented by a set of harmonic functions, of which the one with the fastest growth rate emerges as the dominant initial bar pattern, based on Fourier's theorem (Crosato & Mosselman, 2020). The resulting system of equations flourished in the so-called "Delft approach that analyses the development of periodic steady bars in channels forced by hybrid bars (Struiksma et al., 1985). The system of equations describes the longitudinal profile of the near-bank deviations of flow velocity and bed topography from the normal flow conditions induced by an upstream perturbation - i.e., channel bend, width restriction or expansion, etc. - (Crosato & Mosselman, 2009). The resulting bed shapes are characteristic of the so-called equilibrium bed topography.

Starting from the steady state 2-D depth-averaged continuity and momentum equations and the equations for sediment transport and assuming a transverse periodic shape for the perturbations of flow velocity and flow depth yields to the equations reported below (first-order relaxation equations):

$$\frac{\partial U}{\partial s} + \frac{U}{\lambda_W} = \left(\frac{1}{2\lambda_W}\frac{u_0}{h_0}\right) H,$$

$$\frac{\partial H}{\partial s} + \frac{H}{\lambda_S} = \frac{h_0}{u_0}(b-1)\frac{\partial U}{\partial s}.$$

where:

λ_W: streamwise adaptation length for perturbations in the transverse profile of depth-average streamwise flow velocity.

λ_S: streamwise adaptation length for perturbations in the cross-sectional riverbed profile.

B: degree of nonlinearity of sediment transport on the flow velocity.

The adaptation length λ_W, given by:

$$\lambda_W = \frac{h_0}{2 \cdot C_f} = \frac{C^2 \cdot h_0}{2g},$$

in which

C_f: friction factor defined by $2C_f = \frac{g}{C^2}$.

characterizes the longitudinal distance needed for the decay of perturbations in the transverse distribution of streamwise flow velocity due to an upstream disturbance. The longitudinal profile of the perturbation follows this exponential decay law:

$$u'(x) = \hat{u} \cdot exp\left(-\frac{x}{\lambda_W}\right).$$

The upstream perturbation is dampened by about 36% at a distance from the source of perturbation $x = \lambda_W$ and it is considered completely dampened when reaches the 0.05% at a distance $x = 3\lambda_W$.

Chapter 3

Methodology

3.1 Twinning case: The Room-for-the-River approach and the Po River Renaturation Project

As previously stated, the work that follows is a direct consequence of the European MERLIN project's twinning activities. In fact, this research also tries to encourage and promote the increasing dialogue and knowledge-sharing about river restoration in Europe, specifically between the largest Dutch and Italian River Systems. A summary of the Room for the River approach that has been applied along the Rhine Branches was given in Section 2.1.4, its key principle being "more space for conveyance". With a view to twinning efforts, the suitability of a "Room-for-the-River" strategy for the restoration of the Po River was first questioned. Indeed, as outlined in sections 2.1.4 and 2.2, the Rhine Branches and the Po River are two relatively significant entities on an environmental and economic level that share attributes and issues, such as, for instance, signs of river alterations and functional disequilibrium. Based on these analogies, an attempt was undertaken to examine the applicability of interventions' philosophy implemented on the Rhine Branches to the Po River restoration.

Initially, the following point was outlined in order to answer the question whether the room-for-the-river approach was practicable along the Po River: a comparison of the two river systems is needed, taking into account rivers' characteristics such as hydrological regimes, basin extension, environmental, morphological features etc. However, as the study went on, it became clear that this method was not only unproductive but also probably misguided, especially considering the expression of placeless universalism provided by Fryirs & Brierly (2009). Since river restoration should focus on ecosystem integrity, that depends on how the river behaves and responds rather than how it appears, the authors refer to the place-based guiding image concept as the reference conditions that gives a guidance rather than a template. The latter must be defined in terms of representativeness (diversity), range of behaviour (dynamic), and evolutionary trajectory based on field-based insights into naturalness (Fryirs & Brierly, 2009). Because of this, any comparison for the implementation of analogous restoration measures to river systems that are similar but nonetheless different because of their uniqueness would need a comprehensive, multidisciplinary cognitive analysis. This is needed to avoid employing copy-and-paste solutions. The way in which the Room-for-the-River program's proposals were developed and finally chosen serves as confirmation of this. As was already described, a team of interdisciplinary experts (Q-team) supervised and examined the working process with the goal of ensuring that the spatial quality of

the environment following interventions was attained through the accomplishment of design quality. To that end, sets of quality standards that served as evaluation criteria for the proposed interventions were chosen. These were formulated starting form Vitruvius's key criteria of a good design quality, namely *utilitas* (functionality), *firmitas* (solidity) and *venustas* (beauty or attractiveness) and translated into hydraulic effectiveness, ecological robustness and cultural meaning and aesthetics (Klijn et al., 2013). Only when proposed interventions met those criteria, they were ensured to be suited for the individual existing environment while maintaining its traits and diversities at different spatial scale levels and avoiding falling into the previously mentioned placeless universalism.

Now, such an approach is not practicable in this study considering the significant expertise and time necessary, and it is, at the very least, incompatible with the central objective of this research. It follows that any suggestions made in this study on the potential application of the room for the river measures in the Italian context would be quite fragile and out of place as such a method of river restoration requires a high degree of interdisciplinary understanding.

Consequently, river restoration projects along the Rhine Branches have not been studied aiming at assessing the feasibility of room-for-the-river measures along the Po River. Instead, the main emphasis has been on whether and how the methodology and philosophy of the room for the river approach can be applied to the Po Renaturation Project. After gaining a comprehensive understanding of the changes and alterations that both fluvial systems have experienced in past years and recognizing the current criticalities, further attention was given to Room-for-the-River interventions and relative achievements (paragraph 3.1.1.). Understanding the main reasons that influenced the design of the interventions and taking a close look at the outcomes helps in better appreciate the approach's philosophy and allows to consider if the same methodology might be applied as it is to the Po River. To that scope, a part of the research consisted of field visits to both river systems. In particular, the perspective of the Po River was restricted to the Isola Serafini meander site since it was chosen as a case study for this research. Additionally, it is believed that, given that the study's methodology also entails creating a 2D hydro-morphological model of the Isola Serafini meander, sufficient understanding of the river can be attained to draw up qualitative recommendations for river restoration using "more space for the river" as a guiding principle. Lastly, some considerations were made upon the typologies of interventions planned within the Po Renaturation Project, the measurements and monitoring processes and the participatory one.

Given what has been discussed, it is less acceptable to make assertions like "the Rhine and the Po River Systems are fundamentally different and not comparable." Rather than just copying and pasting what has been done along the Rhine Branches, the objective is here to identify key principles that may be elaborated and applied to the Po River case.

3.1.1 Field visits along the Rhine Branches

During the time of this research field visits to both fluvial systems were conducted. In this regard, a special occasion was the "Field visit Room for the Rhine Branches" organized by *Rijkwaterstaat* and *Deltares* within the context of the MERLIN project. During the MERLIN's field visit it was possible to appreciate the results obtained along the Rhine Branches by recent implementation of Room for the River approach explained in paragraph 2.1.4. and by previous restoration projects.

Figure 24. Locations visited along the Rhine Branches. 1: Biesbosh and Noordwaard; 2: Munnikenland; 3: Buiten Ooij; 4: Afferdensche and Deestsche Waarden; 5: Nijmegen.

Biesbosh and Noordwaard:dike relocation and de-poldering

National Park De Bisbosch and the Nordwaard floodplain extends on a freshwater tidal area enclosed between the North Sea and the Maas and Rhine Rivers. Between the 19th and 20th centuries, reclamation works took place and two new stretches of river were dug aiming at protecting the entire area from flooding, namely the Nieuwe Merwede and the Bergsche Maas (Figure 25). This promoted the increase in number of polders and consequently lowered the flood attenuation capacity of the area (inducing higher flood water levels along the upstream river course) and degraded the natural environment.

By giving the river more space for conveyance, a reduction of the flood water levels along the upstream stretch of the Rhine was achieved and consequently an increase of the flood safety. Meanwhile this ensured the periodic inundation of the floodplain, contributing to nature development. The key aspect of this intervention is that not only farmers can still partially cultivate or farming in the high-water flood areas, rather they can remain in polders even during high flood waters (as demonstrated during the flood event occurred the 10th February 2020). This intervention contributed to the recovery of 477 ha of floodplain area and locally lowered the flood water levels of 27 cm (Klijn et al., 2013).

For that reason, de-poldering of the Noordwaard floodplain was selected to be part of the Room-for-the-River program. The measure consisted in partially digging the main dikes and lowering the heights of the ring of dikes enclosing the area. Moreover, part of the agricultural lands was given back to nature whereas the remaining farms were adapted or relocated on existing or newly constructed dwelling mounds.

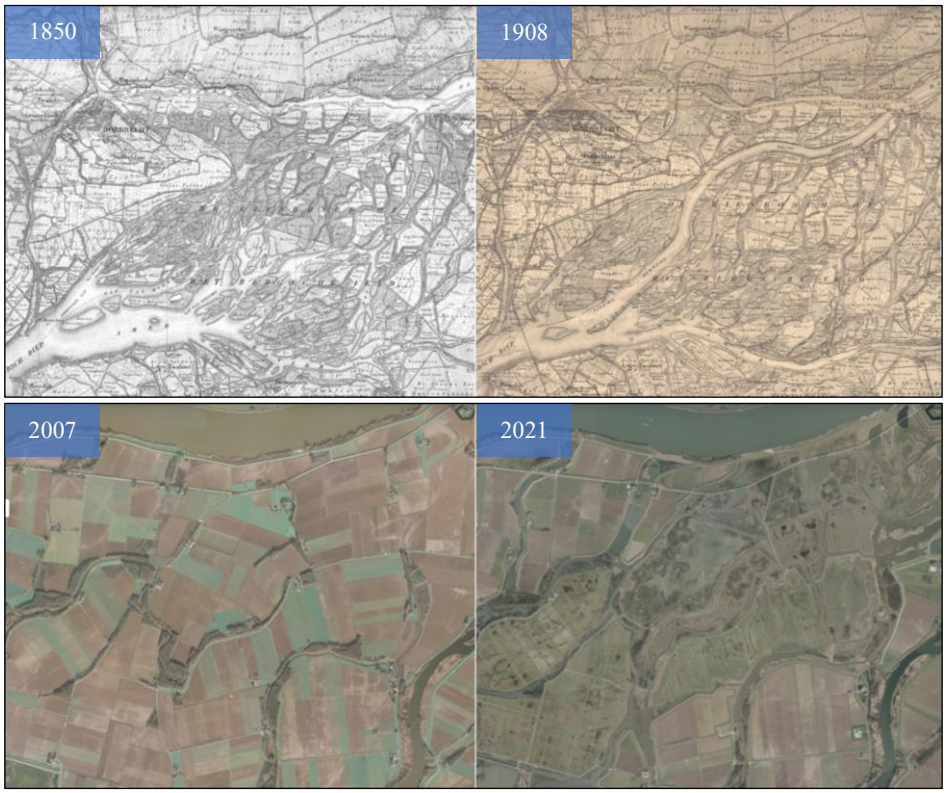

Figure 25. Top: Historical maps of the Biesbosh area. To the left: map of 1850; To the right: map of 1908 after the digging of the Nieuwe Merwede and the Bergsche Mass Rivers; Bottom: Satellite images of the Noordwaard floodplain before (2007, to the left) and after (2021, to the right) room-for-the-river measures. Great portions of polder area were given back to nature by dismission or integration of agricultural fields with river dynamics. In this case the lowering of the main dike visible in the upper part of the maps guarantees lower water levels along the Rhine and development of nature within the floodplain (source: https://www.topotijdreis.nl).

Figure 26. Top left: Aerial photo of flooded Noordwaard floodplain during peak event of the 10th February 2020 (source: https://rijkswaterstaat.nl); Top right: Grazing in the area devoted to nature within the Noordwaard floodplain captured during the field visit; Bottom: photo shot during the field visit from the pumping station showing the integration of agricultural fields with nature areas (source: photos during the field visit shared by Martinengo, M., and Piovani, P.).

Munnikenland: dike relocation and floodplain lowering

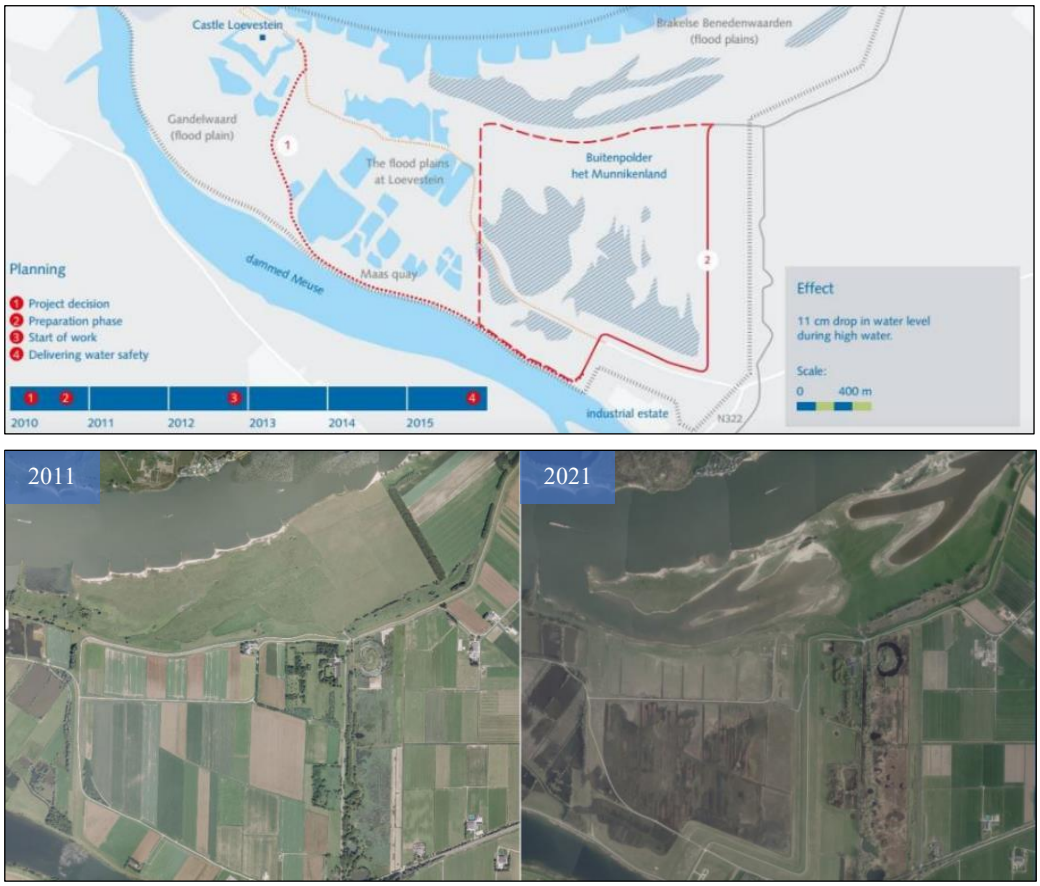

Figure 27. Top: Infographic of the intervention. The dashed red line shows the old dike line that has been dismissed and relocated along the continuous red line determining a great increase of the floodplain area. The dotted red line tracks the heightened access road to Castle Loevestein that can be travelled even when certain high water levels occur (source: Infographics English 2015 by ruimtevoorderivier Stack - Issuu); Bottom: Comparison of two satellite images (2011 and 2021) of the area (source: https://rijkswaterstaat.nl).

A similar approach was implemented at Buitenpolder Munnikenland in which a combined action of floodplain excavation and relocation of main dike permitted the Wall River to reclaim a wide natural expansion area. The enlarged floodplain is then flowed by side channels that, when high discharges come, make the water pass through old agriculture fields converted now in natural areas. The growth of vegetation is controlled by a management strategy that limits plants' heights to excessively increase the hydraulic roughness of the floodplain that could lead to higher water levels. This management is mainly constituted by grazing activities. The added floodplain area accounts for 142 hectares and the hydraulic efficiency of the intervention reached 11 cm (Klijn et al., 2013).

Finally, the newly built dike is intended to serve more than one purpose. At its top, a bike route connects the floodplain region with the historical site of Castle Loevestein, guaranteeing that the area is accessible for leisure purposes.

Figure 28. On the left: Grazing activity taking place during the field visit within the floodplain, next to the navigation channel; On the right: view of the Buitenpolder Munnikenland from the newly constructed dike that serves as a pedestrian and cycle path.

Buiten Ooij: storage area

Since the beginning of the 20th century, one of the flood defence strategies adopted along the Rhine Branches was the use of overflow areas. These were built backward of the main dikes, at lower level with respect of the adjacent zones and connected to the river by a section of dike reduced in height. All these types of structures were abandoned due to the rising demand for land and the understanding of the detrimental impact on flood safety caused by ice jamming, namely due to the slowing of the current downstream of these overflow regions (Silva et al., 2001). Overflow areas were located especially along the Waal, also next to the Ooijpolder where nowadays stands the temporal inundated floodplain of Buiten Ooij.

Figure 29. On the left: schematization of the Buiten Ooij floodplain showing the three ways of water entering the storage area depending on the discharge flowing along the Waal. Main dikes (winter dikes) are highlighted by the red line whereas summer dikes are coloured in yellow; Top right: the sluice positioned at the downstream end of the floodplain area (corresponding to the lowest arrow of figure on the left), (source: from Kurstjens et al. (2020)) ; Bottom right: Photo of the floodway shot by the middle overflow dike looking downstream (source: photos shot during the field visit shared by Martinengo, M., and Piovani, P.).

A temporal inundated floodplain is defined as "*the zone of the floodplain that is inundated almost yearly during late winter and early spring floods (supplemented with local rain or groundwater), which physical and chemical conditions result in a characteristic community of faunal species with adapted life strategies*" (Kurstjens et al., 2020). The Buiten Ooij area accounts for a total of approximately 80 ha of lowered floodplain. The main connection between the Waal and the floodplain area is composed by a floodway and a sluice (the lower arrow on the left of Figure 29) that is maintained open during high flows and then closed during summer, to hold back water in the floodplain. Two other stretches of summer dikes are defining the area of possible overflow. The floodplain served as a pilot field study aiming at understanding which areas of the Rhine's fluvial system could have more chances to redevelop temporal inundated floodplain mechanisms. Results of the study concerning the determining conditions necessary for the ecological functioning of these types of areas are shown by Kurstjens et al. (2020).

Afferdensche and Deestsche Waarden: floodplain lowering and side channel excavation

Flood safety requirements were the main reasons for which also the floodplain at Afferdenche and Deetsche Waarden was restored. This project is composed by a set of combined measures aiming at turning a partially inactive floodplain to a natural and recreational area. The objective was achieved by excavating a main side channel passing through the floodplain, lowering dikes and the floodplain's ground levels.

Figure 30. Satellite image of the floodplain at Afferdenche and Deetsche Waarden showing the connection of the floodplain area with the main channel through a series of side channels and areas reduced in height.

The development of a side channel significantly affects the flow conditions, which in turn impact morphological and sediment transport processes. Repetitive dredging is required to maintain appropriate low bed level in the floodplain and sufficient water depth in the main channel to not hinder navigation. Indeed, sedimentation is expected to occur both on the main channel and in the floodplain.

From an ecological perspective, the side channel should be left unrestricted so that it can meander and migrate laterally, promoting the processes of erosion and deposition. However, this lateral movement must be controlled and kept to a minimum, especially considering the risks it may pose to the stability of the main embankments. A brick factory that had been located on the banks of the main channel had to be removed as part of the project in order to make more room for nature

(converted into grass and rough terrain). Additionally, a particular vegetation management method was chosen for this location that still involves grazing.

Figure 31. Top: Photo internal to the floodplain; Bottom left: Photo showing a side channel internal to the floodplain (source: source: photos shot during the field visit shared by Martinengo, M., and Piovani, P.); Bottom right: Aerial photo of high-water levels condition before room for the river measures (source: Rijkswaterstaat (1999)).

Nijmegen: floodway excavation

The city of Nijmegen is positioned on the hydraulic left of the Waal River where the course forms a sharp bends. The city has always been threatened by flooding of the Waal River and more recently, in reason of the bottleneck formed thereby by the urban areas of Nijmegen and the adjacent village of Lent. When the new approach of giving more space to the river as an innovative flood risk management arise, the Nijmegen bottleneck was immediately considered as a possible intervention to be implemented.

The intervention consisted in the excavation of a floodway on the inner bend of the river in an area previously devoted to urban setting that guarantees the lowering of high flood water levels. This called for several additional steps to be taken. The side channel was mostly created in an area where a housing project had been approved and there were already standing structures. Therefore, not only relocations or removal took place, but a modification of the urban planning became necessary. The dikes were set back of approximately 350 m and new dikes constructed on the newly formed and inhabited island. New bridges were designed to connect the island with the inland.

Figure 32. Top: Cartographic maps of the area of intervention before and after the creation of the floodway (source: https://www.topotijdreis.nl); Bottom: Aerial photos before and after the room for the river measure (online sources).

As a result of these interventions the narrow river section was widened, the Waal gained more space for conveyance and consequently high-water levels were reduced, resulting in a high hydraulic efficiency (up to 34 cm according to Klijn et al. (2013)). Moreover, the entire project area was planned to be an urban park where to develop nature and recreational activities (boulevard, festival ground, event terrain, rowing course etc.), strongly improving the spatial quality of the site.

But the ability to find a win-win solution between river management and policy makers was the actual added value of Nijmegen's room for the river project. While the area's hydraulic safety improved, the municipality of Nijmegen was able to seize the opportunity for creating new development plans to the north of the city, particularly because the municipality's new bridge requirement was included in the project.

3.1.2 Field visit on the Po River

The filed visit at Isola Serafini held at the beginning of July 2022 during the severe drought that characterized all the summer period. The primary goal of the visit was to gain a visual impression of the study area to better understand the main issues that were revealed by the conducted literature review. In order to make a comparison with what was observed during the field visits along the Rhine Branches, attention was also paid to the layout of the riparian and floodplain zones. Short time available and the wide presence of private properties limited the surveying area. Hence, some of the photos reported below are integrated from material provided by ADBPO (2005a).

During the field visit water levels were extremely low as testified by locals who guided within the river area. The ADBPO's bulletin of 11 July, 2022 (Osservatorio Permanente) reported an observed discharge of 163 and 240 m^3/s on the day of the field visit for the Piacenza and Cremona hydrometric stations, respectively. This implies that the power station was switched off during the visit, as it was, and that a minimum discharge was conveyed on the tailrace (Figure A-2 in Appendix A) while at least 100 m^3/s were flowing along the meander (as required with the MVF). This is the discharge that occurs on average about 250 days per year (see Figure 56) considering the operation rule of the barrage, meaning that these are the ordinary water levels reached in the mender loop for most of the year.

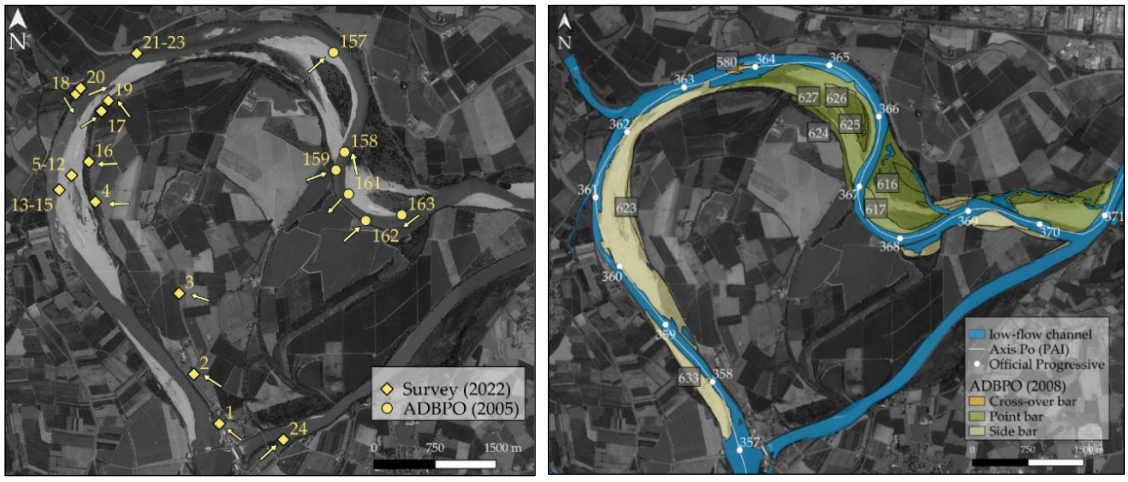

Figure 33. On the left: Location of all photos shot during the field visit and those integrated from ADBPO's material (2005). More detail of locations of pictures in Figure A-1 in Appendix A; On the right: Bar classification made by ADBPO (2008b). Labelling of bars derives form elaboration of GIS features provided by ADBPO and it has the only purpose of facilitating the reading of the report), (sources: GIS features provided by ADBPO and base map by Google).

Bar categorization produced by ADBPO (2008b) is reported in Figure 33 with labels solely relative to the most significant bars considered in the present study. Immediately downstream of the barrage, a side bar (633) emerges on the hydraulic left and extends for approximately two kilometres up to official progressive 359, around the zone of flow crossover between bar 633 and bar 623. It's a bare bar with areas of pioneer vegetation growing on fine sand, and no permanent vegetation appears to be sprouting. According to ADBPO (2005a), the submerged discharge of the bar is 3,000 m^3/s, and its evolutionary tendency appears to be regulated by the barrage's operational rules, which resulted in the increasing deposition of sediments on its surface.

Figure 34. Photo n°1: View of bar 633 in the downstream direction.

During the flood event of 2000, a local scour of the bank in the hydraulic right opposite to the bar occurred, necessitating urgent action with sandbags to stabilize it (Figure 35). It should be noted that the right bank line is inclined of about 25° with respect of the inflow direction from the barrage and, additionally, bar 633 could be responsible for a further concentration of the flow in the outer bend, increasing the hydraulic pressure against bank defence.

Figure 35. To the left: Photo of people working for guaranteeing the stability of the bank (source: extracted from Master of Science Thesis "Analisi idrodinamica bidimensionale dell'evento di piena dell'Ottobre 2000 sul Fiume Po in corrispondenza di Isola Searafini" – Marsiglia, L.); To the right: Schematization showing the inclination of the outflow of the barrage relative to the direction of the right bank line.

In the years between 1978 and 1991 stretches of defence works were built between official progressive 358 and the Adda River mouth on both banks of the river (purple lines in Figure 36). Of the entire erosion area (orange area) that ranged between progressive 359 and 361 less than half (red area) is nowadays left free to erode (bank erosion is depicted on top of Figure A-4 in Appendix A). These measures may be required to safeguard both the Castelnuovo Bocca d'Adda urban area (positioned west of the area) and the main embankments from the direct impact of hydrodynamic pressures. By doing so, the river lost a large part of its incised channel that is currently largely used for agricultural fields and poplar groves. Furthermore, the riparian vegetation is restricted to a few meters wide discontinuous bend (Figure A-4 in Appendix A).

The construction of the longitudinal wall located on the hydraulic right just upstream of official progressive 359 (Figure 36), on the other hand, contributed to the formation of an overleaf depositional area that established a eutrophic standing water habitat (Habitat 3150-Natura 2000) and promoted the growth of riparian forest with poplars and willows (Habitat 9A20-Natura 2000).

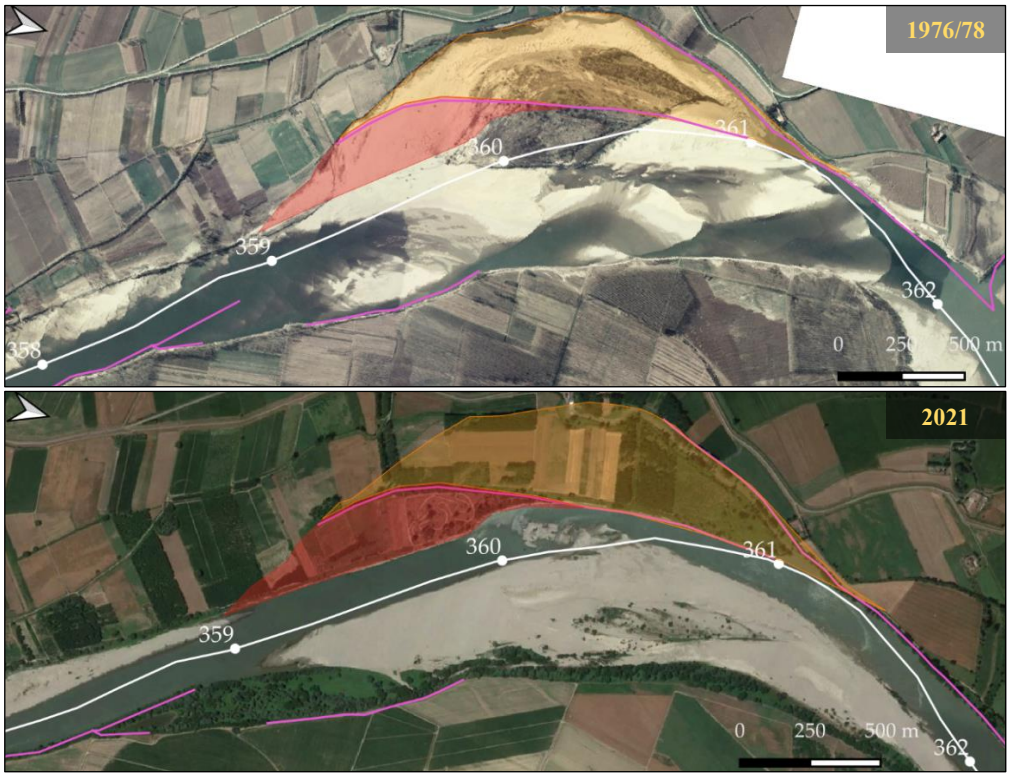

Figure 36. Segment of the meander between progressives 359 and 361 was characterized by wider channel sections associated to an erosional left bank and a more complex and heterogeneous morphology (image on top). Bank defences (pink lines) were still not built. After bank defences' construction, the low flow channel was straightened, and parts of the channel (yellow and orange area) were presumably nourished. Nowadays (image on bottom), the yellow area is completely disconnected from the river dynamics (being completely protected by bank defences while the orange area is facing bank erosion at the downstream end (source: GIS features from ADBPO and base maps from Geoportal Emilia-Romagna).

The apex of the deposition area generated by the longitudinal wall coincides with the beginning of side bar 623. It is divided from the latter by a relatively narrow deep band which continues within the bar, generating a side channel and widening moving downstream, which separates the highest part of the bar from the right bank. The side channel is clearly distinguishable within the bar because of a steep swale that delimits the two parts of the bar at different bed elevation, generating a topography like a scroll bar. It was not possible to get information on the origins of the side channel, but orthophotos show that it was formed prior to the construction of the hydropower plant in 1955 (Figure 13). The flow over the meander was substantially reduced when the barrage was built, resulting in large portions of bedforms emerging from the water surface due to the lowering of ordinary water levels (orthophoto of 1970 of Figure 13). Sand mining and sediment mobilization are likely to have occurred during the construction of defensive works (the locals reported that mobilization of sediments was carried out regularly in past time as river management activity). As a result, the actual layout of bedforms might emerge from a mix of natural and anthropic activities above which effects of sediment transport alteration and regressive erosion induced by the operational rules and the meander cut-off (1951) respectively, have been overlapping.

Figure 37. Top: Photo n°5 showing bar 623 in the upstream direction. The side channel internal to bar is visible on the left divided from the low-flow channel in the right by the highest and vegetated part of the bar; Centre: Photo n°10 shot above the ridge highlighting the elevation gap between the two parts of the bar; Bottom: Photo n°6 showing the downstream segment of bar 623.

At the time of the field visit the side channel was dry with a bare soil, except for a small segment at its inlet with some vegetation growing. By contrary more advanced successional species can be found on the ridge of the swale as well as in the centre of the channel further downstream where a belt of post pioneer species grows (Figure 38). This vegetation growth enhances sediment retention and therefore the local rising of bed elevation, potentially leading to morphological inactivity of this part of the channel. Elevated and vegetated portions of the channel, however, enhance trapping of woody material, contributing to habitats development, organic matter supply and defining the environmental gradient within the incised channel.

Figure 38. Top: Photo n°7 revealing high vegetation growing in a central position downstream of bar 623, next to the low-flow channel; Centre: Photo n°11 shot above the ridge, in the upstream direction, and showing the local vegetation patterns ; Bottom: Photo n°12, analogous to photo n°11 but shot in the downstream direction, revealing the presence of large woody debris deposited within the elevated area of the bar.

As described in paragraph 2.2.4, the excessive extension of bars with respect of the wet channel is one of the hydro-morphological alterations along the meander. Indeed, apart from the lowered water stages induced by the hydropower station's regulation, topographic surveys and digital terrain models available show cross sectional profiles of the channel characterized by a narrowed and deep low-flow area and a relatively elevated part of the channel that seems to be disconnected form the ordinary regulated flow dynamics (Figure 39). This elevation gap determines a certain degree of lateral discontinuity internal to the incised channel, consequently a reduction of fluxes transversal to the main flow and therefore a lowering of the floodplain-main channel dynamics interaction. According to what expressed in paragraph 2.1, the desired degree of connectivity should be determined through ecosystem-based approach that linked hydrodynamic conditions with vegetational and fauna survival ones (see Geerling et al., 2006). From a hydraulic point of view this translate into the assessment of inundation maps that define the frequency of flooding of

floodplains and into the computation of related flow depths and velocity and shear stresses. For this analysis to be accurate, a real 2D topographical reference of the channel is necessary, but this was not currently available. For that reason, the present study concentrated only on the assessment of how the topography could be influenced in its morphological development.

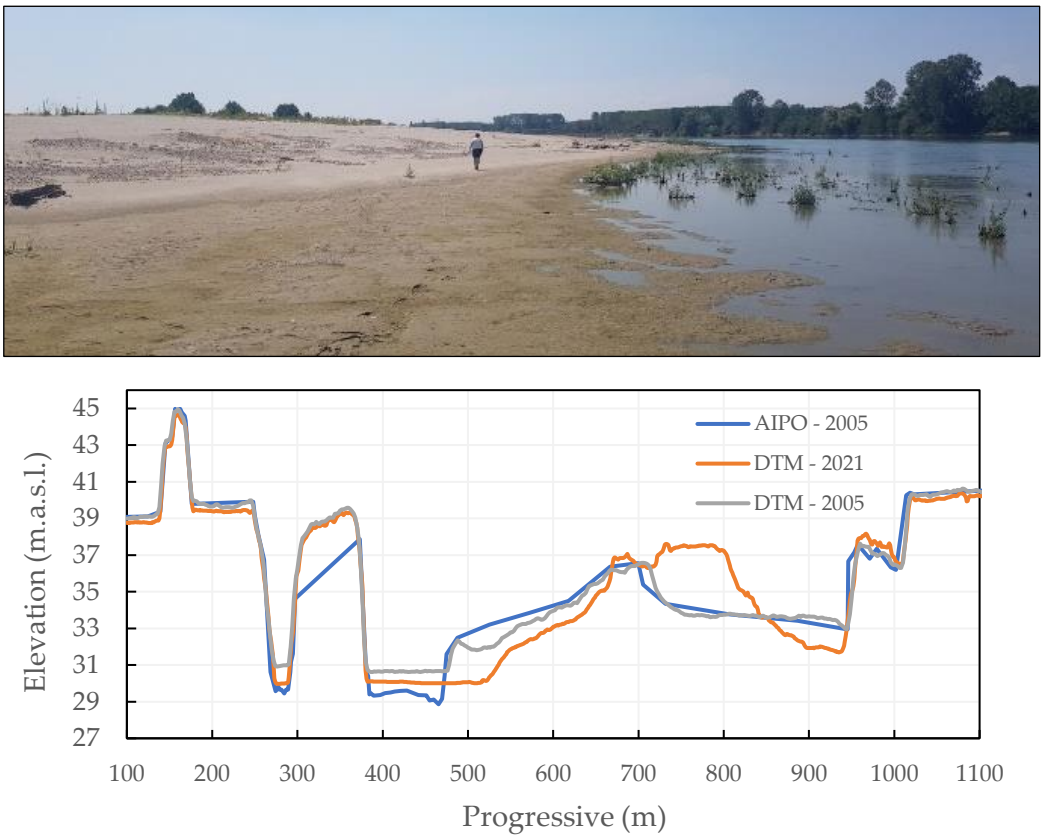

Figure 39. Top: Photo n°8 depicting bar 623 in the upstream direction. It is possible to appreciate the existing elevation gap between the low-flow channel and bar surface; Bottom: comparison of cross section S24C as depicted by the topographic survey AIPO-2005, the DTM-2005 and the DTM-2021 (ADBPO).

Vegetation's colonization of bare bars has been especially taking place between official progressives 363 and 369 (Figure 40). This segment is characterized by a meander train of two meander bends imposed by training walls progressively built after the occurrence of the meander cut-off (1951). The river flows along its trained low-flow channel, occupying a relatively small portion of the entire incised channel and because of the deepening of the bed, the latter can convey even ordinary peak discharges. The first meander bend account for a bend length of around 3 km that encompasses a point bar (627) in which two other units can be identified (Figure 33), a side channel (ridge and swale topography) and a fluvial island (bar 626). The fluvial island (Habitat 3240/3270 - Natura 2000) appears to be morphologically stable especially because of the relative higher elevation and vegetation that has become established in time.

Figure 40. Top: Photo n°20 revealing forest vegetation along the right bank of the channel, upstream of bar 627; Photo n°158: lateral view of the fluvial island (provided by ADBPO).

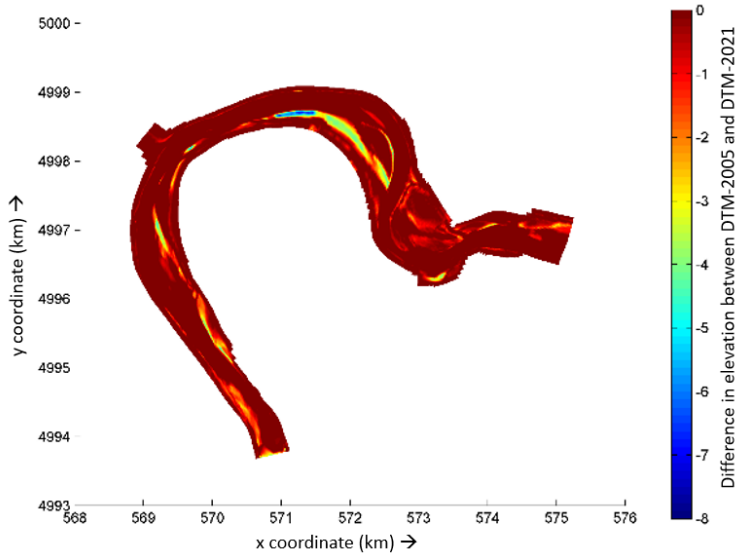

Figure 41. Graph generated with QUIKPLOT reporting the bed elevation reduction resulting from the difference between DTM-2005 and DTM-2021 provided by ADBPO. Both side channel internal to bar 623 and internal to bar 627 faced erosion. It must be specified, however, that the erosion occurred along the second side channel could be associated to excavations of sand connected to activities of the close quarry.

Side channels represent a key feature from an ecological point of view, providing areas of lower flow velocities and shear stresses, constituting sheltered zones for aquatic species, and contributing to the overall biodiversity of the fluvial system. These generally face aggradation, especially because of rooted vegetation growing on their bed and banks acting as a trap for sediments. The internal ridge of the side channel results to be highly vegetated by softwood forests (Figure 42) but the side channel experienced erosion between 2005 and 2021 (as shown by the difference in elevation between DTM-2005 and DTM-2021 of Figure 41). Insights on the evolutionary trend could be gained by mean of a 2D hydro-morphological model capable of properly simulate lateral flows, eventually integrating into the model the effect of vegetation on sediment transport.

Figure 42. On the left: Extract of the orthophoto image of 2003 with no vegetation on the bar surface except for the fluvial island; On the right: Satellite image of 2020, high vegetation growing in the area upstream of the fluvial island (sources: ADBPO and Google).

Because of the existence of bank defences, the left bank's retreat between the Adda River's mouth and official progressive 366 is halted. The same applies for the right bank between official progressives 367 and 368 (Figure A-6). Along the first stretch, bank defences are critical because they keep the main dike, which is largely located close to the incised bank (less than 200 m), from being directly exposed to the stream's hydrodynamic pressure. The deepening of the low-flow channel, which is leaning on the outside bends, might cause instability issues in the defence works, therefore ADBPO (2005b) is planning to modify the low-flow channel set-up by excavating the side channel internal to the point bar and nourishing the channel in the outer bend.

Figure 43. Top left: View of the Po River from the Adda River mouth on top (Photo n°20bis). The left bank is protected by defences. Above, photo n°22, shot from the left bank (the one cited above) in the upstream direction; Top right: Photo n°23, another viewpoint from which is clearly seen the current status of bank defences defending the steep bank; Bottom: Photo n°157, bank defences in 2005 (source: ADBPO).

River training has also particularly impacted the morphology of the meander. Starting from progressive 366 a series of three side-alternated longitudinal walls completely define the morphology of the course. Especially the first longitudinal wall determined the creation of a deposition area, nowadays classified as a point bar (bar 616). ADBPO (2022) is also planning to partially lower the height of the longitudinal training wall located in the left bank between progressives 366 and 367 (Figure 44). The overleaf deposition area (bars 616 and 617) constituting the point bar of the second meander bend is indeed highly vegetated except for the apical area of the point bar and for a side channel that from the head of the longitudinal training wall cuts the point bar in two vegetated halves. Between the bar and the left bank, a permanently submerged side channel exists. Because of the training wall's excessive height, the latter is predicted to receive water solely from downstream, even during peak flows, hence its contribution to sediment dynamics seems to be negligible.

Figure 44. Top: Photo n°159 showing the longitudinal training wall located between progressive 366 and 367; Centre: Photo n°162, depicting bar 6l7 and 617, namely the depositional area overleaf of the previous longitudinal training wall. This part of the river was in past time an active part of the incised channel (source: ADBPO); Bottom: A picture of the Po River shot from the section just downstream of the conjunction between the tailrace and the meander loop. It is possible to appreciate the extent of the point bar located on the hydraulic left at the conjunction mainly generated by the upstream longitudinal training wall (source: Google Earth).

Isola Serafini has traditionally been a thriving riverside entity. Inhabitants were settling here to practice a sustainable exploitation of river resources; foraging and agricultural production were prevalent, and fishing was frequently the only source of wealth. However, in the context of economic progress, depopulation occurred, and vacant lands were turned to extensive agricultural fields. These have been using river resources in an unsustainable manner and deprived the region of vast natural area.

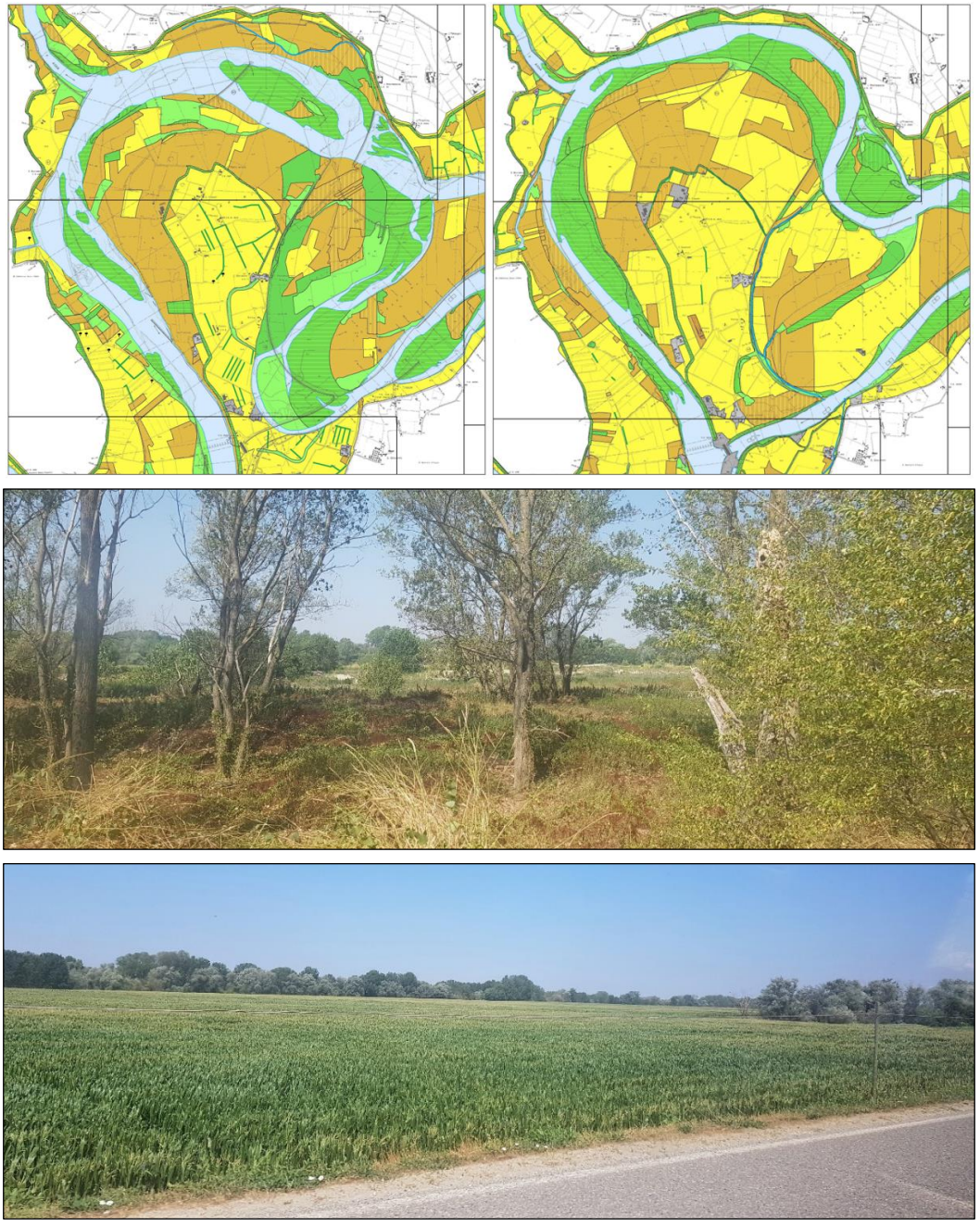

Figure 45. Floodplain Photo 4 and 3 Top: Comparison between 1954 Land use map of 1954 (on the left) ;2002 land use map (on the right). Yellow and orange areas indicate arable and agricultural lands whereas green areas refer to woodland and wetland areas. For a more detailed description of the map see ADBPO (2010); Centre: Photo n°4 showing a segment of the riparian belt separating the incised channel from agricultural fields; Bottom: Photo n°3 depicting one of the numerous intensive agricultural filed of Isola Serafini (largely, corn maize plants, as in this case).

But contextually to the economic development, depopulation process took place and dropped land were converted to extensive agriculture practices. Indeed, as the locals remark, the traditional willow and poplar forests that formerly characterized Isola Serafini are now a fading memory, while the many identities that cohabit are sometimes at odds with one another, resulting in an unbalanced landscape destitute of its own identity (as described in Isola dei tre ponti).

This can be seen by comparing the two land use maps depicted in Figure 45. The 1954 map displays Isola Serafini after the meander cut-off but prior to the erection of the hydropower plant. The abandoned course (i.e., the Dead Po) generated wide woodland areas (areas in green) with high environmental value, and while early traces of river training and expanding farmlands were discernible, the boundaries between the incised channel and surrounding floodplain were less defined. The current configuration shows an expansion of agricultural fields, particularly along the Dead Po area, and surviving natural river area is only internal to the incised channel. Moreover, some of theme, such as the area of bar 616, are disconnected from the river dynamics. The field visit supported the preceding; the riparian strips are nowadays restricted to thin, discontinuous bands of vegetation, whereas floodplain zones, external to the incised channel, are almost entirely dedicated to fields of intensive agriculture (Figure A-3 and Figure A-4).

3.2 Implementation of a 2D hydro-morphological model: Sound engineering checks

Modelling river morphodynamic in two-dimensional depth-averaged numerical models requires a comprehensive understanding of several key aspects, including the numerical and physical concepts that define the model, model artefacts, and experience with their application in real rivers (Mosselman & Le, 2016). A comparison with the modelling approach used in the Netherlands will be made through the text since hydro-morphological modelling approach implemented on Rhine Branches provides the fundamental knowledge for this case study.

It is important to emphasize the heuristic value of models applied to natural science. Since natural systems cannot be modelled using a limited number of independent parts they are, in fact, never closed. Thus, it is conceptually impossible for such models to be validated, verified, or calibrated when their goals are to replicate reality (Oreskes et al. 1994). In light of this, it is crucial to keep in mind that lack of data shouldn't prevent the development of a model because natural systems are dynamic, which restricts the validity of observations and measurements over time and exemplifies the inherent unpredictability of all models, even those built on massive data sets.

Models, however, can be effective tools for identifying data that need to be collected or directing further analysis to be done to close any knowledge gaps that may exist (Mosselman & Le, 2016), as well as for supporting hypotheses, evaluating discrepancies in other models, and performing sensitivity analyses (Oreskes et al. 1994). This research, for which data availability is limited, also

aim at improving general understanding of a complex, altered system like the one on Isola Serafini and offering valuable information for river management and restoration efforts.

Two-dimensional morphological models are developed by *Deltares* as tools for targeting sediment management strategies and investigating induced consequences by interventions and maintenance plans along the Rhine branches (Mosselman, 2009a). Model construction, calibration, and application are the three sequential steps that make up the general framework used at *Deltares* for 2D hydro-morphological models dealing with sediment management.

Construction. The computational grid is built with an appropriate resolution (grid cells dimension) based on the hydro-morphological features of interest. Generally, the computational grid inside the main channel has a higher resolution than the floodplain regions. The grid will then be projected on the available topographic feature to interpolate bathymetric data to allocate at each grid cell. Roughness values are assigned uniformly to the entire domain or discretized as space varying value through the adoption of bedform roughness predictors and vegetation models. Depending on data availability model calibration can be performed, for instance, by using two topographic references that describe the initial and final conditions of a period that have been well monitored in terms of liquid and solid flow.

Calibration. Calibration strategy is typically divided in:

i) Hydrodynamic calibration: tune the hydraulic roughness to achieve the lowest differences in water levels or flow rates between the simulated and the observed values. The discharge distribution at the bifurcation serves as another calibration criterion for the Rhine Branches.

ii) 1D morphodynamic calibration: define a sediment transport formula that properly reproduces cross sectional average values, such as annual sediment load and morphological characteristics of the river (i.e., bedforms celerity or annual bed level changes) and eventually calibrate the parameters of sediment transport predictor. It is crucial to have a comprehensive understanding of the sediment transport behaviour of the river, as well as sediment transport measurements to compare with the model results and topographic surveys repeated in time.

iii) 2D morpho-dynamic calibration: recreating the actual bar-pool patterns, the 2D behaviour of the river is finally investigated. To do this, one must calibrate the bed topography patterns (transverse slopes in bends and the position of crossing between two opposite bends), tune the bed slope effect (parametrized by A_{sh} and B_{sh} factors), obtain bed topography amplitudes (bar's height), and tune the helical flow effect due to curvature (parametrized by E_{spir}).

Application. 2D hydro-morphological models are commonly used to assess the local effects caused by groins or longitudinal dams, or to plan suitable dredging or nourishing programs. Two more issues are the interpretation of spiral flow in bends and the morphodynamic consequences of the construction of fixed layers along channel beds. Anyway, morphological modifications occur on a greater time scale than the hydrodynamic ones, but the computational time of morphological

models must be reasonable. In response to this, *Deltares* developed a simulation management tool that involves processing hydrological data. Based on statistical analysis for prolonged time series, the typical hydrograph is schematized into representative discharges. The time series is first transformed into a probability density function, after which it is converted into a cumulative density function and sorted into steps that are representative of the river under study's hydrograph. Quasi-steady simulations are thus run with water input made up of steady state discharges. This enables the application of the so-called morphological acceleration factor, which assumes that bed form velocity is significantly slower than stream velocity and that the morphological process can be sped up by applying a multiplication factor.

3.2.1 Creation of the model domain: computational grid and topography

The construction of the computational grid requires the determination of the domain extent and grid cell size.

Longitudinal domain extent

The barrage induces backwater effect that extends upstream for approximately 30 kilometres (Maselli et al., 2018). Thus, the first hypothesis for the domain extent was the one in the upper part of Figure 46, with inflow and outflow open boundaries located at the hydrometric stations of Piacenza and Cremona, respectively (the two orange dots in Figure 46). The barrage defines a hydraulic disconnection between upstream and downstream stretches and its section can be imposed as an inflow open boundary for a restricted domain that includes valley sections only. Sediment rates entering the inflow open boundary are largely attributed to sediment balance mechanisms that shape the longitudinal river profile and for which a 1D approach appears to be preferable (Deltares, 2022, personal communication). A hybrid 1D-2D approach could have been adopted to model the course upstream and downstream of the barrage, respectively but it would have taken far too long in compared to the time available for this research. Sediment input was determined by imposing specific sediment boundary condition as it will be described below. The second hypothetical domain, displayed at the bottom left of Figure 46, was delimited by an open inflow boundary at the barrage and an open outflow boundary at the hydrometric station of Cremona. It should be noted that the incision of the tailrace is a 1D issue that is completely unrelated to the purpose of the study, which is to quantify 2D hydro-morphological effects. As a result, the model may ignore the tailrace. The model extent on the bottom right of Figure 46 was indeed chosen to be the design one.

The design model domain begins at the Isola Serafini barrage and ends about 400 meters upstream of the junction of the meander loop and the hydropower plant's tailrace. The reasons for which it was decided to end it before of the Cremona's hydrometric station were related to computational time, overall accuracy, and data scarcity. Removing from the model the section of the river between the tailrace and the meander's confluence and the Cremona hydrometric station required the imposition of a discharge rating curve as a downstream boundary condition at the end of the

meander. This was possible using data on water level slopes from a previously available 1D hydraulic model (ADBPO, 2005a). It was believed that increasing the computational time by imposing the boundary condition at the hydrometric station would not have resulted in an increase in the model's overall accuracy. The uncertainties in defining all the model's various inputs, among which the unknown relationship between the Adda discharge and the outflow of the barrage, were introducing a higher level of uncertainty. A variability interval for the discharge rating curve was identified to test the influence that a variation in the assigned water level could have on shear stress distribution along the meander. The topographical references available along the meander loop were the Po River Basin Authority's Digital Terrain Model of 2005 (hereafter DTM - 2005) and nine topographic cross sections surveyed by AIPO in 2005 (hereafter PO 2005 - AIPO). The DTM - 2005 was not integrated with bathymetric measurements, consequently the elevation of the bed topography was not entirely known. This made it impossible to create a model with real topography that covered both the meander loop and the stretch upstream of the Cremona hydrometric station.

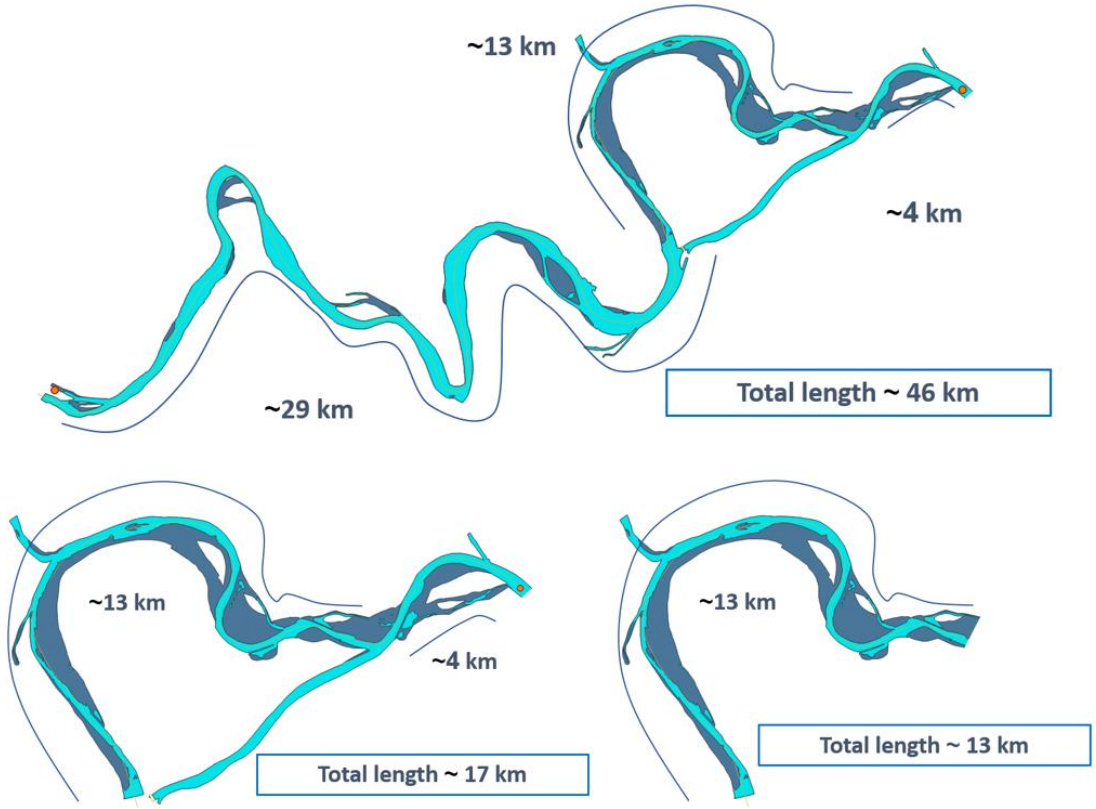

Figure 46. Different proposals for the computational model extent hypothesized during the model construction.

Lateral domain extent and grid cell size.

The computational grid should be designed in such a way that the grid discretization is dense enough to accurately replicate the cross-section profile (including bank lateral slope) while resulting in reasonable computational times. Based on previous modelling experience, the appropriate number of cells required to ensure accurate depiction of the main channel was determined to be eight for the Rhine Branches (Yossef, 2016). It is generally recommended to generate it iteratively, starting with a coarser resolution and refining it based on the required level

of detail of hydrodynamic attributes. Construction of the computational domain for the Isola Serafini case study presented a challenge in terms of ensuring sufficient overall quality criteria and did not follow to this iterative procedure. Indeed, according to the Deltares (2018), the grid must meet the following criteria:

- It must fit as closely as possible to the land-water boundaries (in short land boundaries) of the area to be modelled;
- It must be orthogonal, namely grid lines must intersect perpendicularly;
- The grid spacing must vary smoothly over the computational region to minimize inaccuracy errors in the finite difference operators.

Delft3D's modelling suite includes the program RGFGRID with which to generate the curvilinear grid. Land boundaries and, preferably, topography should be considered when creating a curvilinear body fitted grid. Land boundaries were determined by converting the shape files (the polygons coloured in dark and light blue in Figure 46) of both low flow channel and bankfull channel (ADBPO, 2005b) to.ldb files using QUICKPLOT. The topography was provided by the DTM - 2005 and can be visualized with QUICKIN alongside land boundaries (Figure 47). The grid should avoid producing staircase effects, which occur when the grid is not properly aligned with the topography. Furthermore, is recommended to stretch grid cells in the main flow direction up to an aspect ratio of 3 to 4 for a more efficient compotation. Thus, rectangular grid cells that are elongated along the main flow direction are preferable to square grid cells.

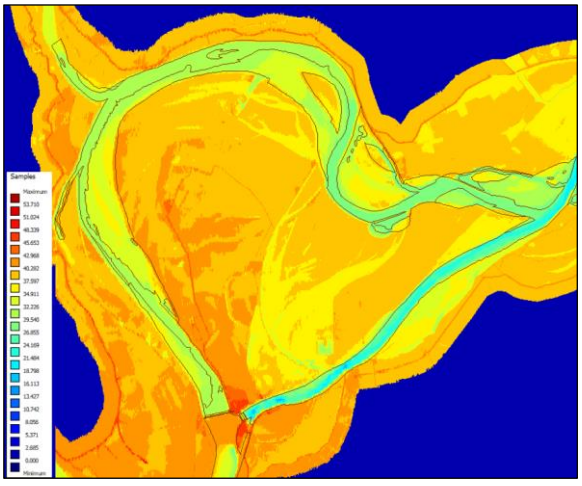

Figure 47. Screenshot of QUICKIN displaying the loaded DTM-2005 as a .xyz file together with land boundaries generated by the shape files of low-flow and bankfull channels.

The grid's lateral extent followed the bank lines defined by the bankfull channel's shape file and was extended outwards of approximately 100 m. This decision was taken after ascertaining that discharges of interest for modelling were always contained within the incised riverbed, with no flow interesting adjacent floodplains. It took time to design a grid whose longitudinal development followed the primary flow direction as closely as possible while also meeting adequate quality criteria. This was particularly challenging for the stretch of the river between progressive 366 and 369 where the low-flow channel follows the navigation curves imposed by the training walls defining a meander bend that spans an approximately 180° angle. The design grid is reported in

Figure 48 whereas grid quality properties map with which to check the quality of the grid are reported in Appendix B.

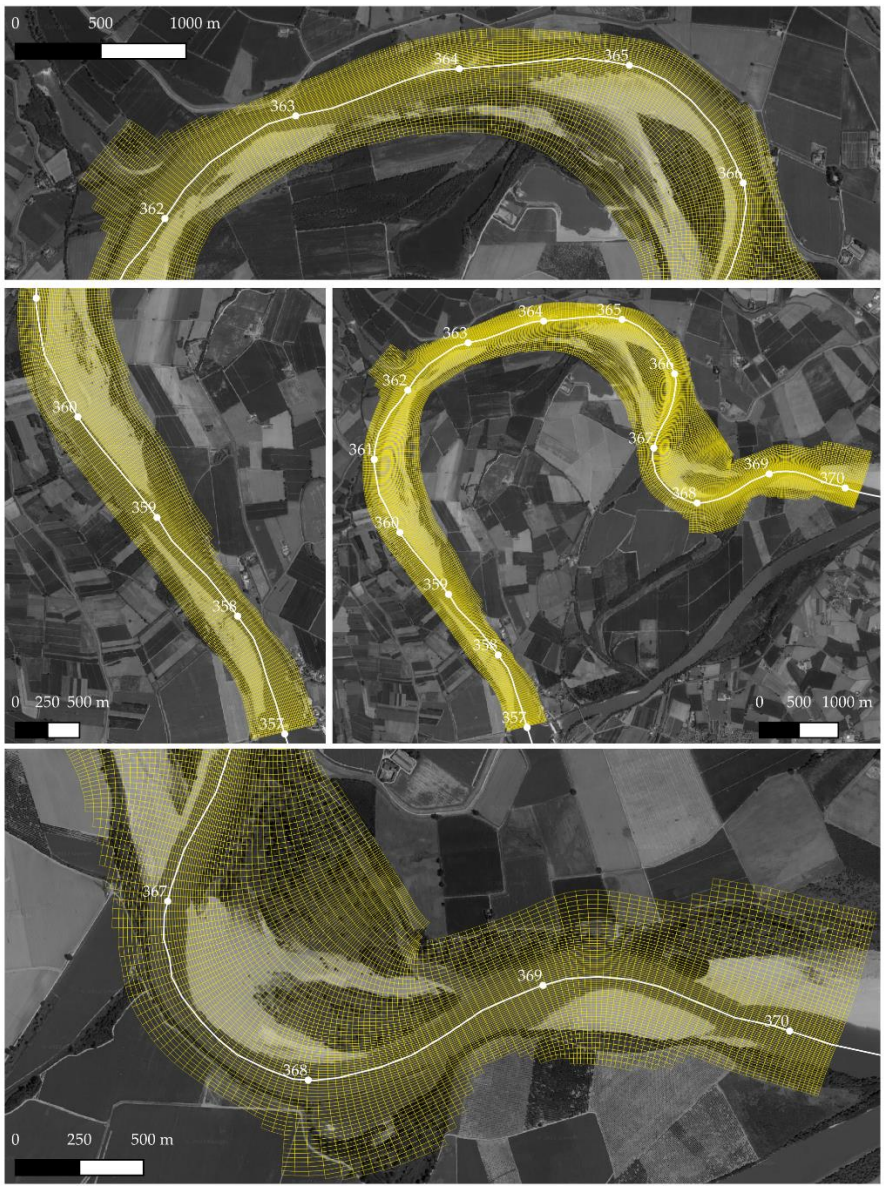

Figure 48. Screenshots of the computational grid.

The grid is composed by M=76 columns and N=458 rows and a total of active grid cells (cells that are used for the computation) equal to 24267. The grid cell dimensions are variable with cell length (M-direction) that varies between 25 and 7 m and cell width that ranges from 37 to 12 m.

Model topography from topographical data processing

The input .dep file was created with the QUICKIN tool, where the available DTM, previously converted from raster to sample files with QGIS (from .asc to .xyz format), was interpolated upon the previously constructed computational grid imposing specific interpolation settings. Each computational cell was associated to a specific interpolated value of the bed elevation (Figure 49). The resulting depth file (named DTM – Topography) was affected by the water table detected with

the LIDAR measurement and is therefore unsuitable for modelling. This required for the selection of an alternative method of analysis that plants to generate a reference topography representative of the real one in which to assess potential restoration measures. This entailed starting morphodynamic modelling without first performing a hydrodynamic calibration to tune the roughness of the channel.

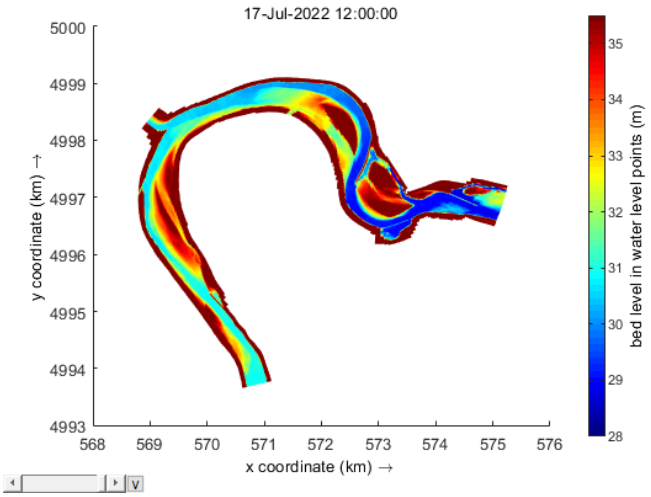

Figure 49. Graphs showing the bed level points of the computational grid with a manual colour limits scale to understand more easily which parts of the channel are known and which part of the DTM detected the water table.

3.2.2 Sound engineering checks on a transversely flat bed

The following step of the research aims at reproducing the basic morphological functioning of the river and investigate how the river's current bar patterns can develop obtaining a reference topography to be used as topographical basis for further simulations of restoration measures. That was possible by assessing the morphological modifications induced by specific water inputs on a transversely flat topography while performing a sensitivity analysis of the various physical modelling parameters. Specifically, morphological parameters A_{sh}, B_{sh} and E_s that parameterize the effect of gravity pull along the transverse slopes and spiral flow on sediment transport and the degree of nonlinearity od sediment transport were varied to investigate changes in the morphological development of the course. Moreover, this permitted to avoid possible modelling artefacts in morphodynamic processes such as the one connected to sub-grid features of the topography (Deltares, 2022, personal communication). Dunes and local scours could indeed promote specific morphodynamic development and affect the assessment of the actual general behaviour of the river. Flattening the channel topography guarantees that sub-grid variations are erased. Such methods of analysis have been applied by *Deltares* in past studies although no studies were available as literature references.

Inherently, the question of which part of the entire domain needed to be flattened arose, and the answer was that it depended on the specific discharge under investigation. Each discharge is associated with defined water stage along the meander, and thus with specific wet area widths that vary along the river course. The widths of the channel to be flattened could be considered, as first

approximation, the widths of the wet areas associated with the specific discharge analysed. This required the understanding of water levels reached for the various flow magnitudes.

The transversely flat topography was generated using the procedure explained below and these data:

- DTM - Topography: the depth file previously created in QUICKIN from the DTM - 2005;
- PO 2005 - AIPO topographic surveys;
- Water levels results from the 1D hydraulic model made by ADBPO (2005a).

PO 2005 - AIPO cross sections are the topographic references of the 1D hydraulic model (ADBPO, 2005a) that provides model results for water levels reached at each cross section for a set of analysed discharges (Table 3 and Figure 50).

Table 3. Water levels for each analysed discharge in the 1D hydraulic model (ADBPO, 2005a) at each cross section of the topographic survey PO 2005 – AIPO. Water levels at the Closing section were evaluated by interpolation.

AdbPo (2005a) - water levels (m.a.s.l.)							
Sections	progressive (m)	Discharges (m^3/s)					
		500	1000	2000	3000	4000	5000
S24	357,482	33.500	34.600	35.700	36.800	37.790	38.628
S24B	358,934	32.437	33.883	35.455	36.487	37.411	38.191
S24C	361,286	31.680	33.058	34.671	35.742	36.698	37.520
S24D	363,320	31.078	32.407	33.976	35.007	35.919	36.713
S24E	364,844	30.782	31.981	33.543	34.593	35.525	36.348
S24F	366,354	30.001	30.994	32.547	33.728	34.748	35.646
S25	368,675	28.762	29.857	31.641	33.025	34.190	35.190
S25_02	369,364	28.170	29.466	31.363	32.764	33.917	34.912
S25_03	369,838	27.846	29.360	31.347	32.779	33.951	34.956
Closing s.	370,588	27.794	29.287	31.252	32.666	33.817	34.811

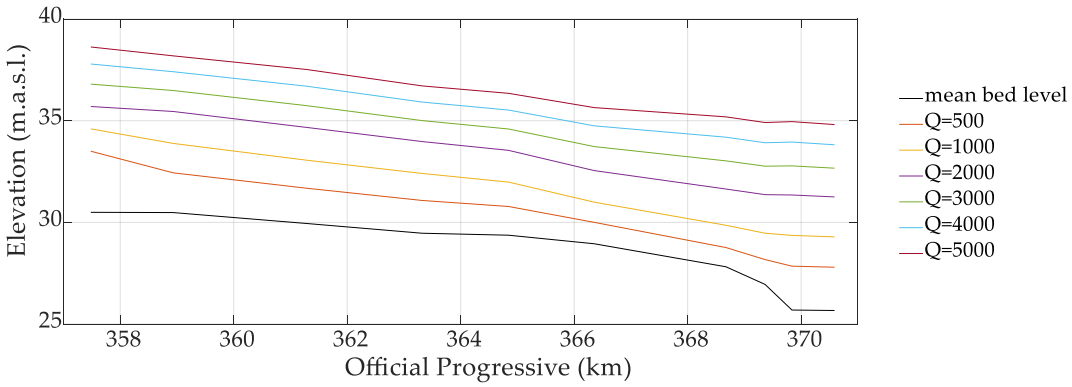

Figure 50. Graphic representation of longitudinal free surface profiles computed by the 1D hydraulic model (ADBPO, 2005a) along with the estimated mean bed level longitudinal profile.

Using representative N-columns of the computational grid, the same cross sections could be qualitatively identified on the computational grid (Figure 51 and Table 4). Each cross-sectional

topographic survey was thus associated with a single N-column of the computational domain as reported in Table 4.

The next step consisted of creating a depth file in QUICKIN that replicated the water table for each discharge (named WT - Qn). The construction process is explained referring to a discharge of 5000 m^3/s. Once the discharge was set, water levels were imposed at each of the N-columns, and water level values were assigned to all grid cells via linear interpolation between two consecutive cross sections' values (top of Figure 52).

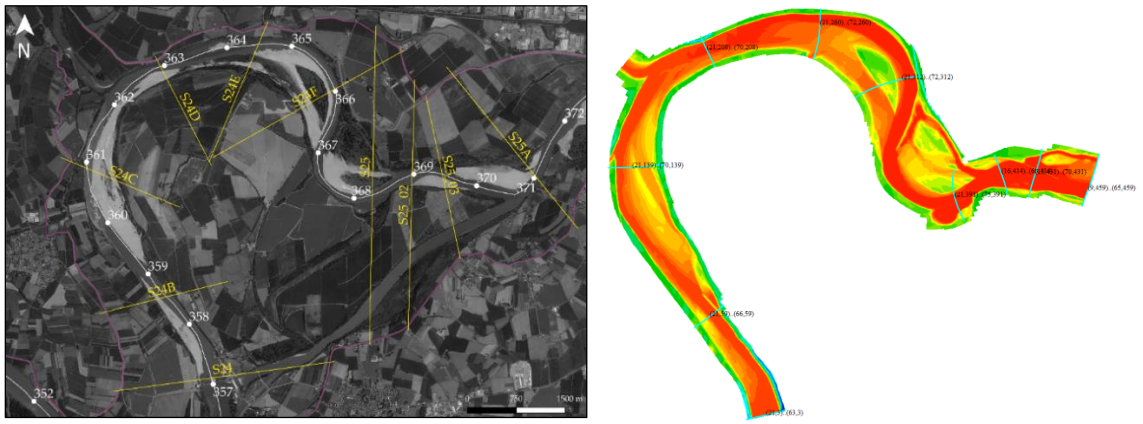

Figure 51. On the left: Locations of cross-sectional topographic surveys PO 2005 – AIPO along the meander of Isola Serafini; On the right: Location of N-columns identified in the computational grid that can be considered representative of the topographic surveys.

Table 4. Selected match between the cross-sections PO 2005 - AIPO and the N-columns of the computational domain.

Sections	N-column 2D model	Official Progressive (m)
24	3	357,482
24B	59	358,934
24C	139	361,286
24D	208	363,320
24E	260	364,844
24F	312	366,354
25	391	368,675
25_02	414	369,364
25_03	431	369,838
closing s.	459	370,588

Once the depth file for the water table was generated, it was combined with the depth file DTM - Topography (representing the bathymetry detected by the LIDAR). These two files were first converted to .mat format using QUICKPLOT, then loaded into *Matlab* and processed as matrices through a simple algorithm (bottom left in Figure 52). Components of the computational domain that were not submerged by the water table, returned positive difference between the matrices DTM - Topography and WT - Q_n. Negative components, namely the computational domain's submerged portion, were replaced by nan (bottom right in Figure 52). The resulting matrix was then saved as a sample file and imported into QUICKIN to generate a new depth file.

Cells with nan values of the new depth file had to be assigned new values to generate the transversely topography. This was achieved by applying a single value of bed elevation to the N-

columns cross sections and then interpolating again to assign the remaining grid cells a depth value. Two options were considered to determine the uniform value of bed elevation to impose at the N-columns cross sections:

i) Mean bed elevation of the submerged part of the channel could have been evaluated and applied to each N-column cross section of the computational grid since water levels were known for each PO 2005 - AIPO cross section along the meander from the 1D hydraulic model (ADBPO, 2005a). The mean submerged elevation was computed using *Matlab*. Depth values for all grid cells were then computed by linear interpolation between two consecutive cross sections, resulting in the depth file named IF – MS – Q_{5000}.

ii) The second option was based on referring to the mean bed level identified by ADBPO (2005a) at each PO 2005 – AIPO cross section, resulting in the creation of a depth file named IF – M – Q_{5000} to be applied indistinctly for each discharge.

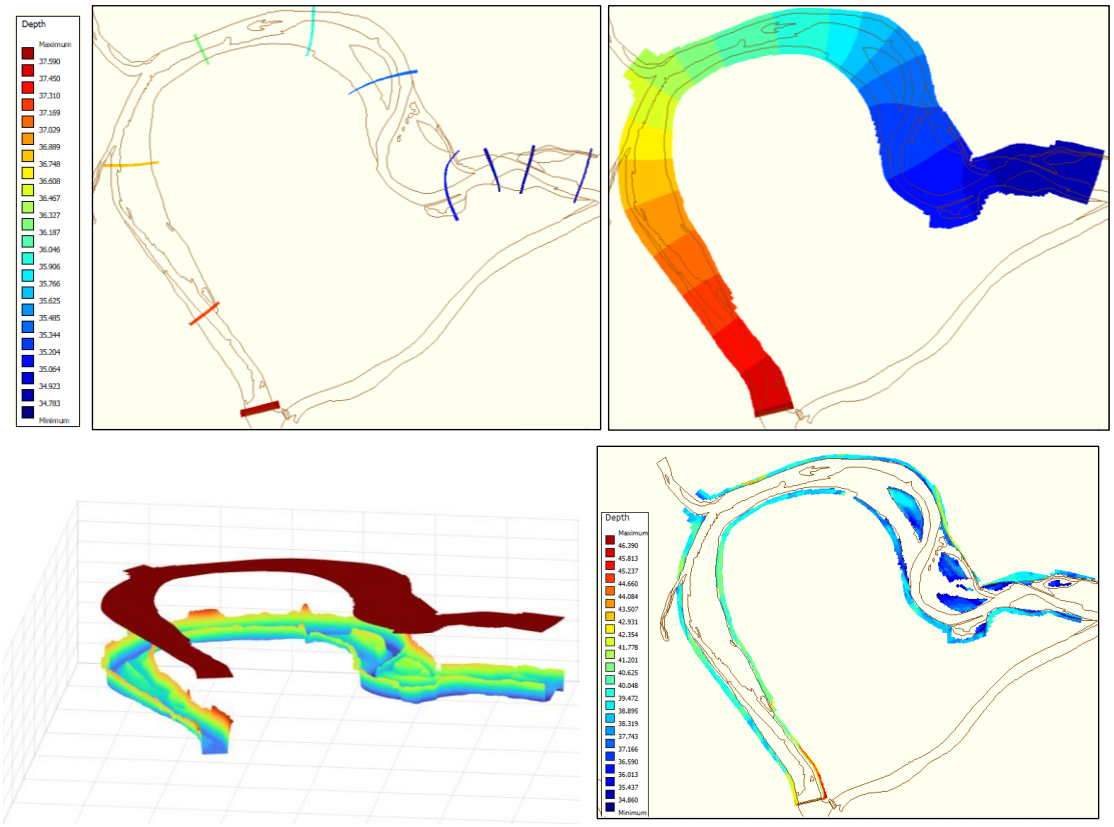

Figure 52. Top: Construction of a depth file (WT – Q_{5000}) representing the water table associated to a discharge of 5.000 m3/s along the meander loop. Firstly constant values to each of the selected N-column of the computational grid were assigned (top left) then by linear interpolation between each consecutive n-columns bed elevation value was assigned to each cell composing the computational grid; Bottom left: Representation of the two generated depth file, the one (DTM - Topography) associate to the topography detached by the DTM-2005 (below) and the other (WT – Q_{5000}) reproducing the water table (above); Bottom right: resulting bed level points of the computational grid after the subtraction of WT – Q5000 topography to the DTM- Topography.

The 1D hydraulic model also evaluated water levels for 6,000, 7,000, 8,000, and 9,000 m^3/s, but these discharges appeared to be too high and with an associated frequency of occurrence that was too low to be meaningful for modelling purpose. For the reasons outlined above and those that follow, the discharge of 5,000 m^3/s was chosen to be the one to primarily investigate. Firstly, the meander loop's formative discharge was estimated to be between 4,000 and 5,000 m^3/s (Filippi et

al., 2013). Secondly, the submerging discharge of bars should be considered to set a limit to discharges to be analysed since the main objective was to reproduce existing bedforms. The submerging discharge of bars 626-625 and 616 were estimated at 4,000 and 7,000 m^3/s, respectively (ADBPO, 2005b). The fluvial island coded 625-626, however, was not completely submerged when generating a flat bed at 9,000 m^3/s (presumably because the DTM detached the high vegetation therein). Finally, the discharge of 5,000 m^3/s enabled the generation of a flat topography entirely contained within the computational grid's lateral banks. Longitudinal training walls that were submerged by the water table were assigned nan values during the construction process. Consequently, the depth file had to be modified by resetting their effective elevation.

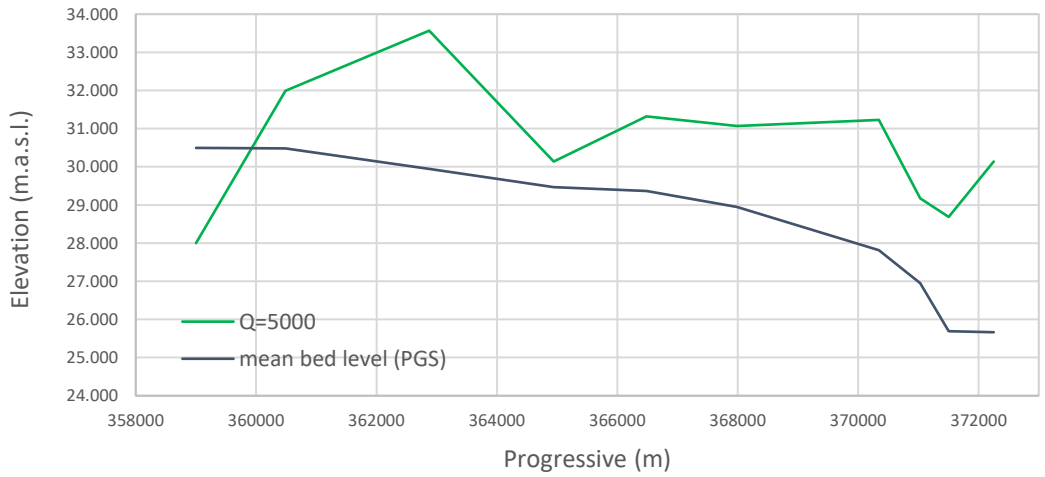

Figure 53. The only two longitudinal bed level profiles that were used for generating the transversally flat bed.

Table 5. Bed slopes of each segment between adjacent topographic survey encompassed in the model.

segments	Length (m)	Bed slope (‰)						
		mean bed level (PGS)	Q_{500}	Q_{1000}	Q_{2000}	Q_{3000}	Q_{4000}	Q_{5000}
S24 – S24B	1452	**0.01**	-2.39	-2.57	-2.91	-4.04	-4.08	**-3.98**
S24B – S24C	2352	**0.22**	-0.33	-0.67	-1.21	-0.47	-0.66	**-0.66**
S24C – S24D	2034	**0.23**	0.83	0.64	1.38	1.42	1.66	**1.66**
S24D – S24E	1524	**0.06**	0.18	-0.32	-0.71	-0.76	-0.80	**-0.77**
S24E – S24F	1510	**0.28**	-0.28	0.80	0.50	0.18	0.18	**0.17**
S24F – S25	2321	**0.48**	0.47	0.60	0.99	1.19	1.22	**-0.07**
S25 – S25_02	689	**1.27**	0.23	-0.33	-0.17	-0.43	-0.86	**3.00**
S25_02 – S25_03	474	**2.68**	2.98	2.01	-0.82	-0.37	-0.10	**1.03**
S25_03 – closing s.	750	**0.03**	0.85	0.59	0.77	-2.09	-1.91	**-1.93**

It was also decided to begin simulations with topography where there was no fluvial island coded 625-626, making the bed as flat as the adjacent areas. This means that two bathymetries with different longitudinal bed slopes (the first evaluated by considering the mean bed level of the submerged part of the known cross sections and the second evaluated by considering the mean bed slope from the 1D model (ADBPO, 2005a)) and two similar bathymetries without the fluvial island were generated. After the initial bathymetries were created, the analysis was primarily based on

changing the values of the sediment transport and morphological parameters. To obtain the real bars patter, values for the degree of nonlinearity of sediment transport b and morphological parameters Ash, Bsh and Espir were varied. Simulation results were visually compared with the DTM - Topography map and graphically compared by projecting, for each cross section known from the topographical surveys, the known and simulated topography.

Simulation' inputs were progressively defined by analysing modelling results. Consequently, it was decided not to report here the simulations' summary and to explain the modelling process directly in paragraph 4.1.1. Simulations were run until morphological changes along the channel were no longer considered significant (up to three months for the lower degree of non-linearity of sediment transport considered). Inflow rate at the barrage (5,000 m^3/s) was imposed as a uniformly distributed release from the eleven gates that comprise the barrage.

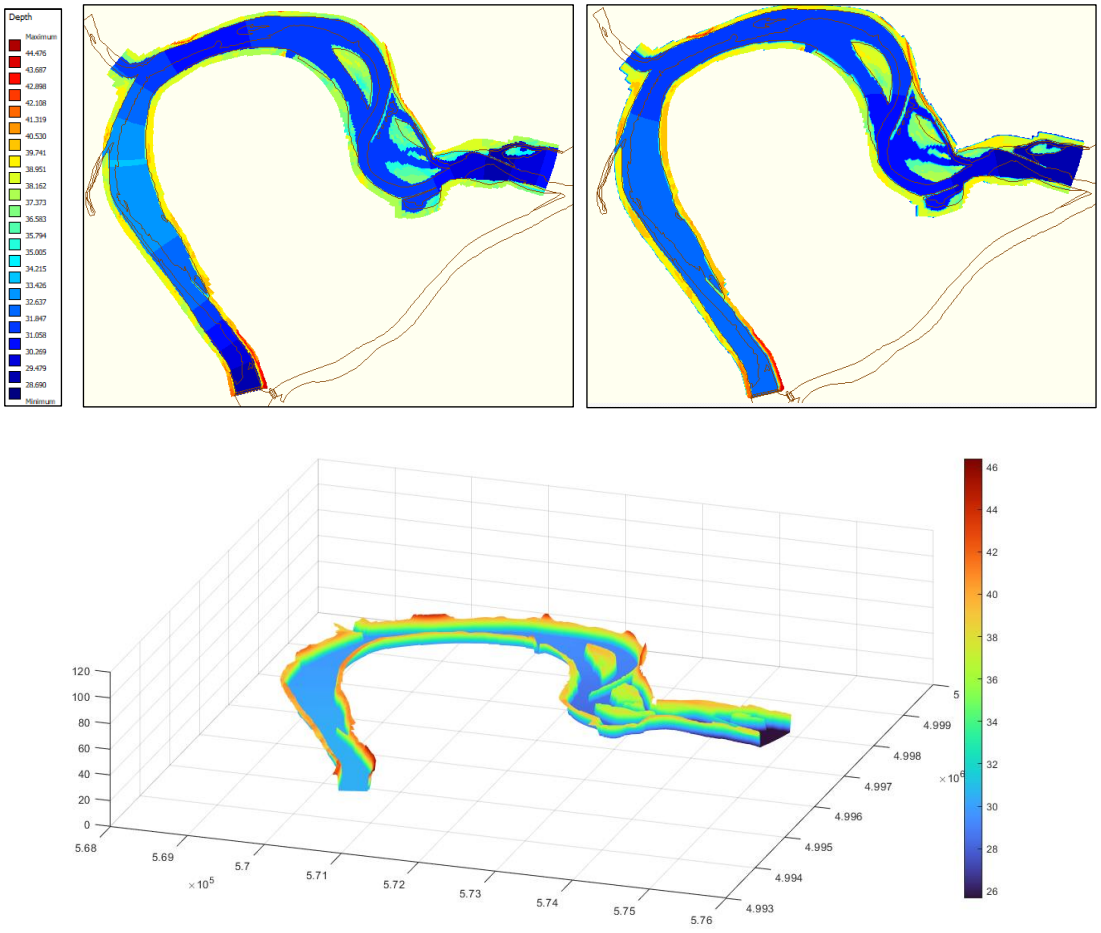

Figure 54. Top: Screenshots of the two initial bathymetries generated, namely IF - MS - Q_{5000} on the left and IF - M - Q_{5000} on the right, visualized within QUICKIN; Bottom: 3D visualization of the transversely flat topography IF - M - Q_{5000}.

3.2.3 Other modelling inputs

After having generated the input file for the computational grid and bathymetry (MDF-file) the user is required to define all parameters necessary for the Master Definition Flow file:

- *Time frame*: The Data Group Time frame is composed by the reference date, simulation start time, simulation stop time and time step. Beginning with the reference date, the start and stop times define the time frame for the simulation that will be computed. Accuracy of results, that depend on the Courant-Friedrichs-Lewy number, is primarily affected by the time step (CFL). Its definition depends on the average values of the grid cell spacing in both directions.

- *Processes*: Processes to include in the analysis by definition of the physical processes (e.g., wind, tidal forces, wave) and related constituents (such as salinity, temperature, and tracers) in the Data Group Processes. The following options were chosen for the morphological and sediment transport processes: Sediment as constituents (non-cohesive) and Secondary flow as physical processes.

- *Initial conditions*: Water level, sediment concentration, and secondary flow velocity values were required as initial conditions given the processes chosen in the previous step. These can be assigned as values from a previous calculation or as uniform spatial values (map or restart file). For each executed analysis, a test simulation was run for a time frame of six hours with uniform initial water level values and null values for secondary flow and sediment concentration generating a restart file to be used as initial condition for the simulation.

- *Boundaries*: Two different boundary conditions needed to be specified: flow conditions and transport conditions. The former type was specified as a total discharge through the imposition of a Time-series whereas the latter consisted of sediment concentration [kg/m^3], which was imposed to be zero for all open boundaries.
  - *Inflow boundary conditions*: Two open boundaries made up the model (Figure 55); the first was located at the barrage, and the second was located on the Adda River.

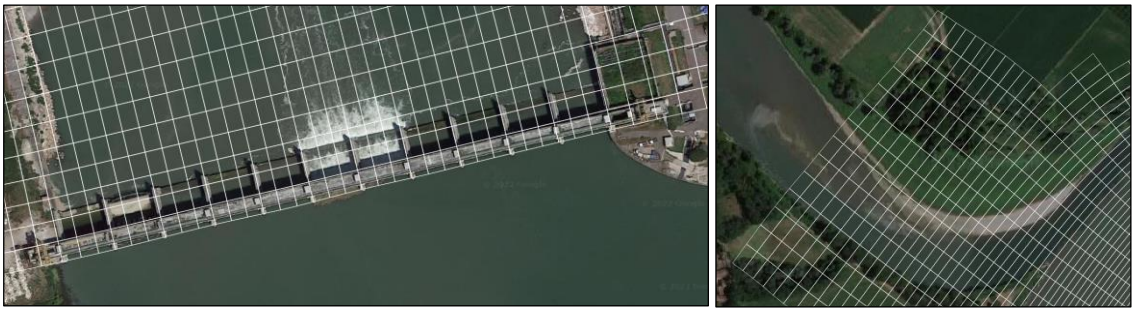

Figure 55. On the left: Principal open boundary located at the barrage of Isola Serafini; On the right: Second inflow open boundary located next to the Adda River mouth.

Only 33 of the total 43 grid cells that constitute the first inflow open boundary were internal to the hydraulic structure from which the water enters the system (three grid cell per flood gate). Thus, on grid cells external to the barrage, both flow and transport conditions were imposed as null whereas it was possible to impose different water and sediment releases passing from each cell composing the flood gates to reproduce any kind of operation rule. The second open boundary was defined by a total of 14 grid cells. The four external cells to the hydraulic right and hydraulic left of the Adda River, being

outside of the incised channel, were imposed to be constantly null in terms of discharge and sediment concentration. Connecting the Adda discharge with the discharge released by the barrage was challenging. The Po River's discharges over a period of 30 years were examined by *ARPA Emilia-Romagna* accessing Annali idrologici determining the relative mean monthly discharges as well as the mean annual hydrographs (Figure 56). Discharges at Piacenza can be considered equal to the inflows to the hydropower plant since contributions to the Po River discharge of the of the two tributaries between Piacenza and the barrage, the Nure and Chiavenna Rivers (Figure 57), are negligible. Characteristic discharges for the Adda River were provided by *ARPA Lombardia* through an estimating method (Bilancio idrico) applied to the period 2001-2015 relative to a closing section positioned at the Adda's mouth. Also, *ARPA Lombardia* provides measured data at Pizzighettone hydrometric station positioned around 14 km upstream of the Adda River mouth relative to a measuring period of two years only (2019-2020).

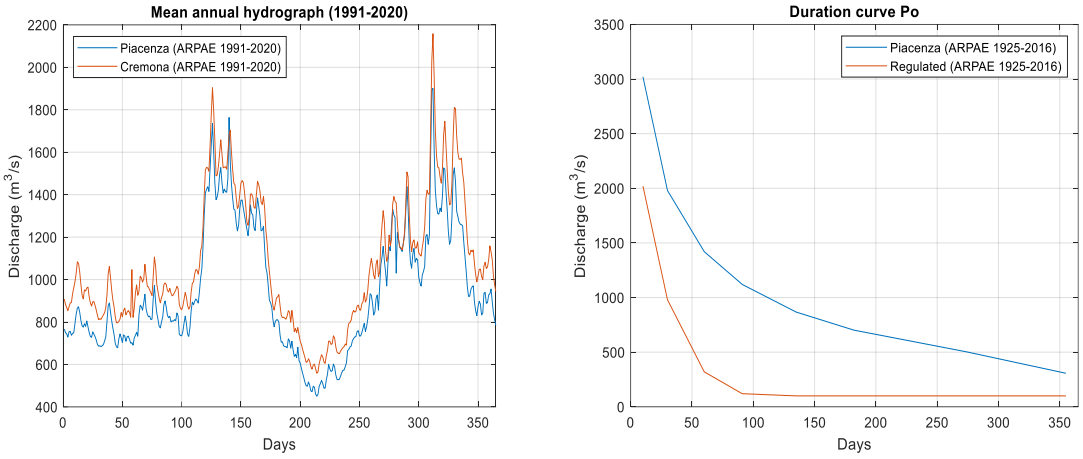

Figure 56. On the left: Mean annual hydrograph evaluated at Piacenza and Cremona hydrometric station based on daily discharges provided by Annali Idrologici for the period 1991-2020; On the right: Duration curves of the natural flows estimated with data of Piacenza's hydrometric station (i.e., discharges at Piacenza are equal to incoming discharges to the barrage) and of the regulated flows estimated by applying the operation scheme of the barrage to the natural flows.

Figure 57. Locations of the point of measure used for analysing water discharges.

It was attempted to calculate Adda River's discharge by difference between daily measured discharges at Cremona and Piacenza. It turned out, however, that the

hydrometric station in Cremona (downstream) consistently recorded lower values than those recorded in Piacenza (upstream), on the occurrence of medium and high daily discharges. Given the frequency of occurrence of this fact it was impossible to exclude from the calculation such daily measurements and thus estimate in that way the Adda's discharges.

Table 6. Summary of mean monthly discharges evaluated for the Po and the Adda Rivers.

Mean monthly discharges (m^3/s)												
	Jan	Feb	Mar	Apr	May	Jun	Jul	Aug	Sep	Oct	Nov	Dec
Po - Cremona (ARPAE 1991-2020)	922	872	969	1001	1555	1223	732	674	1002	1223	1592	1144
Po - Piacenza (ARPAE 1991-2020)	764	737	836	881	1441	1123	611	557	864	1154	1377	952
Po Cremona-Piacenza (ARPAE 1991-2020)	158	135	133	120	114	100	121	117	138	69	215	192
Adda - Bilancio Idrico (ARPAL 2001-2015)	181	182	179	194	286	189	146	143	156	189	296	206
Adda - SIDRO (ARPAL 2019-2020)	188	109	112	132	213	287	111	119	220	440	409	339

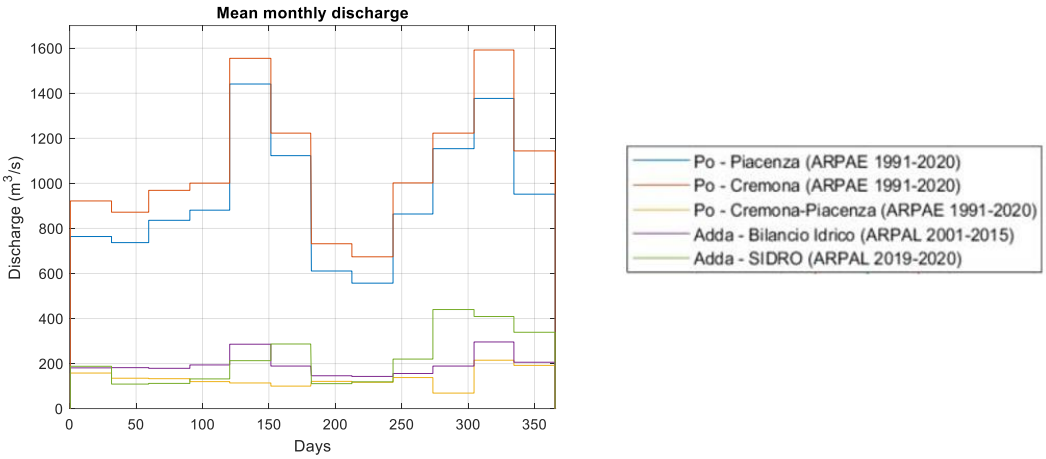

Figure 58. Comparison of the mean monthly discharges evaluated.

– *Outflow boundary conditions*: The outflow open boundary was positioned around 400 m upstream of the conjunction where the bathymetry of the cross section is not completely known (not in the submerged part). For that reason, the shape of the submerged part of the cross section was guessed by examining the elevation of the talweg of the nearby known cross sections S25-03 and S25A. (topographic survey PO 2005 – AIPO of Figure 59). The talweg's elevation of the closing section was determined by linear interpolation of talweg elevations of the two known cross sections and therefore set at 22.3 m.a.s.l. and consequently the shape of the cross section was drawn (centre of Figure 59). Sediment concentration was set to zero whereas water levels were imposed by setting the discharge rating curve. It was determined by interpolating the free surface profiles from the 1D hydraulic model (ADBPO, 2005a) at the location of the closing section. A range of variability for the water level related to each specific discharge was considered, identifying lower and upper limit curves so

that to test the uncertainty related to its definition. These two curves were created by coupling the water level computed with the lower and higher discharges, respectively, analysed by the 1D model, at each discharge Q_i.

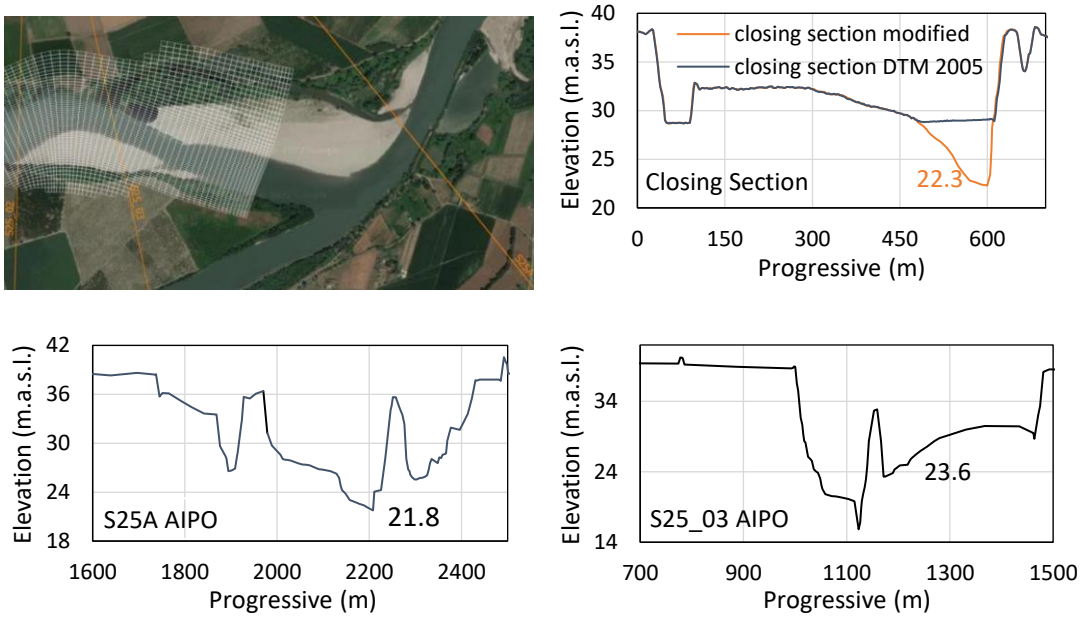

Figure 59. On top left: outflow open boundary located upstream of the conjunction between the meander and the tailrace; On top right: closing cross-section, the orange part is the portion of the channel submerged by water and it was guessed as explained in the text; Bottom: cross section S25_03 and S25A entirely known from the topographic survey.

Two hydrodynamic simulations were thus run by imposing the lower and higher limits of the rating curve in order to compute the difference in water levels reached along the meander and the length of influence of the resulting backwater effect. Figure 61 shows that, for the case of topography IF - M - Q_{5000}, the difference in water levels extended all along the meander but within 10 km from the barrage (official progressive 367) it was lower than 0.5 m.

Table 7. Water level values for each discharge defining the design discharge rating curve (h_{Qi}) and the upper and lower limit curves ($h_{Q(i+1)}$ and $h_{Q(i-1)}$).

		h_{Qi-1}	h_{Qi}	h_{Qi+1}
		(m.a.s.l.)	(m.a.s.l.)	(m.a.s.l.)
Qi (m3/s)	**500**	-	27.794	29.287
	1,000	27.794	29.287	31.252
	2,000	29.287	31.252	32.666
	3,000	31.252	32.666	33.817
	4,000	32.666	33.817	34.811
	5,000	33.817	34.811	35.703

It was crucial to understand what effects a change in water levels could have had, for instance, in bar pattern formation since the goal of the sound engineering checks phase was to assess the morphological development of the course starting from a transversely topography. The variation of the width-to-depth ratio was a good indicator for that, and it appeared to be relatively small when considering that the smallest width of the channel

is equal to 300 m, the average water depth was about 7.5 m (with a maximum variation of 0.5 m in the stretch between the barrage and official progressive 367). Hence, to assess how the downstream boundary condition could eventually affect the morphodynamic development, a series of hydro-morphological simulations were performed imposing the three possible discharge rating curves. Figure 61 clearly shows that changes in the morphological development occur almost exclusively downstream of official progressive 367, i.e., 10 km from the barrage, whereas the topography developed almost identically on the stretch between the barrage and the Adda River mouth.

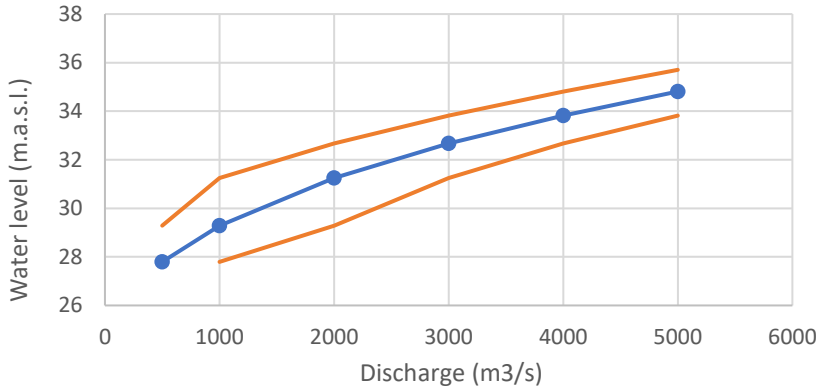

Figure 60. Discharge rating curve and upper and lower limits.

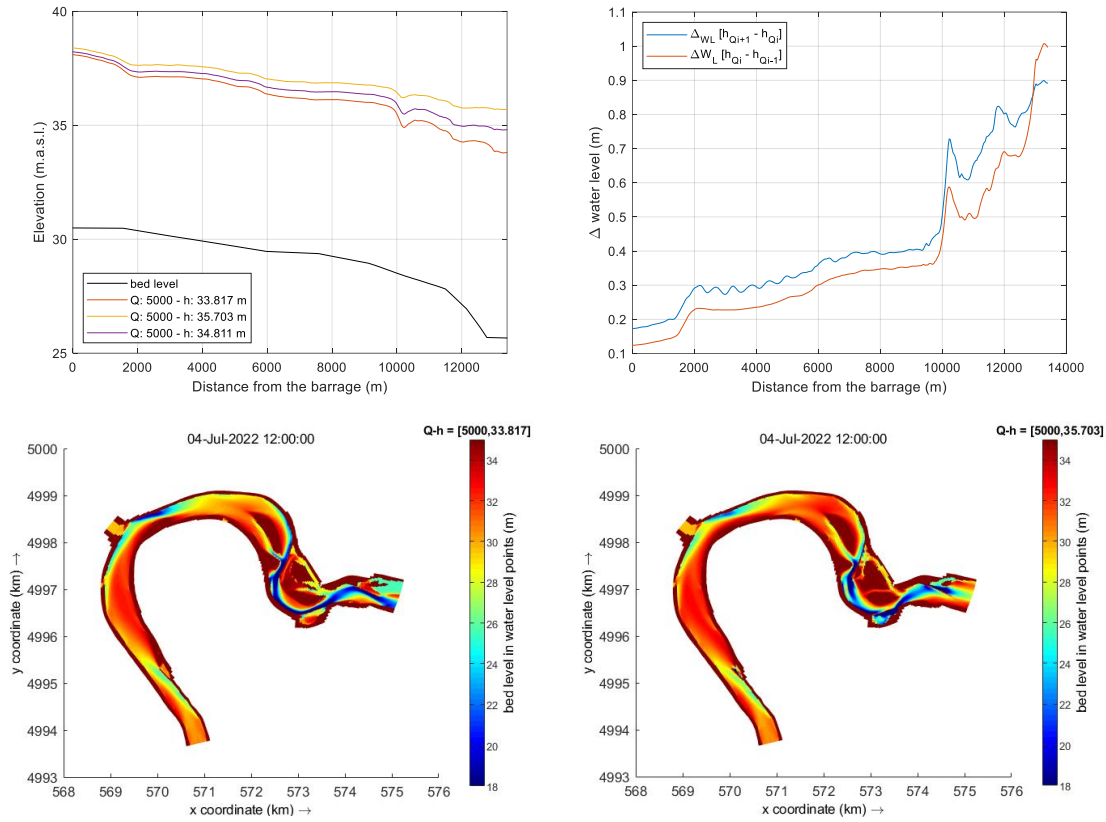

Figure 61. Top left: water level profiles along the meander obtained imposing the three different values of water level for the discharge of 5,000 m^3/s as downstream boundary condition; Top right: Longitudinal profiles of the difference between the water profile obtained through imposing the design discharge rating curve and profile obtained with the upper and lower limit values; Bottom: graphs of the obtained final bed level after three months of computation with a constant discharge of 5,000 m^3/s applying the lower (to the left) and upper (to the right) limit values for the discharge rating curve.

- *Physical parameters*:
  - *Roughness:* and side walls can be specified in that sub-data group. *R*oughness of the bottom can be computed according to three available formulas as uniform or space varying value. In 2D models, a space-varying form is typically used, and its value is iteratively adjusted using a fine-tuning approach based on hydraulic calibration of water levels. Mosselman & Le (2015) identified this approach as a common error in fluvial morphodynamic modelling since inputs force development of morphological patterns. According to the authors forcing a prefixed spatial roughness distribution can prevent the channel to evolve freely, lowering the model's predictive capability. Delft3D-FLOW has been extended with bedform roughness predictors and vegetation models for considering alluvial bed and vegetation flow resistance (trachytope approach) so that to obtain a spatial variation of roughness based on a physical process instead of imposing it preliminary (Mosselman & Le, 2015). Nevertheless, it was applied a constant value for the bottom roughness for the entire domain since the number of uncertainties in the model were high. The Chézy value was imposed to be equal to 45 $m^{1/2}/s$ based on experience (Deltares, 2002, personal communication). Free slip condition was selected for side-walls roughness.
  - *Sediment:* A single sediment fraction composition with a median sediment diameter (D_{50}) of 0.24 mm was chosen for bed sediment composition, as reported by ADBPO (2005b). Moreover, fixed layers were imposed upon grid cells that made up the longitudinal training walls to reproduce structures comparable to non-erodible layers.
    The Engelund-Hansen (1967) formula was selected for computing the transport rates as the sum of bedload and suspended load (total load). The reason for the choice of this formula relies on the assumption that the suspended load is negligible and thus the bed load corresponds to the total load. Based on experience (Deltares, 2022) and because of the lack of prior studies to use as references, the Engelund-Hansen formula was selected to be the more appropriate to adopt. As explained in paragraph 2.3.1., a General Transport Formula was also adopted to test the variation of degree of non-linearity of sediment transport generating a formula in which flow velocity was elevated to the power of 4.2 and 3.8 (based on experience).

  - *Morphology*:
    - Morphological scale factor: Simulations were run applying a unit morphological factor.
    - Spin-up interval before morphological changes: It was selected to be 720 min such that to be sure to reach steady flow before the beginning of morphological modifications.
    - Internal to the .mor file, values for the morphological parameters A_{shld}, B_{shld}, E_{spir} had to be assigned.

- *Monitoring and output*: Monitoring of simulation results can be imposed by the Data Group Monitoring in which one can define:
  - *Observation points*: grid locations, positioned at the computational grid cell centres, in which to store simulations at a user-defined time interval (i.e., water levels).
  - *Drogues*: these are floats that move with the flow and are especially used as tracers to track specific trajectory travelled.

– *Cross-sections*: sections along one of the grid directions through which to compute transport fluxes.

The results are then stored in two main types of files:

– *History files*: files that contains evaluated quantities in the defined Observation points and cross-sections.
– *Map files*: files that contain snap shots of the computed quantities of the entire area.

3.3 Effects of different gates' opening configurations from the Isola Serafini barrage (asymmetrical inflows).

This step of the research aimed to investigate how different flow distributions at the inflow boundary can affect the topography of the meander by conceptually simulating various operation schemes. This can provide useful insights on potentials and limitations related to workable and realistic alternative operation rules. These could be accordingly elaborated with a view to promote specific morphological developments of the meander that are conducive to the rise of more heterogeneous and dynamic processes within the channel. Additionally, these might be useful for reversing morphological alterations that the segment of the river is experiencing such as the excessive deepening of the low-flow channel.

In the previous step, only one discharge from the gates - a uniformly distributed discharge of 5,000 m^3/s across the 33 grid cells that made up the barrage - was tested. Except for the flow distribution at the inflow boundary, the same inputs imposed for the simulation that best fitted the known topography during the sound engineering checks (follow- up call "simulated topography") were applied for additional simulations concerning the effect of asymmetrical inflows. A set of four simulations was executed examining the induced effects of asymmetrical flows again on the initial transversely topography (namely topography IF – M – Q_{5000}). More specifically, the short- and long-term effects were quantified from a hydraulic and morphological perspective, respectively.

Simulations were conducted using four different flow distribution types. Two types of distributions were labelled "asym-sx" and two other "asym-dx" because of unbalanced flow rates toward the hydraulic left and toward the hydraulic right, respectively. The barrage is composed by 11 floodgates each of which represented on the computational grid by three adjacent grid cells. For distribution type "asym-sx" the flow rates were assigned to each of the grid cell making up the open boundary " so that discharges passing through the first five gates to the left (15 grid cells) were twice the value of discharges passing through the six gates to the right (18 grid cells). This distribution type was labelled as "asym-sx-2". A similar distribution type, referred as simulation "asym-sx-4" was generated, but with discharges passing through the left-hand gates being four times higher than discharges passing through the right-hand gates. The other two distribution types

correspond to those just described but with higher discharges assigned to the first five gates positioned on the right-hand gates, defining simulations "asym-dx-2" and "asym-dx-4".

Table 8. Set of simulations executed for the assessment of asymmetrical inflow's effects on the topography.

Code of simulation	Initial topography	Ashld	Espir	b	Q_{Po} / Q_{Adda} (m^3/s)	Q_{sx} / Q_{dx} (m^3/s)
sym	IF-M-Q_{5000}	0.3	1	3.8	5000/0	151.50/151.50
asym-sx-2	IF-M-Q_{5000}	0.3	1	3.8	5000/0	208.30/104.15
asym-sx-4	IF-M-Q_{5000}	0.3	1	3.8	5000/0	256.40/64.10
asym-dx-2	IF-M-Q_{5000}	0.3	1	3.8	5000/0	208.30/104.15
asym-dx-4	IF-M-Q_{5000}	0.3	1	3.8	5000/0	256.40/64.10

3.3.1 Short-term effects

The Delft approach was taken into consideration when quantifying short-term effects in the context of linear bar theory, as described in section 2.3.2. The topography developed forced by asymmetrical steady state discharge at the open boundary, which results in prescribed constant flow velocity and water depth perturbations of the basic state. The basic state referred to undisturbed flow conditions, but as is clear, those cannot exist in the sections of the river being studied. The channel is indeed characterized by a variable width and by bends, such as the one placed approximately 400 m downstream of the barrage. These circumstances cause flow perturbations which disturb the basic state. Therefore, each modelling result of distribution types were compared with the reference condition of the symmetrical inflow from the barrage in order to test the short-term effects of flow distributions at the open boundary. The basic state was thus represented by the hydraulic conditions associated to the symmetrical flow distribution while asymmetrical distributions of flow gave rise to the perturbated state.

Asymmetrical flows would have been redistributed over cross-sections as approaching valley sections. The perturbation term would have disappeared and, at a specific distance from the barrage, transverse profile of depth-averaged streamwise flow velocity would have been the same as that produced by the symmetrical flow. The linear bar theory could be used to determine the so-called adaptation length, the longitudinal distance needed for the decay of perturbations in the transverse profile of depth-averaged streamwise flow velocity, as described in section 2.3.2. Since its value can be estimated with parameters related to the basic state only, modelling results of symmetrical flow distribution simulation "sym" could be used to calculate it.

Transverse profile of depth-averaged streamwise flow velocity in cross sections situated at longitudinal distances from the barrage equal to λ_w and $3\lambda_w$ were subsequently extracted. In fact, the linear bar theory states that the perturbation term should decay by roughly 36% and 0.05%, respectively, at these distances. This procedure is described taking advantage of simulation "asym-sx-2" as an example. The first step in determining the adaptation length was to process the simulation "sym" modelling results: A water depth .mat file was exported from QUICKPLOT and imported into *Matlab* to calculate the adaptation length referring to reach-averaged value of water depth. After processing the modelling results of simulation "asym-i-sx-2", the depth-average velocity in the streamwise direction (n component) was exported as a .mat file and loaded in

Matlab. The N-index of grid cells associated to the previously calculated distances λ_w and $3\lambda_w$ were evaluated and corresponding values of depth-average velocity were graphically compared with analogous value of simulation "sym". The perturbations terms were represented by the difference between the extracted depth-average velocity values of simulations "asym-sx-2" and "sym" (deviation from the basic state). Consequently, for cross-sections located at λ_w and $3\lambda_w$, respectively, it was expected that the mean of deviation terms (one term associated to each grid cell composing the cross-section) would have corresponded to the 35% and 0.05% of the mean perturbation evaluated at the barrage's cross section.

According to section 2.3.1, the hydraulic conditions (flow velocity) in each grid cell were used to calculate the bedload transport. Since the default option of no bed level changes was chosen at the inflow open boundary, the sediment transport was derived from the mass balance at the open boundary points. Modifying the discharge entering the model at each boundary grid cell (modification from symmetrical to asymmetrical inflow) resulted in different flow velocity per grid cell and consequently different rates of sediments entering the system. Therefore, the total rate of sediment at the inflow boundary (at the barrage) was calculated for each simulation executed.

3.3.2 Medium-term effects

The impact that operation rules have on the morphology of the river and, as a result, on the dynamics of sediment transport were referred to as medium-term effects. It must be recalled that, as was previously noted, each asymmetrical flow scenario was followed by a change in the sediment entry rate. Consequently, channel bed was expected to develop because of a combination of different water flow distributions and different sediment input.

Chapter 4

Results

4.1 Sound engineering checks: modelling results

4.1.1 Selection of morphological parameters as developing river topography

Initial simulations

As stated in Chapter 3, discharge for the simulations was set to 5,000 and zero m^3/s for the inflow at the barrage and the Adda River, respectively. The tested initial topographies, reported in Figure 62 and indicated with "1" and "2" respectively were:

- IF-MS-Q_{5000}: generated by transversely flattening the channel bed and imposing as longitudinal slope the one evaluated by computing the mean bed elevation of submerged part of reference cross sections' channel.
- IF-M-Q_{5000}: generated by transversely flattening the channel bed and imposing as longitudinal slope the mean bed slope identified by ADBPO (2005b).

Following preliminary simulations testing different values of morphological parameters (not included in the present report) the inputs listed in Table 9 were selected to run the first two simulations. The known topography, as defined by the DTM-2005, and the morphological development following each of the three simulated months are shown in the following graphs.

Table 9. First two simulations run.

Simulation code	Initial topography	A_{sh}	E_{spir}	b	Incl. island	Q_Po / Q_Adda
1 - 0.3 - 1 - 5 (a)	IF-MS-Q_{5000}	0.3	1.0	5.0	no	5000/0
2 - 0.3 - 1 - 5 (a)	IF-M-Q_{5000}	0.3	1.0	5.0	no	5000/0

Modelling results showed that starting from initial topography 1 alternate bars initially formed in the stretch between the barrage and the Adda River mouth (bar 623 ranging between progressive 359 and 363), but that this pattern eventually changed because of the superimposition of the side bar in the inner bend of the meander. Contrarily, for initial topography 2, no alternate bars were forming, and planar configuration of bar 623 was accurately replicated (even the shallower internal channel was formed). In the first stretch of the meander, until the beginning of the large point bar

627, the model appeared to be accurately capturing the actual bar pattern. Further downstream the side channel internal to bar 627 was not forming for either initial topography 2, whereas the flow appeared to be concentrated in the outer bend and significant deposition occurred in the inner bend.

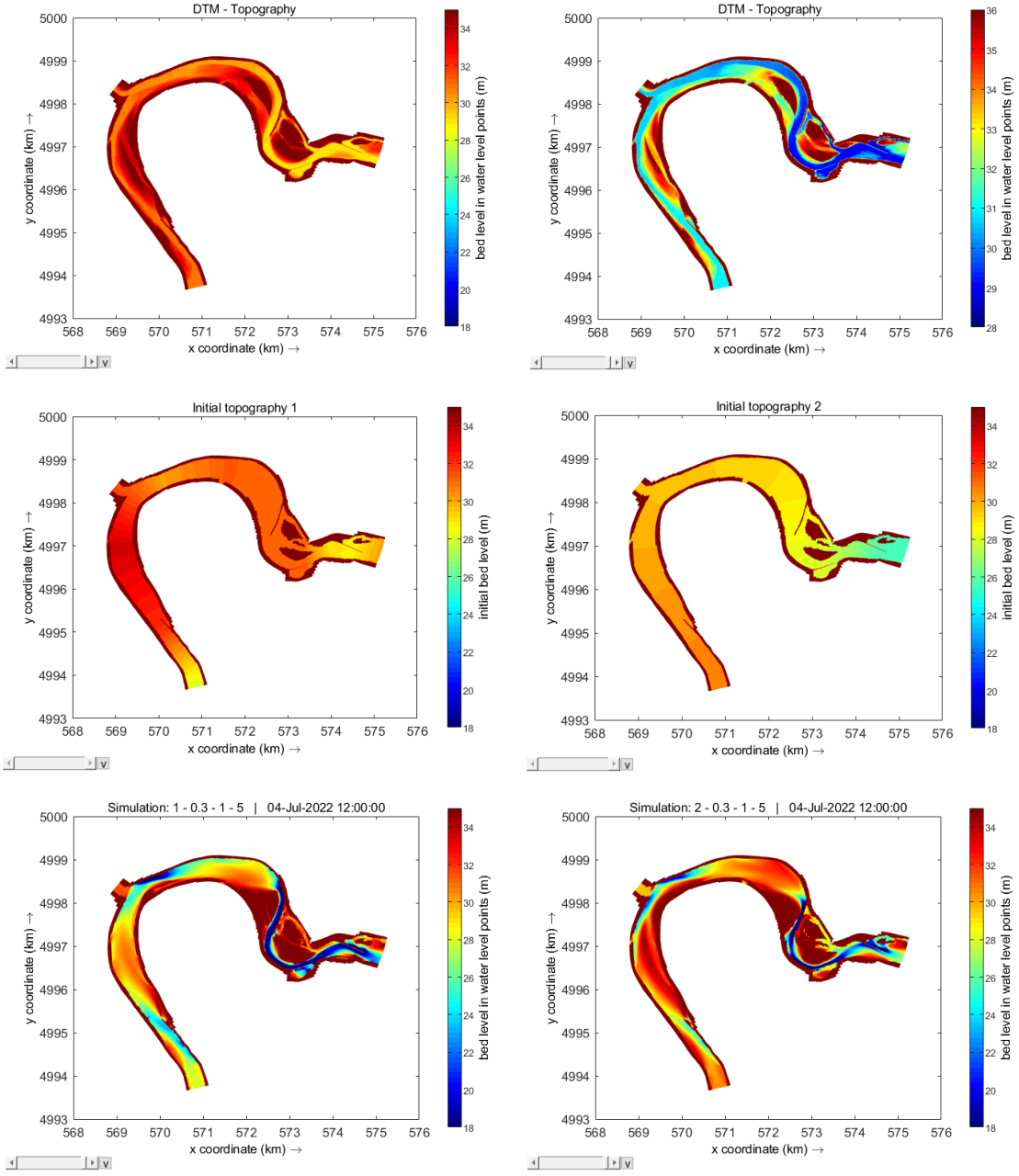

Figure 62. Top: known topography plotted with different colour limits such that to better appreciate known bedforms; Centre: initial bathymetries 1 and 2 without the presence of the fluvial island; Bottom: Results of the morphological development of the river after 3 months of constant flow from the barrage.

Moving to the cross-sectional comparison it was found that cross section S24, the one closest to the barrage, manifested essentially no morphological changes because of the default option imposed for the transport condition at the open inflow boundary.

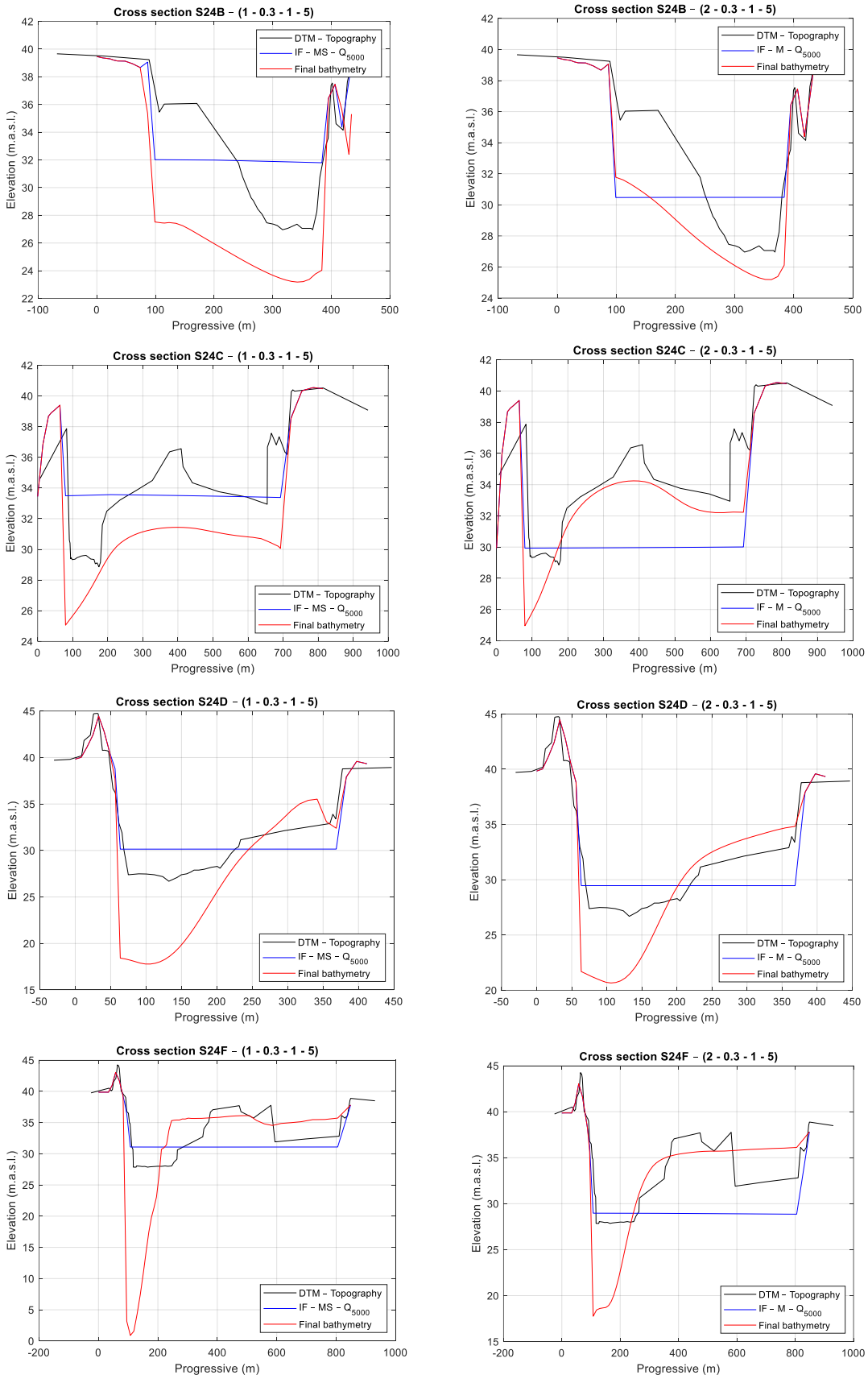

Figure 63. Cross sectional comparison of modelling results with known and initially flat topographies.

Flow conditions at cross section S24 are approximately equal to that in the first row of the domain thus determining negligible modification of bed levels. Literature review did not clarify whether the barrage locally do trap or not sediments. The stretch of the river just upstream of the barrage would probably not undergo changes over the long term, but the operation rule's impulsive activity seems to determine sedimentation during normal flows and sediment flushing during peak discharges. I was decided, however, to adopt the default option for then transport condition given the difficulty in quantitatively estimate the actual sediment regime. Moreover, topographic survey of cross section S24 also detected the local scour immediately downstream of the barrage (see Oldani et al., 2008) that reasonably was generated by local 3D effect, hence the 2D shallow water model is not useful for its investigation.

The bar pattern was correctly captured along cross section S24B for both initial bathymetries (Figure 64), but it wasn't so for bed elevations (especially with topography 1) that resulted extremely reduced. This was presumably attributable to insufficient upstream sediment supply, suggesting that these bars were formed by surplus of sediment transport during peak discharges. This also applied to cross section S24C starting from initial topography 1, whereas starting from initial topography 2 bar 623 was correctly reproduced even though excessive deepening of the low-flow channel occurred.

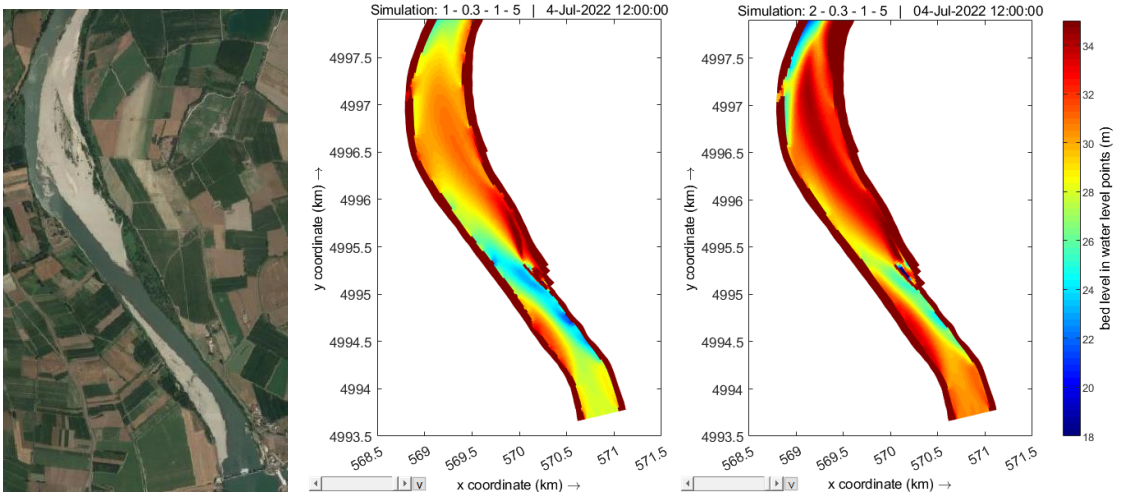

Figure 64. On the left: Orthophoto of 2020 showing the bar pattern along the first 5 km of the mender loop; Centre: Modelling result obtained with initial topography 1; On the right: Modelling result obtained with initial topography 2.

Reduction of the sediment transport's degree of nonlinearity

Results from cross sections S24F (Figure 65) and S25 showed that the channel narrowed and deepened consequently to an excessive erosion of a part of the incised channel. Presumably, the flow seemed to excessively concentrate. Sediment transport rates' measurements were not available from literature, thus also the 1D morphological calibration was not possible such that to assess the more suitable sediment transport formula to be used. Nevertheless, simulations with a lower degree of nonlinearity of sediment transport were run, assuming that, by reducing it and thus by decreasing the effect of sediment removal, the flow would have distributed more uniformly within the incised channel. Based on experience (Deltares, 2022, personal communication), the

Engelund-Hansen formula was replaced with a General formula whose degree of nonlinearity was set to be 3.8. Additionally, an intermediate value of 4.2 and a second simulation imposing b equal to 3.8 with a calibration coefficient twice as large as the first one adopted (α=20 rather than α=10) were tested, resulting in a set of eight simulations to be executed.

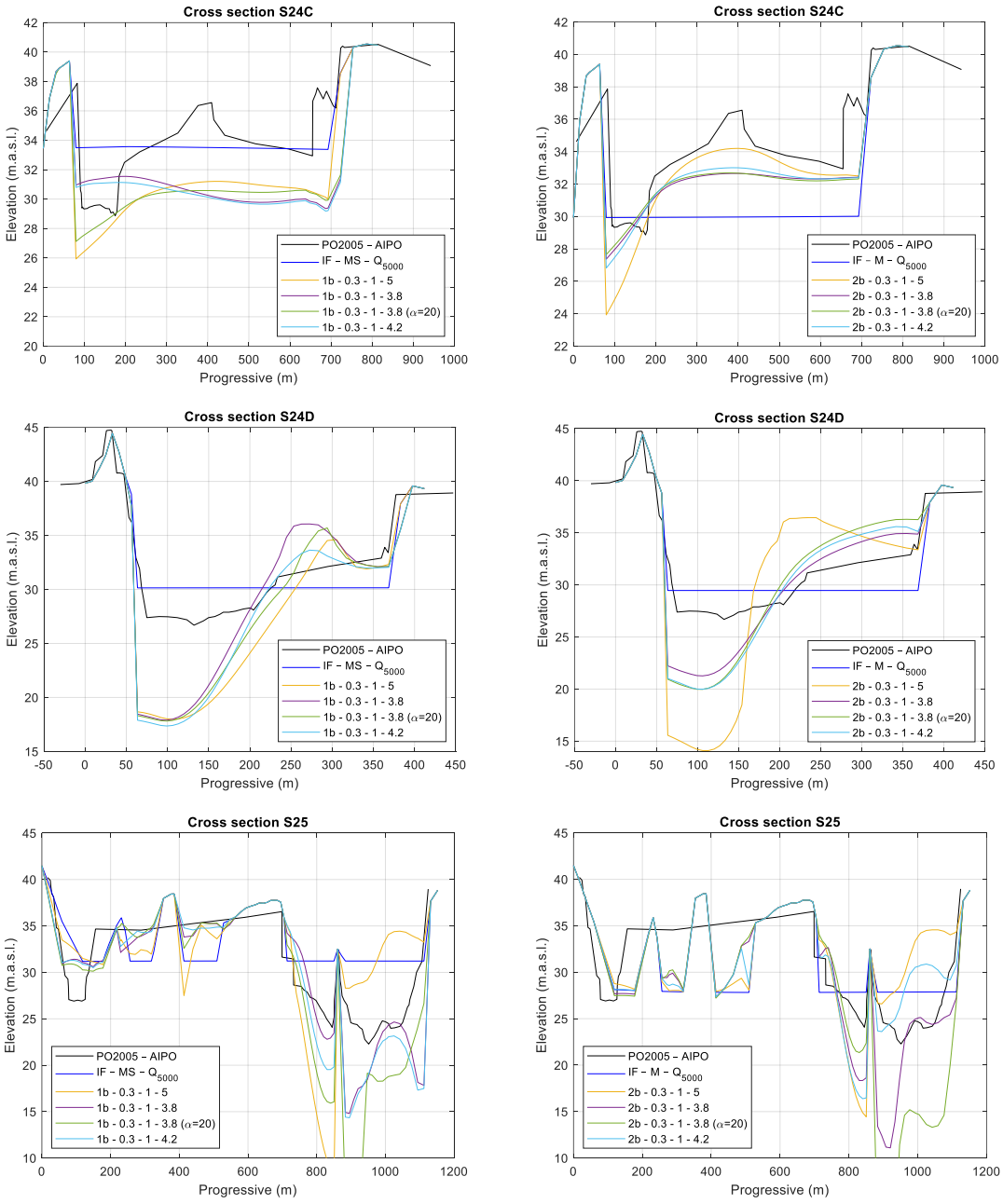

Figure 65. Cross sectional comparison of known and initially flat topographies with modelling results obtained by varying the value of degree of nonlinearity of sediment transport.

The full modelling results are reported in Appendix C. Modelling results demonstrated that, beginning with topography 2 (i.e., IF-M-Q5000), the low flow channel and bars' elevation and bar pattern fit the known topography more closely, as shown in Figure 65. For that reason, it was decided to run further analysis only with initial topography 2. Moreover, less flow concentration was obtained (cross sections S24C and S24D of Figure 65), as expected by reducing the degree of

sediment transport nonlinearity, even though excessive erosion was still taking place next to progressive 367 and further downstream (Cross section S25 of Figure 65).

Table 10. Set of simulations imposing different values for the degree of nonlinearity of sediment transport.

Simulation code	Initial topography	A_{sh}	E_{spir}	b	Incl. island	Q_Po / Q_Adda
1b - 0.3 - 1 - 5 (b)	IF-MS-Q_{5000}	0.3	1.0	5.0	yes	5000/0
1b - 0.3 - 1 - 3.8	IF-MS-Q_{5000}	0.3	1.0	3.8	yes	5000/0
1b - 0.3 - 1 - 3.8 (α=20)	IF-MS-Q_{5000}	0.3	1.0	3.8*	yes	5000/0
1b - 0.3 - 1 - 4.2	IF-MS-Q_{5000}	0.3	1.0	4.2	yes	5000/0
2b - 0.5 - 0.5 - 3.8	IF-M-Q_{5000}	0.3	1.0	5.0	yes	5000/0
2b - 0.5 - 0.3 - 3.8	IF-M-Q_{5000}	0.3	1.0	3.8	yes	5000/0
2b - 0.3 - 1 - 3.8	IF-M-Q_{5000}	0.3	1.0	3.8	yes	5000/0
2b - 0.3 - 1 - 3.8 (α=20)	IF-M-Q_{5000}	0.3	1.0	3.8	yes	5000/0
2b - 0.3 - 1 - 4.2	IF-M-Q_{5000}	0.3	1.0	4.2	yes	5000/0

Sensitivity analysis on the morphological parameters (A_{sh} and E_{spir}).

Modelling results obtained by imposing a degree of nonlinearity equal to 3.8 were the ones closest to the actual topography in terms of shapes of the bars and depth of the channel (Figure 65). Hence, it was decided to run a set of simulations (Table 11) such that to combine different values of the morphological parameters A_{sh} and E_{spir}.

Table 11. Set of simulations imposing different values for the morphological parameters Ash and Espir.

Simulation code	Initial topography	A_{sh}	E_{spir}	b	Inclusion island	Q_Po / Q_Adda
2b - 1 - 1 - 3.8	IF-M-Q_{5000}	1	1	3.8	yes	5000/0
2b - 1 - 0.5 - 3.8	IF-M-Q_{5000}	1	0.5	3.8	yes	5000/0
2b - 1 - 0.3 - 3.8	IF-M-Q_{5000}	1	0.3	3.8	yes	5000/0
2b - 0.5 - 1 - 3.8	IF-M-Q_{5000}	0.5	1	3.8	yes	5000/0
2b - 0.5 - 0.5 - 3.8	IF-M-Q_{5000}	0.5	0.5	3.8	yes	5000/0
2b - 0.5 - 0.3 - 3.8	IF-M-Q_{5000}	0.5	0.3	3.8	yes	5000/0
2b - 0.3 - 1 - 3.8	IF-M-Q_{5000}	0.3	1	3.8	yes	5000/0
2b - 0.3 - 0.5 - 3.8	IF-M-Q_{5000}	0.3	0.5	3.8	yes	5000/0
2b - 0.3 - 0.3 - 3.8	IF-M-Q5000	0.3	0.3	3.8	yes	5000/0

The full results are reported in Appendix D whereas the main ones are shown in Figure 66. Simulations “2b - 1 - 1 - 3.8”, “2b - 1 - 0.5 - 3.8” and “2b - 0.5 - 1 - 3.8” abnormally ended before the end of the computational time frame (set for 04-Jul-2022 12:00:00) and were not plotted in the cross-sectional comparison. Deciding which modelling results fit the topographic survey better was challenging since any method of assessment appeared to be suitable given the complex cross-sectional profile of bars. More emphasis was placed on analysing cross-sections that were closest to the barrage because these were of greater interest for the additional analysis to be performed with the third second research question (i.e., cross-sections S24B/C/D/E). Modelling results of simulation "2b - 0.3 - 1 - 3.8" qualitatively fit the real topography the best when cross sectional profiles were compared.

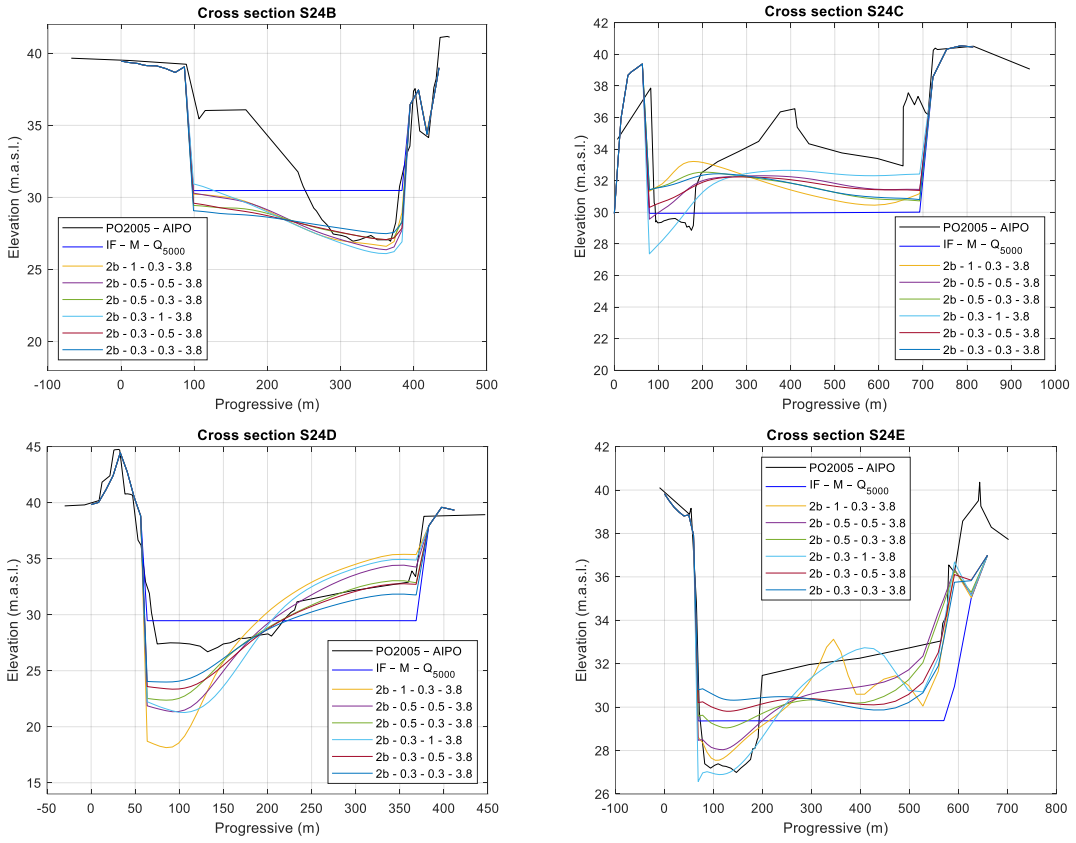

Figure 66. Cross sectional comparison of known and initially flat topographies with modelling results obtained by varying the value of morphological parameters Ash and Espir.

The highest discharge with a sufficiently high frequency of occurrence, 5,000 m^3/s, was chosen to study the morphological development of the channel. It would have been possible to run additional simulations by imposing lower discharges, but it should be noted that by doing so it would have resulted in an initial width-to-depth ratio of the channel being higher, which could have led to the development of multiple bars rather than an alternate bars pattern (Crosato & Mosselman, 2009). A further possible analysis could have concerned the simulation of lower discharges on a transversely flat topography flattened with respect of widths of the channel associated to each specific discharge analysed, as it was tested, indeed. A simulation with 4,000 m^3/s flowing on the initial topography IF-M-Q_{4000} was run but the elevation of bars was, as conceivable, lower than the one obtained with 5,000 m^3/s and therefore farther away from the actual topography.

4.1.2 Other observations from modelling results

Aside from creating a topography that sufficiently replicates the real one, the results also allowed to draw up some conclusions and observations that could be useful for river restoration and management.

Longitudinal training wall between progressive 358 and 359

As previously mentioned, simulation "2b - 0.3 - 1 - 3.8" accurately depicted the zone of crossover of the flow from bars 633 and 623. The talweg moves parallel to the longitudinal training wall from the right bank upstream of progressive 358 to the left bank downstream of progressive 359 passing through sections where the incised channel narrows. Then it proceeds leaning against the left bank for the entire stretch of the course up to the Adda River's mouth. Additionally, it can be noted that the apex of bar 623 coincides with the downstream end of the bank erosion area (Figure 40). With a view to testing whether this configuration depends on the longitudinal training wall and whether the extension of bar 623 is affected by its presence, it was decided to run a simulation in its absence. The simulation was named "no long. train. wall" and consisted of the same inputs of simulation "2b - 0.3 - 1 - 3.8" except for the initial topography that was modified by eliminating the longitudinal training wall, flattening the channel bed and the imposing bed level values of the adjacent cells (top of Figure 67). Results revealed a slight variation in the channel's morphological development, with a less pronounced crossover area even though bar 623 showed nearly identical planar extension and elevation (centre of Figure 67).

This suggested that the longitudinal training wall may be considered irrelevant to the development of bar 623 and consequently for the planimetric layout of the local talweg. Conversely, as stated in section 3.1.2, the training wall induced the depositional area that has been designated as Habitat 3150 and Habitat 9A20 (Natura 2000). Moreover, modelling results indicated that the latter was associated with a zone of low velocities and stagnation of flow that occurs overleaf of the hydraulic structure, contributing to defining more heterogeneous flow conditions within the incised channel (bottom Figure 67).

The longitudinal training wall has also been marked as a non-strategic structure to be monitored in time so that to evaluate its progressive removal (ADBPO, 2005b). Although modelling results indicated that the training wall may be not relevant both to development of bar pattern and generation of the low-flow channel set-up, thus it does not establish unfavourable conditions for the stability of defence works, they also supported its significance in terms of producing heterogeneity and diversity and eventually the training wall may be considered a strategic structure from the perspective of river restoration.

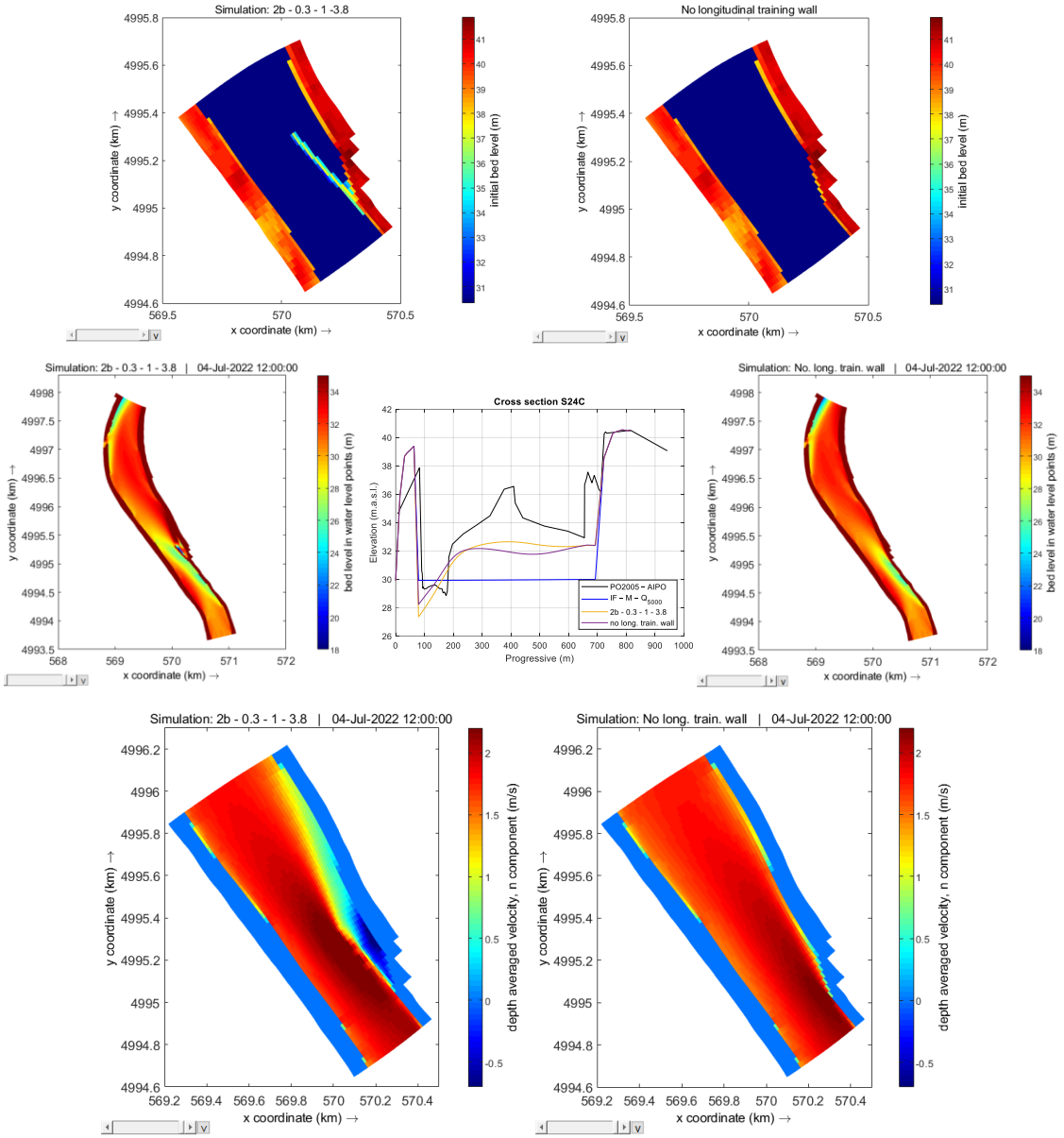

Figure 67. Top: Maps of the stretch with the initial flat topography and the modified one; Centre: Maps of the final bed levels obtained with and without the training wall and cross-sectional comparison of the first downstream cross section (S24C); Bottom: maps of the longitudinal component of the local depth average velocities.

Deepening of the outer bend between the Adda River mouth and progressive 364

All modelling results depicted the local deepening of the thalweg between the Adda River mouth and official progressive 363 (Cross section S24D). This was located upstream of at the apex of the major meander bend where the curvature of the channel is imposing a point bar in the inner bend (downstream end of bar 623), concentrating the flow toward the outer bend (Figure 68). It must be specified that the 2D model was set to compute only bed level changes on grid cells that are submerged and thus ignoring riverbank retreat linked to lateral erosion. As lateral erosion was arrested by grid cells that remained dry, lateral input of sediments was arrested too, and the river was entraining sediment from the bottom only that was therefore eroding along the outer bend. Consequently, stretches of potential bank erosion were detectable in locations where modelling

results showed local deepening of the channel, linked to high shear stress values (such as in Figure 70). Such deepening wouldn't have happened if banks were erodible and lateral movements were kept free, but as it was noticed during the survey, banks are locally protected by bank defences consisting of boulders that prevent lateral erosion (Figure 47).

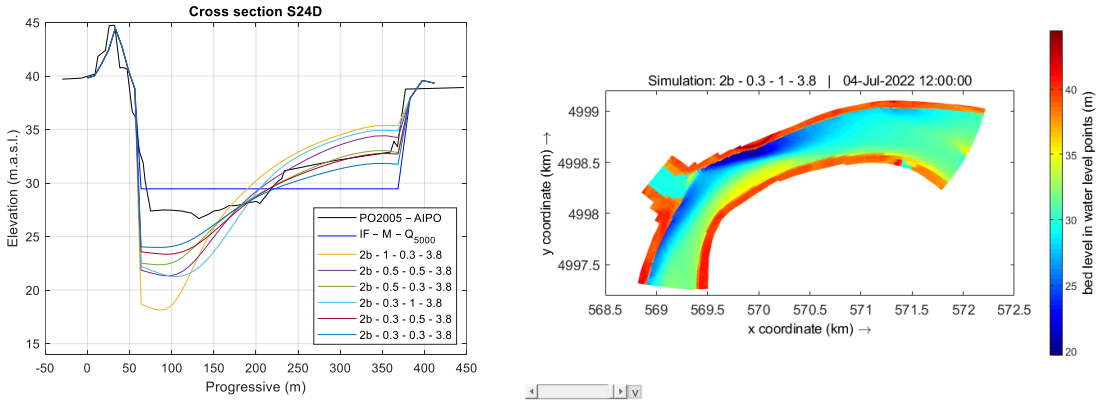

Figure 68. On the left: cross-sectional comparison of the modelling results obtained varying the morphological parameter at cross section S24D; On the right: map of the obtained final bed topography showing the erosion area.

When approaching progressive 362 (just upstream of the Adda River mouth) the width of the incised channel reduces, and the concentrated flow impact against the left bank (downstream of the Adda River mouth). Outwards concentration of the flow was increased by the formation of the point bar along the inner bend adjacent to the area in which secondary flows were higher.

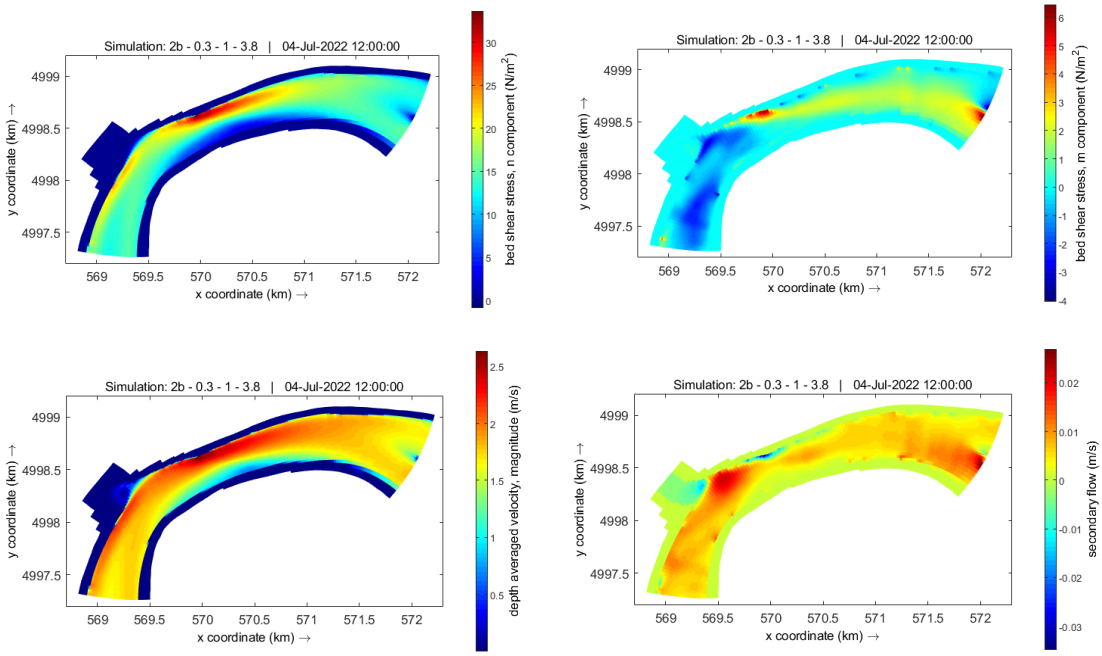

Figure 69. Maps of shear stress and velocity distributions along the stretch that experienced erosion.

If such deepening of the channel predicted by the model is reliable but incompatible with the stability of the defence work, restoration measures may be required. The bank defence is necessary to ensure the main dike stability. It is situated between 30 and 90 meters from the bank line and

replaces the cut bank feature that would have been connected to the point bar forming in the inner bend. The removing of the bank defence may not be affordable up to date without firstly setting back the main dike. Therefore, one option would be to move the main dike outward from the bend and restoring the erodible corridor between the former and the bank line. The so re-established deposition-erosion bank processes could be controlled by implementing adaptive sediment management strategies such as local bank nourishments. Potential bank retreat could also be controlled taking advantage of the sediment trapping action exerted by plants through restoring riparian vegetation.

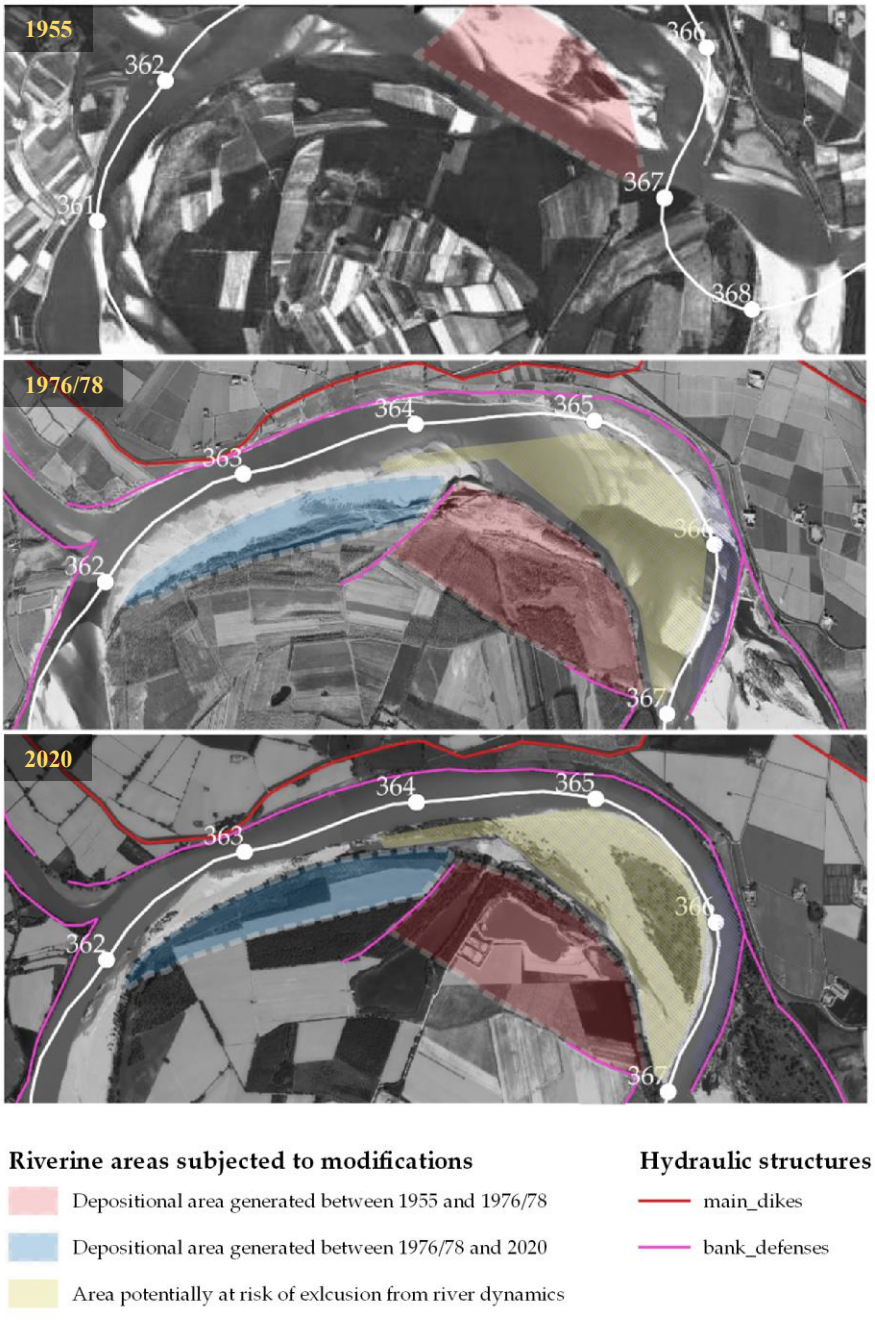

Figure 70. Depositional area generated from 1955 to date.

Other kind of measures could be implemented aiming to enlarge the incised channel by excavating the inner bend and nourishing the low-flow channel (the latter has been proposed by ADBPO

(2005b)). Consequently, a wider wet area would be guaranteed for both low-flow and high-water flow conditions, contributing to redistributing the flow towards the inner bend. With respect of the possible areas of excavation is it worth noting that great portions of the past incised channel are nowadays completely disconnected from the fluvial dynamics. It is the case of the areas marked in red and blue of Figure 69. Apparently, the construction of the defence work located in the hydraulic right between progressives 364 and 365 and the longitudinal wall between progressive 366 and 367 jointly contributed to the deposition of about 85 ha overleaf of the former structure in an area where the course was split in two channels by a central bar. Deposition seems to be occurred even on the side bar located along the right bank between progressive 362 and 364, depriving approximately 45 ha from the river dynamics.

The local deepening, however, detached by modelling results, hadn't been detected by the topographic survey PO 2005 – AIPO. Nonetheless, the entire left bank ranging from the Adda River mouth to official progressive 366 was classified by the Po Basin Authority as a defence work subjected to direct hydrodynamic action (ADBPO, 2005b). Moreover, limited stretches have been identified as prone and potentially prone to erosion and consequently declared as to be monitored over time.

Excessive flow concentration at the longitudinal training wall between progressives 366 and 367

Results showed that the approximately 1,000 m long longitudinal training wall, which is located on the hydraulic left between progressive 366 and 367, was directing the flow against the defence work constructed along the outer bend of the point bar 616.

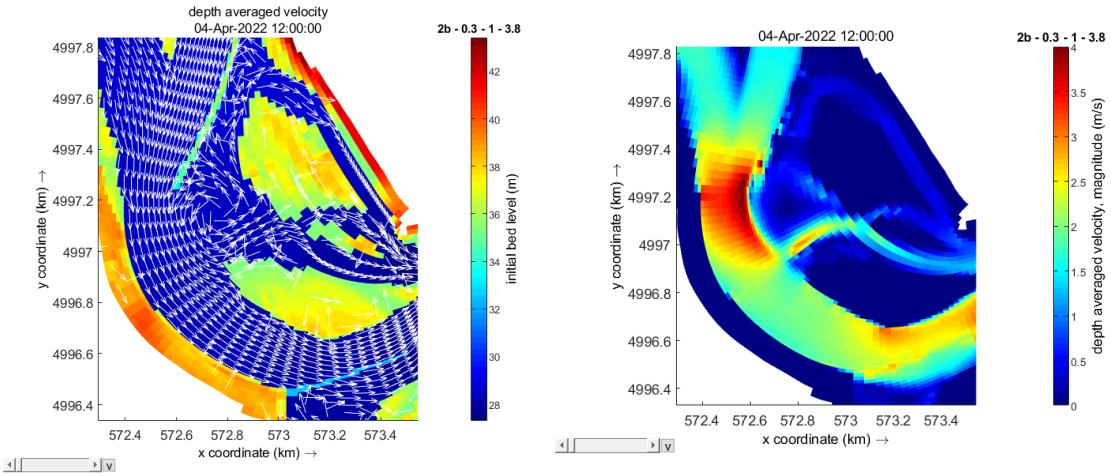

Figure 71. On the left: the flow didn't top the training wall and a recirculation cell formed overleaf of the head of the training wall.

Considering initial conditions (transversely flat topography) the constant discharge of 5,000 m^3/s flowed exclusively through a relatively narrow section of the incised channel's width (200 m over a length of about 900 m) and the longitudinal training wall was not topped by water (on the left of Figure 71). According to ADBPO (2022), only discharges greater than 6,000 m^3/s cause water to flow over the hydraulic structure, so the simulated initial flow conditions could be considered appropriate. The computed main flow followed the navigation curves imposed by the training

works. A recirculation cell separated from the main flow at the head of the longitudinal training wall, and only the smaller secondary channel internal to the bar carried a percentage of the current in the streamwise direction (on the right of Figure 71).

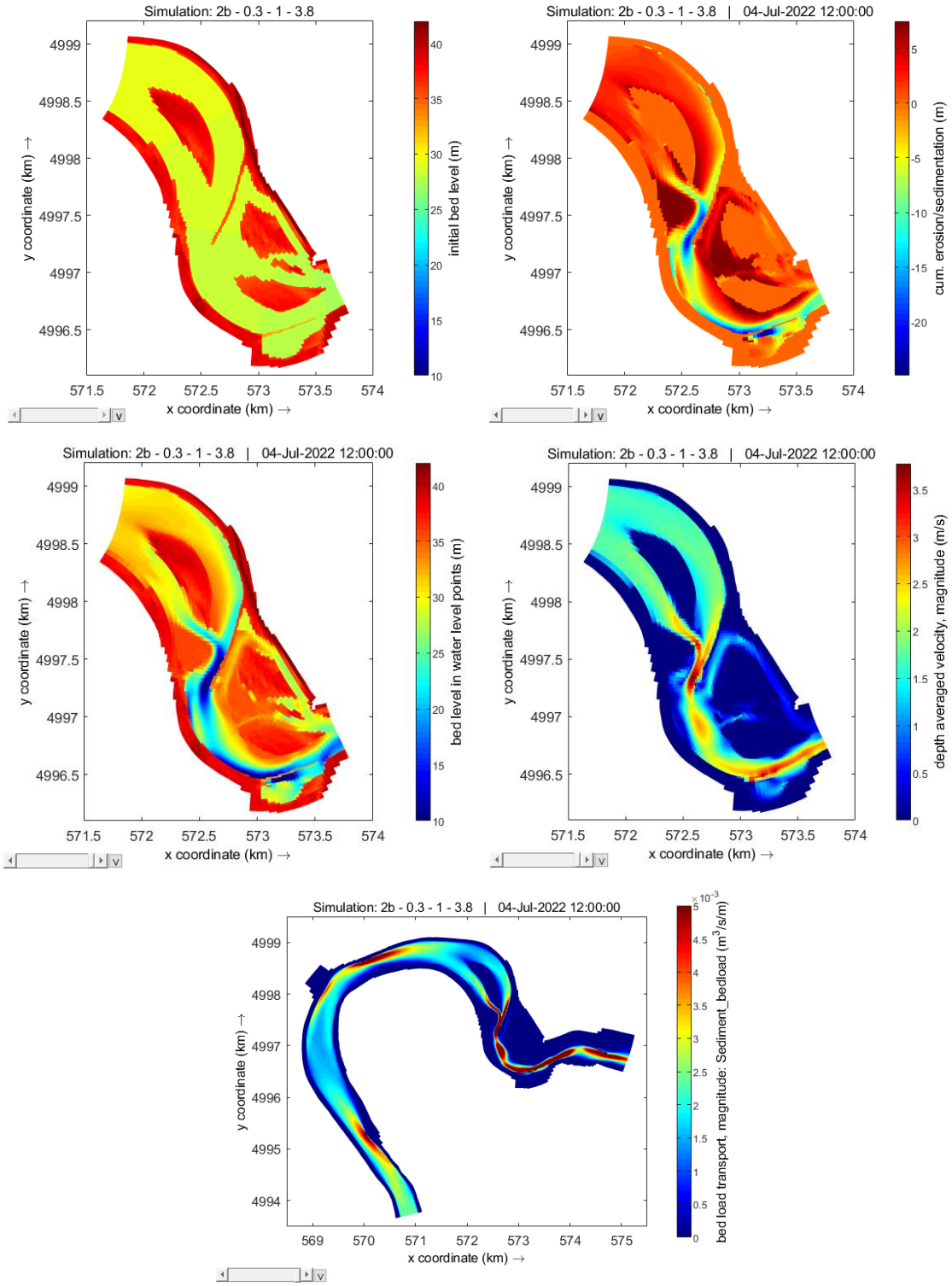

Figure 72. Top: initial bed elevation and cumulative erosion/sedimentation maps; Centre: final topography and depth averaged velocity maps; Bottom: Bed load transport map.

Associated to these flow conditions sedimentation was expected to occur overleaf of the longitudinal training wall, leading to the progressive clogging of the channels inside the depositional area. Indeed, low flow velocities translated into areas of great deposition on the back of the hydraulic structure up to the point that, at the end of the simulation, the flow was entirely conveyed along the outer bend (Figure 72).

Furthermore, the excessive concentration of flow at the head of the longitudinal training wall imposed extremely high flow velocities and associated high shear stresses, which were responsible for the local bed erosion. The flow concentration was further increased by sediment deposition at the outlet of the secondary channel internal to point bar 627, upstream of the head of the longitudinal training wall, resulting in an unrealistic topographic configuration. The other two longitudinal walls located further downstream contributed to restrict morphological dynamics such that effective sediment transport from progressive 367 to the end of the computational grid took place only in a narrow section of the channel (Figure 72).

To summarize, the applied method did not permit t to accurately reproduce the topography of this stretch of the meander with, and thus the obtained results must be regarded as purely qualitative. Nonetheless, the findings supported the necessity of lowering the height of the longitudinal training wall, as proposed by ADBPO (2022).

4.2 Hydro-morphological influence of asymmetrical inflows from the barrage

4.2.1 Short-term conditions (hydraulic)

Following the procedure explained in section 3.3.1, λ_w was assessed for simulation "sym", obtaining a value of 735 m. Graphs of Figure 73 report the transverse profile of depth-averaged streamwise flow velocity obtain for simulations "asym-sx-4" and "asym-dx-4" at the barrage and at distances of λ_w and $3\lambda_w$ from the barrage along with corresponding value of the symmetrical simulation. Each transverse profile consisted of point values associated to each of the grid cell that makes up specific N-column of the computational grid, namely the first one referring to the barrage and the N-column which mean distance from the previous one was equal to λ_w and $3\lambda_w$.

Perturbation of the transverse profile of streamwise velocity at the barrage progressively decayed moving downstream. At a distance of $3\lambda_w$ from the barrage the perturbation term was almost completely vanished, and the transverse profile of asymmetrical simulations approximately correspond to the one of symmetrical inflow. Table 12 reports the values of mean perturbation in the transverse profile of depth-averaged streamwise flow velocity $\overline{|u'|}$ computed at the three distances for each simulation along with the corresponding residual percentage that according to

the linear theory should be equal to 36% and 0.05% at distances of λ_w and $3\lambda_w$ respectively. These values were substantially in line with what expected by the Delft approach to the linear bar theory, demonstrating the predictive power of such theory when used as first-assessment analysis.

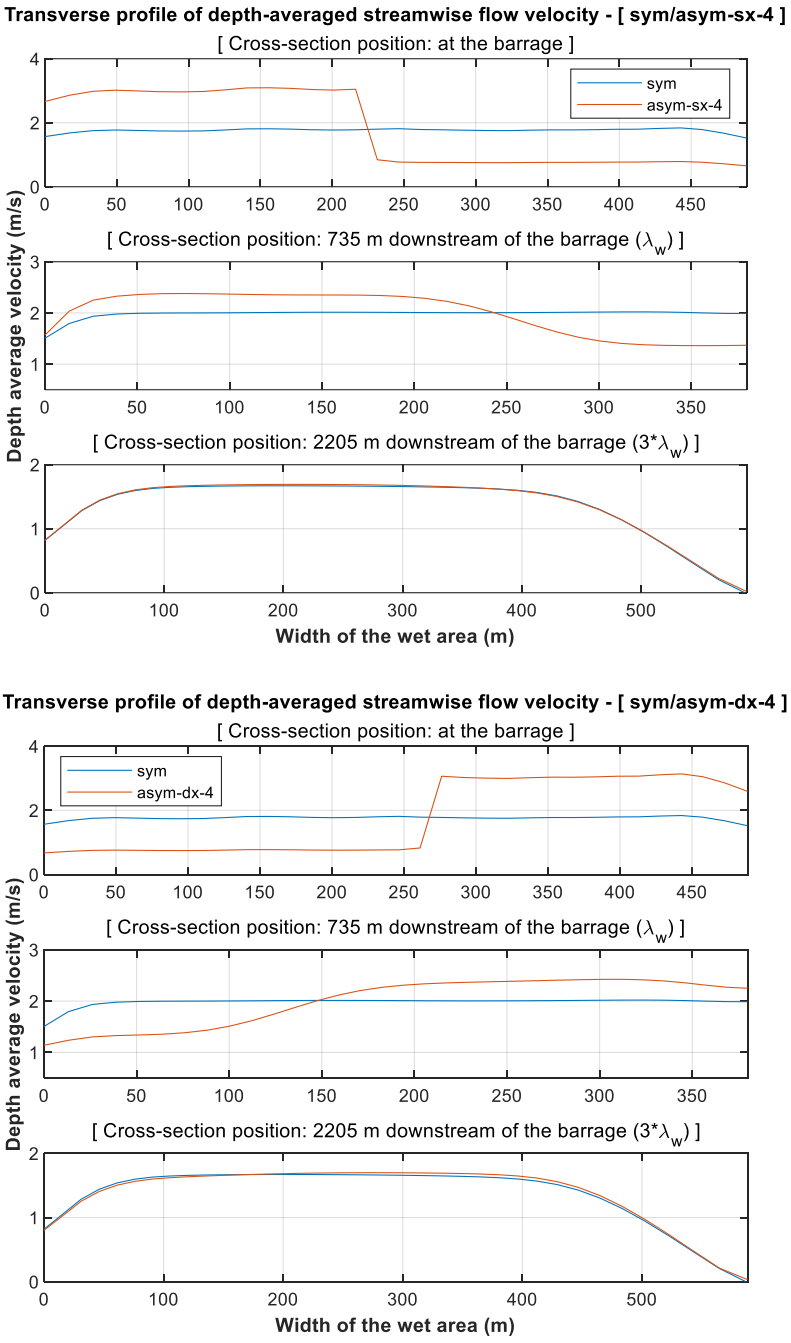

Figure 73. Transverse profiles of depth-averaged streamwise flow velocity obtained for simulations "asym-sx-4" and "asym-dx-4". Results for simulations "asym-sx-2" and "asym-dx-2" are reported in Appendix E.

Graphs on top of Figure 74 show maps of the streamwise component of depth average velocity for simulations "sym" and "asym-dx-4". The cross-sectional distribution of flow for asymmetrical flow corresponded to the one produced with the symmetrical simulation at approximately 2500 m from the barrage, where the incised channel widens, downstream of the narrower sections. Therefore, significant differences between symmetrical and asymmetrical simulations in the

channel topology were not expected to take place when medium-term analyses were performed. But as already mentioned, variations of discharges at the open boundary translates into different sediment rates entering the system and morphological development will be consequently impacted. Table 13 reports the total bed load transport rates at the open boundary for each of the simulations performed as mean bed load transport rate per unit width $\overline{q_{s_i}}$ for the left and right hand of the barrage and as total bed load transport through the entire barrage $q_{s_{tot}}$. The graph of Figure 75 shows cross-sectional profiles of bed load transport evaluated at the first N-column of the computational grid. The total bed load transport of simulation "sym" was approximately the 60% and the 30% of relative values of simulations "asym-sx-2"and "asym-dx-2" and simulations "asym-sx-4" and "asym-dx-4", respectively. Graphs on bottom of Figure 74 reveals that within three times λ_w, the bed load transport occurred almost entirely to the side where the discharge is higher. Further downstream, when the perturbation induced by the asymmetrical flow vanished, the solid transport corresponded to the undisturbed case.

Table 12. Mean perturbation and corresponding residual percentage of transverse profile of streamwise flow velocity.

		Distance from the source of perturbation [m]		
		$s = 0$	$s = \lambda_w$	$s = 3 \cdot \lambda_w$
asym-sx-2	$\overline{\lvert u' \rvert}$ **[m/s]**	0.597	0.202	0.011
	$\%\overline{\lvert u' \rvert}_{res}$ **[-]**		33.8%	1.84%
asym-sx-4	$\overline{\lvert u' \rvert}$ **[m/s]**	1.11	0.376	0.013
	$\%\overline{\lvert u' \rvert}_{res}$ **[-]**		33.9%	1.17%
asym-dx-2	$\overline{\lvert u' \rvert}$ **[m/s]**	0.598	0.204	0.019
	$\%\overline{\lvert u' \rvert}_{res}$ **[-]**		31.4%	3.18%
asym-dx-4	$\overline{\lvert u' \rvert}$ **[m/s]**	1.113	0.381	0.029
	$\%\overline{\lvert u' \rvert}_{res}$ **[-]**		34.2%	2.61%

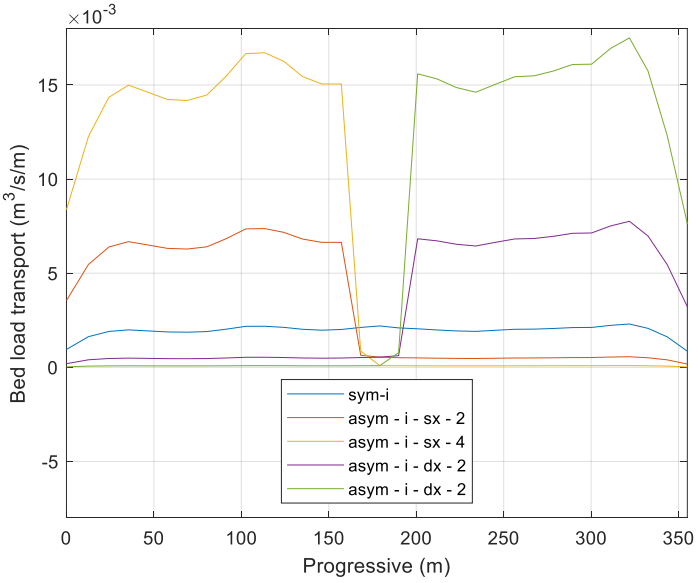

Figure 74. Transverse profile distribution of bed load transport at the first N-column of the computational domain.

Table 13. Mean bed load transport rate per unit width for the left and right half of the barrage.

	$\overline{q_{s_{sx}}}$ [m^3/s/m]	$\overline{q_{s_{dx}}}$ [m^3/s/m]	$q_{s_{tot}}$ [m^3/s]
sym	1.946 x 10^{-3}	1.946 x 10^{-3}	0.714
asym-sx-2	6.428 x 10^{-3}	0.49 x 10^{-3}	1.186
asym-sx-4	14.542 x 10^{-3}	0.122 x 10^{-3}	2.489
asym-dx-2	0.481 x 10^{-3}	6.597 x 10^{-3}	1.184
asym-dx-4	0.116 x 10^{-3}	14.955 x 10^{-3}	2.489

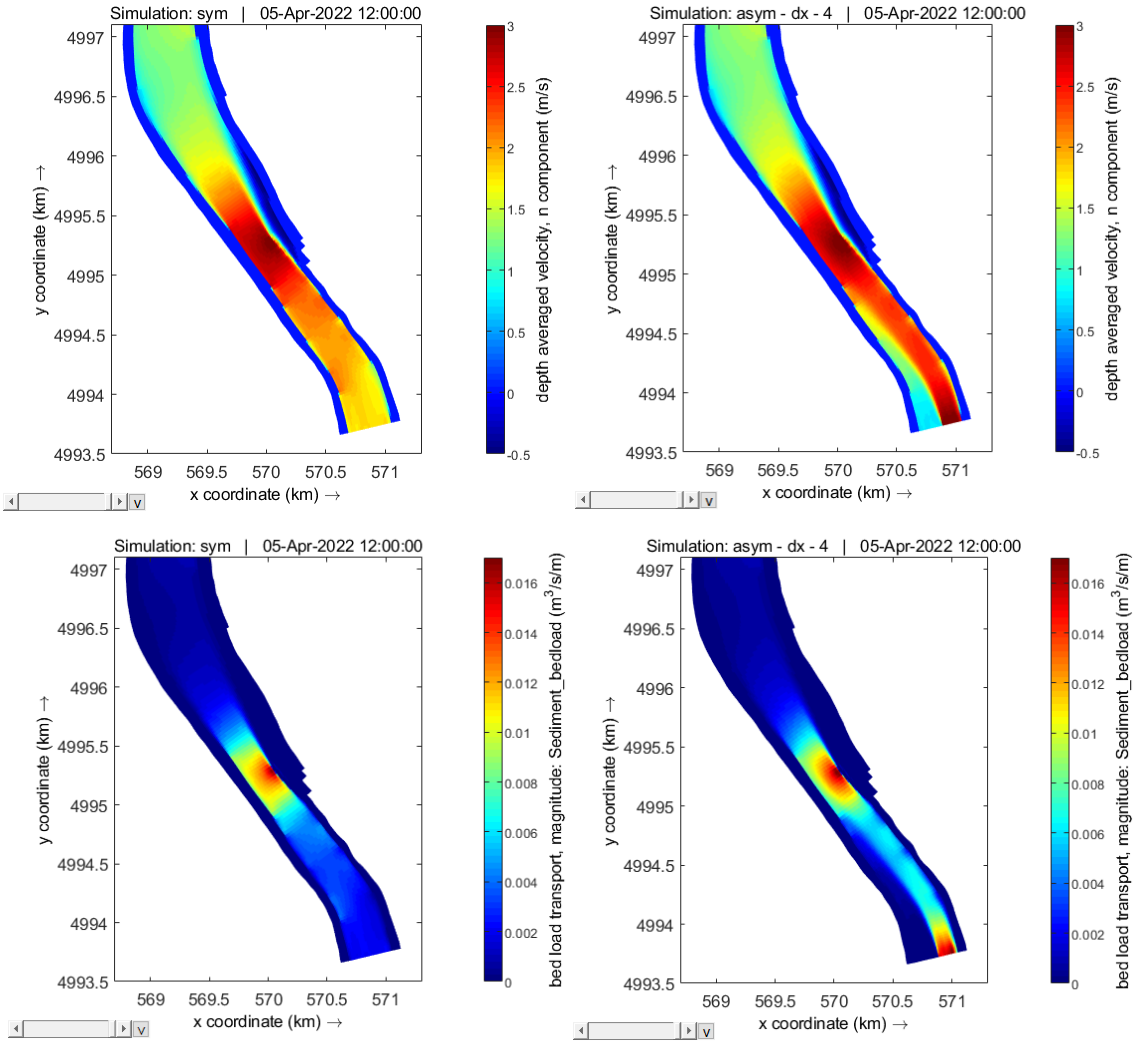

Figure 75. Top: Map of n-component of depth-averaged velocity distribution obtained with simulations "sym" and "asym-dx-4"; Bottom: Map of bed load transport distribution obtained with the same simulations.

4.2.2 Medium-term conditions (morphodynamic)

As was expected given the greater input of sediments from the open boundary, modelling results of simulations with asymmetrical inflows led to higher bedform elevations. In comparison to the scenario of symmetrical flow, simulations with greater rates through the gates on the left side of the barrage showed larger slopes in the shape of cross section S24B (Figure 76 and Figure 77).

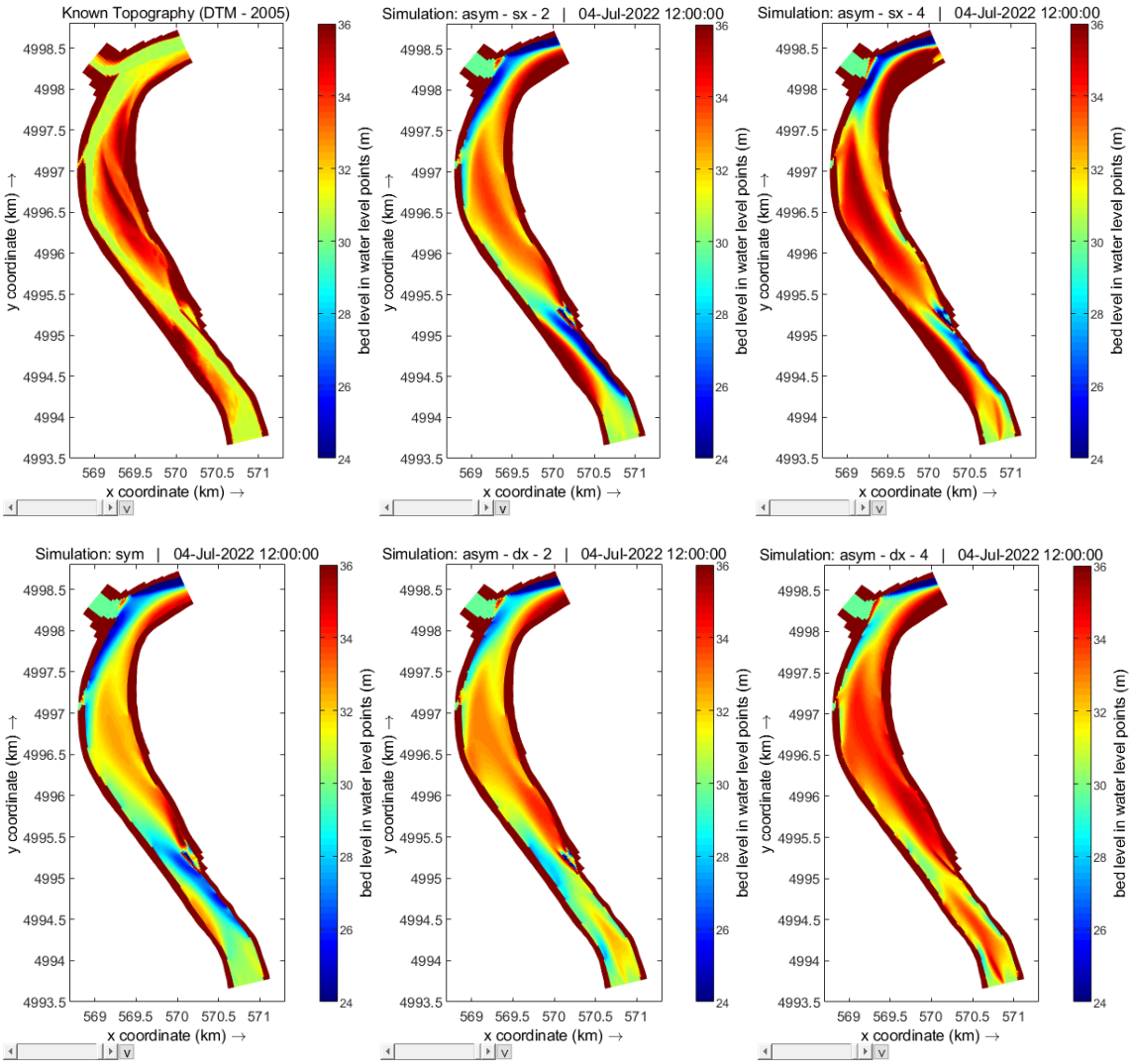

Figure 76. Final bed level distribution obtained with simulations of symmetrical and asymmetrical inflows.

The results of simulation "asym-sx-2" revealed a deeper low-flow channel and a more elevated bar (bar 633), whereas "asym-sx-4" resulted in an average rise in bed elevation of about 2 meters with respect of simulation "asym-sx-2", with cross section S24B that perfectly matched the known one. On the other hand, asymmetrical inflows with higher discharges from the right side of the barrage caused sediment to accumulate in the centre of the channel up to one km and half from the barrage. Furthermore, transverse slope in section S24B was inverted, with bar 633 not developing at all. Simulation “asy-sx-2” led to a slight increase in the elevation of bar 623 at the centre of the channel whereas the bottom of low-flow channel remained at the same level. In contrast, simulation "asy-sx-4" produced more significant changes, with bed levels remaining roughly the same within 200 meters of the right bank, whereas between progressives 100 and 500 of cross section S24C, the channel experienced an elevation increase of roughly 4 meters compared to simulation "sym". With simulation "asym-dx-2," the bed elevation was raised only along the left half of cross section S24C; this rise accounted for around 2 meters on the outer bend, which gradually reduced up to null value reaching progressive 400. Results of simulation "asym-dx-4"

were different from the previous ones since higher bed levels were reached above the region of bar 623 by around 1-2 meters.

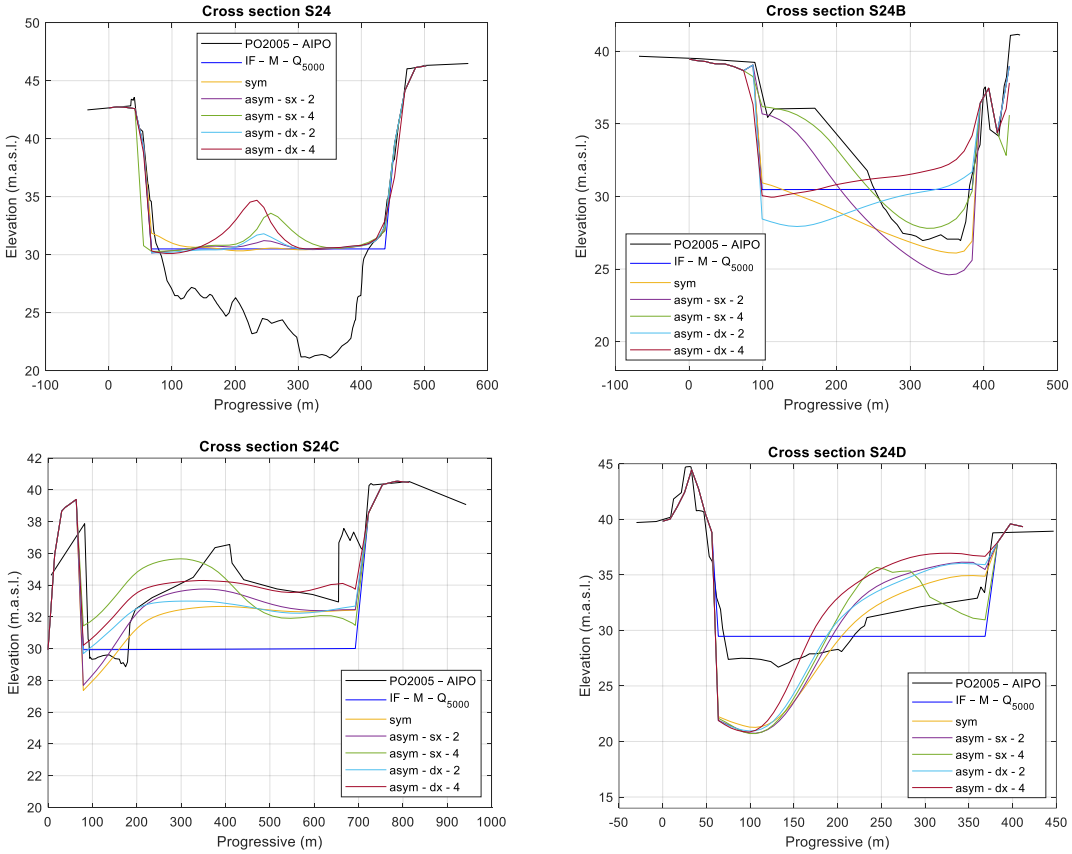

Figure 77. Cross sectional comparison of modelling results obtained with asymmetrical inflows.

The morphological evolution of the channel was roughly the same for all simulations from section S24D to the end of the computational domain. Equal low-flow channel depths were attained along cross section S24D, and almost identical point bar elevations in the inner bend were also reached.

Graphs of Figure 78 show how sediment transport varied from one simulation to the other. The bigger the amount of sediment that was entering the system, the higher the solid transport in the stretch of the river within 4 km from the barrage was. Additionally, it is noticeable that a more heterogeneous solid transport conditions, with areas of larger and lesser transport, manifested in the case of a greater inflow from the left side of the barrage (i.e., simulations “asym-sx-2” and “asym-sx-4”). Additionally, the secondary channel inside of bar 623 exhibited greater solid transport rates, especially in simulation “asym-sx-4”.

Overall, it can be concluded that the elevation gap between the low flow channel and the top of the bars increased due to larger releases from the left side of the barrage. However, with simulation "asym-sx-4," the outer bend next to cross section S24C experienced a significant elevation rise. The depth along the outer bend eventually reached the same height as the secondary channel inside bar 623, which may be a good condition for improving the transport dynamics along the latter. Conversely, simulations characterized by more flow from the right side of the barrage appeared to

produce flatter incised channel bathymetries, which could mean that the heterogeneity and dynamic conditions of the channel substantially reduced.

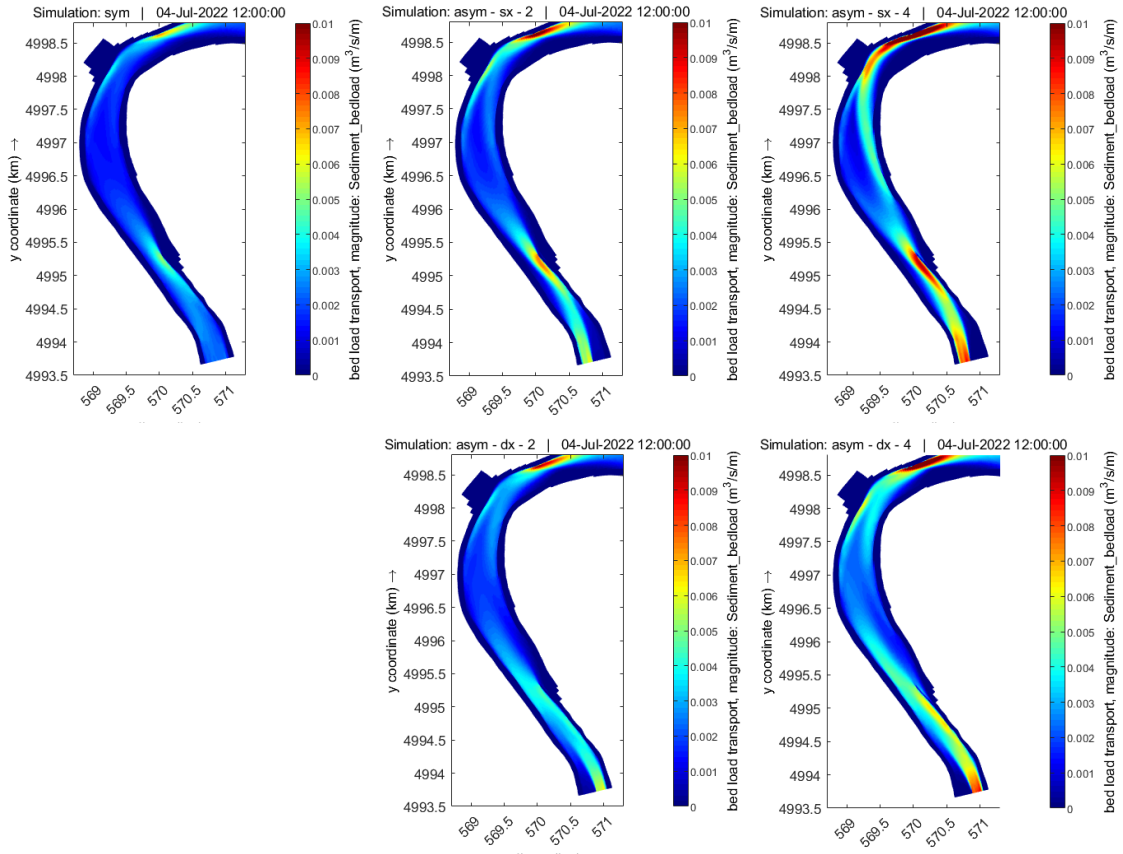

Figure 78. Maps of bed load transport obtained with symmetrical and asymmetrical inflows.

4.3 Twinning: Out-scaling of the Room-for-the-River approach to the Po River's restoration

Sections 2.1.4 and 3.1.1. explain how the Room-for-the-River approach, based on the principle of giving the river "more space for conveyance", translated also into more space for nature and dynamics. Moreover, as Mosselman (2022) remarked, a key message to take away is about "the importance of events and seizing of opportunities" to produce a paradigm shift in ordinary managements that can opens to fresh perspectives and create new possibilities by rejecting conventional thinking. In this regard, the present research was conducted during a period of prolonged and severe drought on the Po River (see ADBPO's 18/2022 Bulletin), demonstrating how urgent the problem of climate change's impacts is. The expectation is that the drought crisis will serve as a launchpad for a new approach to river and water resource management, like what happened in the Netherlands with the major problem of hydraulic safety.

The importance of floodplains and wetlands in sustaining the ecological integrity of river systems and providing ecosystem services, and thus in addressing climate change, is nowadays recognised, and confirmed throughout Europe (European Commission (2003a); European Environmental Agency (2019)). It was believed that the Po River Renaturation Plan appears to put too little emphasis on drought mitigation, underestimating the importance of sponge functions that provide peak attenuation and groundwater recharge, which floodplains should offer. On the contrary, the Plan recognises the significance of returning space to the river as evidenced through the proposal of interventions such secondary channel reopening and reactivation. However, since these measures are intended to rehabilitate river dynamics and promote biodiversity conservation, a better understanding of which hydro-morphological processes are expected to recover is required. To that end, 2D modelling might be a valuable tool for supporting the Po River restoration.

The question then emerged as to whether such new river space might be perceived as space for storage rather than for conveyance. The Room-for-the-River programme refers to different types of water storing, namely detention (i.e., "case di espansione" typically adopted along Italian rivers), storage and flowing storage (Silva et al., 2001). Since these measures generally entail substantial structural changes to the existing environment, they must assure respect for local natural features and landscape, and cultural characteristics, that is the improvement or conservation of spatial quality. Regarding the case study of Isola Serafini, water storage may be adopted, especially given the lack of active floodplains of the riverine area (Filippi et al., 2013) and the reduced flows along the meander. Left hand of Figure 79 illustrates the extensions of "Fascia di mobilità di progetto" (green areas) and "Fascia di tutela morfologica ed ambientale" (orange areas) mentioned in section 2.2.1. Even though these places are no longer active in normal hydro-morphological dynamics, they should be preserved for their landscape and environmental value due to the existence of riparian and aquatic habitats. Yet, the second map in Figure 79 shows that the same lands to be protected are now planned for arable corps and poplar groves.

The Po Renaturation Plan frequently refers to the reduction of the artificiality of the river as a restoration measure aimed to reduce human impact on the river. Since artificiality doesn't seems to be a common term generally used for describing man-induced river modifications, it could be useful to recall the concept of naturalness that may be considered to opposite of artificiality (but

as it was defined by Fryirs & Brierley (2009), see in section 2.1.3.). Naturalness is also related to how people perceive their surroundings and, as a result, to the site-specific notion of spatial quality. Hence, cultural values that define a territory's and its inhabitants' identities can also be related to naturalness (consider the Dutch polders, man-made landscape features that are now listed as UNESCO heritage sites for their historical and cultural significance, or Mosselman's observations (2022) about the historical use of Dutch rivers). Thereby, the Room-for-the-River programme never addresses the goal of reducing river artificialization, but rather focuses on the restoration of river functionalities and ecosystem services that may be obtained by operating on the existing river status.

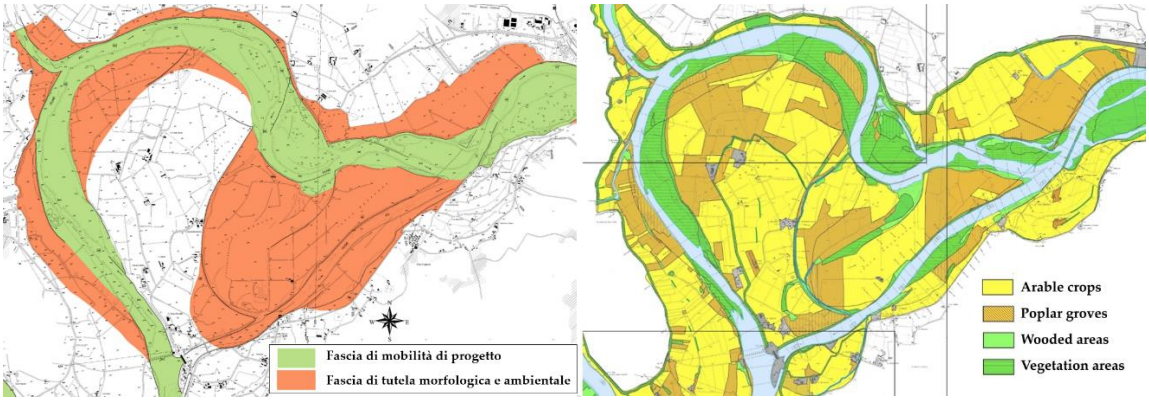

Figure 79. On the left: Map of *Atlante delle fasce di mobilità morfologica* (ADBPO, 2008c); On the right: Map of land use (ADBPO, 2010).

Based on that definition of naturalness, the primary objective of river restoration should be to examine the boundary conditions that determine the river system's naturalness and whether these permits or not to accomplish biodiversity conservation goals and ecosystem services compliance.

Turning back to the case study of Isola Serafini meander, the hydropower plant construction caused significant river alterations and modified the boundary conditions, changing the naturalness' state of the meander which may differ from the past one. Modification of boundary conditions is also imposed by climate change effects (reduced precipitations and runoffs) and consequences of human exploitation of river resources (sediment supply and water regulations). For instance, restoration of the meander may require the assessment of the current and the optimal frequency of flooding of bars necessary to habitats conservation. Also, it may be crucial to assess if there is sufficient flow to ensure hydro-morphological processes within the incised channel to regulate heterogeneity and fluvial dynamics. The present study instead, analysed the possibility of enhancing the meander's heterogeneity by taking advantage of the barrage's boundary condition.

A 2D hydro-morphological model of the meander was developed based on the modelling approach used along the Rhine Branches. Eventually, the applied methodology differed from the latter, owing to limited data availability. Firstly, no hydrodynamic calibration undertaken no bathymetric data for the whole channel was available. Another significant limitation for applying the Dutch approach was the lack of reference data (measurements or estimations) for sediment transport rates, which made it impossible to choose the appropriate solid transport formula to employ. In contrast to the Rhine modelling, where data availability is not a constraint, only the annual sediment transport capacity estimate was available from literature, and only a few numerical

analyses of the Po River's hydro-morphology have been performed to date. Another significant difference between modelling the Rhine and the Po River is the level of complexity of the incised channel. The Rhine's channel bends are generally less sharp than those of the Po River, which complicates the construction of a high-quality computational grid (referring to the quality criteria exposed in section 3.2). Also, the cross-sectional geometry and width of the Po River's channel appears to be less regular than that of the Rhine.

Nevertheless, aside from data availability, numerical models applied to the natural sciences should provide a heuristic value (Oreskes et al. 1994), and hence neither the model develop during this research nor those employed along the Rhine Branches can guarantee that the river would behave as predicted. As one contributor to this study expressed, "all models are wrong, but some are useful" (George Box, 1976). Because rivers are complex systems, it is impossible to predict how they will respond to modifications with any degree of certainty. Furthermore, because the goals of river restoration projects may be achieved in the long-term, coping with them necessitates adaptive thinking. This latter must be supported by field observations, which must be analysed in association with a comprehensive understanding of river structure, behaviour, and evolution (Fryirs & Brierley, 2009). As a result, it is clear how river restoration is prone to failure in the lack of an appropriate monitoring programme that may serve as a guide also once measures are implemented.

The last valuable message that the Dutch experience may offer is about participation. One of Room for the River's other major strengths was its capacity to integrate society from the project's beginnings. In fact, the project would have needed a considerable amount of government investment (2.3 billion euros), as well as sacrifices from the population, such as home removals or land expropriations. To encourage acceptance, it was vital to establish not just sound democratic control over the projects, but also transparent and open communication with the community and local authorities. This led in the Room-for-the-River programme adopting the "Planning Kit" tool and forming the "Q-team" to strengthen connections between the individuals and professionals. This also fostered the involvement of new stakeholders, enabling the multi-objectivity of initiatives and the establishment of synergies (what Klijn et al. (2013) refer to as *genius loci*).

Chapter 5

Conclusions

The present dissertation was conducted as part of the European MERLIN Project's twinning activities between the Room-for-the-River programme and the Po Renaturation Plan. 2D hydro-morphological approaches were introduced from the Room-for-the-River programme in the Netherlands aiming at assessing 2D hydro-morphological effects relevant to river restoration by investigating the case study of Isola Serafini in the Po River.

The question of which 2D modelling approach could be applied with existing knowledge was firstly posed, and a 2D hydro-morphological model of the meander was created using Delft3D-4. Nevertheless, the applied methodology deviated from the reference approach primarily due to a lack of data for model construction and calibration. Above all, bathymetric data for the whole channel were missing, making hydrodynamic calibration impossible. Moreover, since no estimates or modelling results on sediment transport were available, 1D morphodynamic calibration was also not feasible. As a result, the adopted modelling phase, called "sound engineering checks" was intended to replace the morphodynamic calibration phase of the Ducth approach by investigating the impact that crucial 2D hydro-morphological effects could have on the morphological development of the meander. The spiral motion and the gravity pull along the transverse bed slopes effects were the most important to address since they are crucial for formation of bars in curved channels. This modelling technique did not require full topographical information of the meander as it was possible to reproduce existing bedforms and generate a full 3D topography to be used for further model applications by simulating the morphological development of a transversely flat topography of the meander while adjusting the values of the parameters that parameterize the 3D effects inside the 2D model. Additionally, modelling results revealed useful insights for river restoration such as identification of potential areas of bed erosion adjacent to defence works or the influence of training walls on the morphological development of the incised channel. It should be emphasized, however, that given the type of simulations conducted and the assumptions made about the unknown data, these findings are merely heuristic in nature and cannot be regarded valid for design purposes. To that end, comprehensive new data collecting is necessary to increase the accuracy and reliability of modelling, as it has been done for the Rhine in the Netherlands.

This preliminary phase allowed us to answer the second research question, which was how and to what extent alternative barrage operation rules could influence the morphological development of the meander. According to the modelling results, the hydraulic effects of asymmetrical inflows from the barrage are limited to around 2 km from the barrage since flow redistribution along the transverse profile of the channel occurred entirely within this distance. Asymmetrical inflows, on the other hand, result in more sediment entering the system than symmetrical ones. Therefore, medium-term effect (morphologically) of such operation rules was extended to a greater distance

from the barrage, namely 6 km, generating flatter or more heterogenous topographies, depending on the inflow distribution. Operation rules with higher flow rates on the left side of the barrage led to greater bedform heterogeneity, with shallow water areas shifting from the outer to the inner bends. Similar operation rules might be used to increase the complexity of the bedform pattern within the incised channel and to promote sediment mobilisation on the internal side channel of bar 623. Conversely, even if spatial topographic heterogeneity was decreased, operation rules with greater flow rates on the right side of the barrage might be applied to increase lateral connectivity within the incised channel by reducing the elevation gap between bars and low-flow channel. Nevertheless, the potential of alternative operation rules relies on the possibility to regulate sediment rates through the gates rather than just water inflow distribution. Thus, it is necessary to better understand how sediment may be transferred from upstream to downstream of the barrage, which appeared to be the determining factor for accomplishing significant topographical modifications. Although it was assumed in these scenarios that no bottom changes occurred upstream of the barrage, it is worth mentioning the recognised impulsive sediment-transport mechanism induced by the barrage's operation rules (ADBPO, 2005b; Maselli et al., 2018) that may be in contrast with the modelling assumption.

Finally, some considerations can be made about what the Po River restoration can benefit from the Room-for-the-River's expertise. The first key learning from the Room-for-the-River programme might be the importance of seizing the opportunity provided by a crisis to develop innovative ideas and approaches. Analogously to the Dutch hydraulic safety problem, the prolonged drought along the Po River might serve as a steppingstone for a novel approach to river management. This is especially important given the inherent drought mitigation capacity that floodplains can provide, and that river restoration should try to rehabilitate and protect, but that did not appear to be among the Po Renaturation Plan's core objectives. To that end, given that the Po Renaturation Plan recognises the necessity of giving the river more space, it was questioned whether "more space for storage" could be a more appropriate principle to apply to the Po River restoration rather than "more space for conveyance" as was applied in the Netherlands. This last question can only be answered through a field-based approach aimed at preserving and improving the spatial quality of the environment (as outlined in sections 3.1 and 4.3) while assessing hydro-morphological processes required for rehabilitation of river functionalities. Such functionalities might rely on hydro-morphological processes to be restored and hence their assessment is crucial for river restoration effectiveness. The Room-for-the-River measures were planned also to provide the river more space for dynamics and nature, but dynamics and nature were intended to be controlled and limited (i.e., restricting lateral migration for side channels and implementing cyclic floodplain rejuvenation, respectively). It was found that a better understanding of how to manage such processes is required for the Po Renaturation Plan. Lastly, the Dutch experience demonstrates the importance of planning multi-objective measures to attain cost-effective river management and avoiding top-down decision-making processes by ensuring direct multistakeholder and population participation beginning with the intervention planning stages.

Chapter 6

Recommendations

An attempt was made to employ the Dutch modelling approach to the restoration of the Po River. Since data availability was limited and the reference strategy was not fully practicable, the model developed for the Isola Serafini meander in the Po River was ultimately affected by several assumptions. Yet, significant insights on the morphological behaviour of this segment of the Po River are thought to have been obtained. As a result, the applied modelling technique can be utilized in circumstances where data availability is restricted, especially as the model itself may guide new data collection and additional analysis to be performed.

Follow-ups on the models may be carried out with the goal of increasing the reliability of the modelling results and exploiting Dutch expertise. These recommendations might be beneficial:

- Perform hydraulic calibration: To dispose of a full topographic representation of the channel, new topographic and bathymetric measurements are required. As data discrepancies were found during the building of the Isola Serafini model, consistency checks on water levels data and discharge-rating curves between hydrometric stations and former modelling may be required.
- Perform 1D morphodynamic calibration: It may be essential to verify previous conclusions on annual sediment load by developing a new 1D morphodynamic model of the Po River course. Setting up a monitoring plan and repeating bathymetric surveys at the beginning and end of the monitored time span might provide crucial details on annual bed level changes. Since measurements of solid transport may be challenging to conduct, encouraging new modelling may be vital for greater understanding of the river's sediment transport behaviour and selecting the most suitable sediment transport formula to use in modelling.

Some open questions crucial for the Isola Serafini meander restoration remain, among them:

- Given the reduced dynamics induced by the operation rules, is there sufficient flow to guarantee active hydro-morphological processes?
- Which is the degree of lateral connectivity within the incised channel necessary to biodiversity conservation?

In the interest of restoring the entire course of the Po River, it is recommended that:

i) Establish multidisciplinary work teams and engage with local entities;
ii) Improve the monitoring system;
iii) Recognise ecosystem conservation targets;
iv) Select which hydro-morphological processes should be recovered to achieve these objectives.

To that end, the continuation of 2D modelling is recommended, and the twinning activity can give opportunities for exploration into both the modelling approach and governance aspects. Managers of the Po could benefit from Dutch experiences with stakeholder involvement, interdisciplinary teams and monitoring programmes. Meanwhile, managers of the Rhine could benefit from Italian experiences with freshwater supply in periods of draught that are expected to become more prominent according to scenarios of climate change. Carrying out twinning activities between managers of the Rhine and the Po Rivers then appears to be crucial for mutual benefit.

References

ADBPO (Autorità di Bacino del Fiume Po), (2005a). Studio di fattibilità degli interventi di gestione dei sedimenti alluvionali dell'alveo del fiume Po nel tratto confluenza Tanaro-confluenza Arda.

ADBPO (Autorità di Bacino del Fiume Po, (2005b). Programma Generale di Gestione dei Sedimenti Alluvionali dell'alveo del Fiume Po. Stralcio Confluenza Tanaro-Confluenza Arda.

ADBPO (Autorità di Bacino del Fiume Po), (2008a). Il recupero morfologico ed ambientale del fiume Po: Il contributo del Programma generale di gestione dei sedimenti del fiume Po. *Diabasis*. Reggio Emilia, Italy.

ADBPO (Autorità di Bacino del Fiume Po), (2008b). Atlante Geo-morfologico. Fiume Po da confluenza Stura di Lanzo a Pontelagoscuro. Parma, Italy.

ADBPO (Autorità di Bacino del Fiume Po), (2008c). Fasce di Mobilità del Fiume Po da confluenza Stura di Lanzo all'incile del Po di Goro. Atlante Cartografico. Edited by Aimar, A., Camorani, G., Colombo, A., Filippi, F., Merli, C. Parma, Italy.

ADBPO (Autorità di Bacino del Fiume Po), (2010). Atlante dell'uso e coperture del suolo del Fiume Po. Fiume Po da Torino all'incile del Po di Goro. Edited by Farioli., C., Camorani, G., Filippi, F., Pegazzano, A. Parma, Italy.

ADBPO (Autorità di Bacino del Fiume Po), (2022). PNRR-M2C4 INVESTIMENTO 3.3 Rinaturazione dell'area del Po. Programma d'Azione. Edited by Segreteria Tecnica ADBPO with contributions from AIPo, Regione Piemonte, Regione Lombardia, Regione Emilia-Romagna, Regione Veneto.

Agapito A. L., Romano B., Iemma A., (2020). Riqualificare l'Italia. Proposte per un piano di ripristino ambientale e di adattamento ai cambiamenti climatici. WWF Italia ONLUS.

Bandrowski, D. J., Lai, Y. G., Bradley, D. N., Murauskas, J., (2015). River restoration decision analysis – 2D hydrodynamic approach to project prioritization.

Baptist, J. M., Penning, E. W., Duel, H., Smits, J. M. A., Geerling, G. W., Van der Lee, G. E. M, Van Alphen, J. S. L., (2004). Assessment of the effect of cyclic floodplain rejuvenation on flood levels and biodiversity along the Rhine River. *River Res. Applic*., 20:285-297.

Bernardi, D., Bizzi, S., Denaro, S., Dinh, Q., Pavan, S., Schippa, L., Soncini-Sessa, R., (2013). Integrating mobile numerical modeling into reservoir planning operations: The case study of hydroelectric plant in Isola Serafini (Italy). *WIT Transactions on Ecology and the Environment*, 178,63–75.

Bassi, S., Bolpagni, R., Pezzi, G., Pattuelli, M., (2015). Habitat di interesse comunitario in Emilia-Romagna. L'aggiornamento della Carta degli Habitat nei SIC e nelle ZPS dell' Emilia-Romagna. Regione Emilia-Romagna, Direzione Generale Ambiente, Difesa del Suolo e della Costa, Servizio Parchi e Risorse forestali.

Bizzi, S., Dinh, Q., Bernardi, D., Denaro, S., Schippa, L., Soncini-Sessa, R., (2015). On the control of riverbed incision induced by run-of-river power plant. *Water Resour. Res.*, 51,5023-5040.

Bornette, G., Amoros, C., Lamouroux, N., (1998). Acquatic plant diversity in riverine wetlands: the role of connectivity. *Freshwater Biology*, 39,267-283.

Brinke, W. ten, (2019). Sediment management in the Rhine catchment: Research inventory for the Dutch Rhine and an advice at the catchment scale. *Blueland Consultancy*, supervised by Schielen R. and Kruijshoop J. (Rijkswaterstaat).

Brinke, W. Ten & Zetten, R. van, (2021). The story of the Rhine branches. *Rijkswaterstaat (RWS), Platform Rivierkennis*. Rijkswaterstaat Report Database, PUC_633896_31.

Camporeale, C., Perruca, E., Ridolfi L., Gurnell, A. M., (2013). Modeling the interactions between river morphodynamics and riparian vegetation. *Reviews of Geophysics*, 51(3),379–414.

Chavarrias, V., Ottevanger, W., Mosselman, E. (2020). Morphodynamic modelling over alluvial and non-alluvial layers. 11205235-016-ZWS-0006_v0.1, Version 0.01,2020-12-09, final.

Christiansen, T., Azlak, M., Ivits-Wasser, E., (2019). Floodplains: A Natural System to Preserve and Restore. *EEA Report*, Luxembourg.

CIRF, (2006). La riqualificazione fluviale in Italia. Linee guida, strumenti ed esperienze per gestire i corsi d'acqua e il territorio. Nardini, A., Sansoni, G. (curatori) e collaboratori, *Mazzanti Editori*, Venezia.

Comune di Monticelli d'Ongina, (2008). Variante PAE 2008. Relazione Idraulica. Comune di Monticelli d'Ongina (Italy).

Colombo, A., Filippi, F., (2008). La conoscenza delle forme e dei processi fluviali per la gestione dell'assetto morfologico del fiume Po. *Biologia Ambientale*, 24(1),331-348.

Crosato, A. & Mosselman, E., (2009). Simple physic-based predictor for the number of river bars and the transition between meandering and braiding. *Water Resources Research*, 45(3).

Crosato, A. & Mosselman, E., (2020). An integrated Review of River Bars for Engineering, Management and Transdisciplinary Research. *Water*, 12(2), 596.

Deltares, (2018). DELFT3D-FLOW, User Manual. Deltares, Delft (NL). Version:3.15,SVN Revision:57696.

ENEL, (2010). Raggruppamento impianti idroelettrici di Castellanza. Centrale di Isola Serafini. DPT – Sede distaccata di Milano.

ENEL, (2012). Centrale idroelettrica di Isola Serafini. Regolamento di gestione delle paratoie. Enel green Power S.p.A., Area Italia e Europa. Unità Territoriale Emilia Romagna, Toscana e Marche.

European Commission, (2003a). Horizontal guidance on the role of wetlands in the water framework directive. Guidance document No 12. Guidance document n°12.

European Commission, (2019). Second River Basin Management Plans – Member State: Italy. Brussels, 26.2.2019 SWD (2019) 51 final.

European Commission, (2021). Biodiversity Strategy 2030. Barrier Removal for River Restoration. Luxembourg: Publications Office of the European Union.

European Environmental Agency, (2019). Floodplains: a natural system to preserve and restore. 2019-51 pp. ISBN 978-92-9480-211-8. doi:10.2800/431107.

Evers, M., (2016). Integrative river basin management: challenges and methodologies within the German planning system. *Environ Earth Sci*, 75:1085.

Filippi F., Pavan S., Piovani P., (2013). IQM del fiume Po da Isola Serafini a confluenza Mincio. Studio di impatto ambientale del "Progetto definitivo degli interventi relativi alla sistemazione

a corrente libera del Fiume Po nella tratta compresa tra Isola Serafini e foce Mincio per consentire il transito di unità di navigazione della V classe CEMT". AIPo.

Fryirs, K. & Brierley, G. J., (2009). Naturalness and place in river rehabilitation. Ecology and Society, 14(1),20.

Geerling, G., W., Kater, E., van der Brink, C., Baptist, M., J., Ragas, A., M., J., Smits, A., J., M., (2008). Nature rehabilitation by floodplain excavation. The hydraulic effect of 16 years of sedimentation and vegetation succession along the Waal River, NL. *Geomorphology*, 99 (2008), 317-328.

Guerrero M., Di Federico, V., Lamberti, A., (2013). Calibration of a 2-D morphodynamic model using water-sediment flux maps derived from an ADCP recording. *Journal of Hydroinformatics*, 15(3),813-828.

Junk, W. J., Bayley, P. B., and Sparks, R. E, (1989). The flood pulse concept in river-floodplain systems. *Can. Spec. Publ. Fish. Aquat. Sci*, 106,110–127.

Kleinhans, M., G. & van den Berg, J., H. (2011). River channel and bar patterns explained and predicted by an empirical and a physics-based method. *Earth Surf. Process. Landforms*, 36, 721-738.

Klijn, F., de Bruin, D., de Hoog, M.C., Jasen, S., Sijmons, D.F., (2013). Design quality of room-for-the-river measures in the Netherlands: role and assessment of the quality team (Q-team). *Int. J. River Basin Manag.*, 11(3),287-299.

Klijn, F., Asselman, N., Wagenaar, D., (2018). Room for the Rivers: Risk Reduction by Enhancing the Flood Conveyance Capacity of the Netherlands' Large Rivers. *Geosciences*, 8(6),224.

Kurstjens, G., Nijssen, M., van Winden, A., Dorenbosch, M., Moller Pillot, H., van Turnhout, C., Veldt, P., (2020). Natte overstromingsvlakten in het rivierengebied. Ecologisch functioneren en ontwikkelkansen. *Rapport 2020/OBN237-RI*. VBNE, Driebergen.

Lanzoni, S., (2012). Evoluzione morfologica recente dell'asta principale del Po. *Accademia Nazionale dei Lincei*. Atti dei Convegni Lincei. Giornata Mondiale dell'Acqua, marzo 2012.

Marsiglia, L., (2010). 2D Hydrodynamic Analysis of the October 2000 flood on the Po River at Isola Serafini. Tesi di Laurea in Ignegneria per l'Ambiente e il Territorio. Università degli Studi di Parma

Maselli, V., Pellegrini, C., Del Bianco, F., Mercorella, A., Nones, M., Crose, L., Guerrero M., Nittrouer, J.A., (2018). River morphodynamic evolution under dam-induced backwater: An example from the po river (Italy). *Journal of Sedimentary Research*, 88(10),1190–1204.

Montanari, A., (2012). Hydrology of the Po River: looking for changing patterns in river discharge. *Hydrol. Earth Syst. Sci.*, 16,3739-3747.

Montgomery, D. R. & Buffington, J. M., (1998). Channel process, classification and response. *River Ecology and Management*, 112,1250-1263.

Mosselman, E., (2007). "Room for the River": Nuova gestione della difesa idraulica e nuove opportunità di progettazione ecologica e paesaggistica in Olanda. Fiume, paesaggio, difesa del suolo. Superare le emergenze, cogliere le opportunità – Atti del convegno internazionale (Firenze, 10-11 Maggio 2006), a cura di Michele Ercolini – Firenze: Firenze University Press (Luoghi e paesaggi;3).

Mosselman, E., (2009a). River morphology and river engineering at Deltares. Journal of the Saint Petersburg State University of Waterways Communications (Журнал университета водных коммуникаций), 2009:62-76.

Mosselman, E., (2009b). Strumenti per la partecipazione pubblica. *Pense & Maravee*. Luglio 2009, Anno 18 – n.3, p.10-11.

Mosselman, E. & Le T. B., (2015) . Five common mistakes in fluvial morphodynamic modeling. *Advances in Water Resources*, 93,15-20.

Mosselman, E., (2020). Studies on river training. *Water*, 12,3100.

Mosselman, E., (2022). The Dutch Rhine branches in the Anthropocene. Importance of events and seizing of opportunities. *Geomorphology*, 410(2022) 108289.

Noss, R. F., (1990). Indicators for monitoring biodiversity: A hierarchical approach. *Conservation Biology*, 4(4),355-364.

Oldani, G., Gigli, P., Jappelli, R., Maugliani, V., (2008). Interventi di salvaguardia della traversa Isola Serafini sul fiume Po. *L'Acqua, Associazione Idroelettrica Italiana*, 5(25).

Oreskes, N., Shrader-Frechette, K., Belitz, K., (1994). Verification, Validation and Confirmation of Numerical Models in the Earth Sciences. *Science*, *New Series*, 263(5147),641-646.

Paoletti A., Braga G., Colombo A., Croci S., Peduzzi G.B., Savazzi G., (2007). La gestione dei sedimenti alluvionali dell'alveo inciso del fiume Po. *L'Acqua*, n. 2/2007.

Piégat, H., Darby, S., E., Mosselman, E., Surian, N., (2005). A review of techniques available for delimiting the erodible river corridor: A sustainable approach to managing bank erosion. *River Res. Applic*. 21: 773-789.

Provincia di Mantova, (2005). Gruppo di Lavoro "Fiume Po". Relazione conclusiva. Area Ambientale, Servizio Acqua e Suolo – Protezione Civile.

Provincia di Piacenza, (2011). PIAE 2011 con valenza di PAE del Comune di Monticelli d'Ongina. Relazione di compatibilità idraulica.

REFORM, (2015). REFORM 2015 - A fresh look on effective river restoration: Key conclusions from the REFORM project. Policy brief, Issue No.3, December 2015.

Regione Lombardia, (2018). Layman's Report. Restoring connectivity in Po River basin opening migratory route for Aci-penser naccarii and 10 fish species in Annex II. Life-Natura program (Life 11Nat/IT/188).

Rijkswaterstaat, (1999). Afferdensche en Deestsche Waarden. Inrichtingplan 1999, ON-rapport-99-001.

Rinaldi, M., Surian, N., Comiti, F., Bussettini, M., (2016). IDRAIM – Sistema di valutazione idromorfologica, analisi e monitoraggio dei corsi d'acqua – Versione aggiornata 2016 – ISPRA – Manuali e Linee Guida 131/2016, Roma, gennaio 2016.

Schippa, L., Pavan, S., Colonna, S., (2006), River Po low water training: The importance of mathematical modeling to support designing activities. *River Flow 2006*, vol.2. Ferreire R. M. L., Alves E. C. T. L. and Leal J. G. A. B., pp. 1973–1983, London, U. K.

Schirmer, M., Luster, J., Linde, N., Perona, P., Mitchell, E. A. D., Barry, D. A., Hollender, J., Cirpka, O. A., Schneider, P., Vogt, T., Radny, D., Durisch-Kaiser, E., (2014). Morphological, hydrological, biogeochemical and ecological changes and challenges in river restoration the Thur River case study. *Hydrology and Earth System Sciences*, 18(6),2449–2462.

Silva, W., Klijn, F., Dijkman, J., (2001). Room for the Rhine Branches in The Netherlands. What the research has taught us. *Tech. rep., WL* | Delft Hydraulics report R3294, Delft, The Netherlands.

SIMA (Società Idroelettrica Medio Adige), (1960). Hydroelectric development of River Po at Isola Serafini.

Struiksma, N., Olesen, K. W., Flokstra, C., De Vriend, Dr. H. J., (1985). Bed deformation in curved alluvial channels. *Journal of Hydraulic Research*, 23:1,57-79.

Tockner, K., Malard, F., Ward, J. V., (2000). An extension of the flood pulse concept. *Hydrol. Process*, 14(16-17),2861-2883.

Vesipa, R., Camporeale, C., Ridolfi, L., (2017). Effect of river flow fluctuations on riparian vegetation dynamic: Processes and models. *Advances in Water Resources*, 110,29-50.

Ward, J. V., Tockner, K., Schiemer, F., (1999). Biodiversity of floodplain river cosystems: ecotones and connectivity. *Regulated Rivers: Research & Management*, 15(1-3),125-139.

Wohl, E., Angermeier, P. L., Bledsoe, B., Kondolf, G. M., MacDonnel, L., Merritt, D. M., Palmer, M. A., Poff, N. L. R., Tarboton, D., (2005). River Restoration. *Water Resources Research*, 41(10).

Wohl, E., (2017). Connectivity in rivers. *Progress in Physical Geography*, 41(3),345-362.

WWF, (2006). Applying the principles of integrated water resource and river basin management – an introduction. A Report to WWF_UK prepared by: Jones, T., Newborne, P., Phillips, B.

Yossef, M., F., M. (2016). Morphological model of the River Rhine branches in the Netherlands from the concept to the operational model. Deltares, PowerPoint presentation.

Zhang, Y., Huang, C., Zhang, W., Chen, J., Wang, L. (2021). The concept, approach, and future research of hydrological connectivity and its assessment at multiscales. *Environmental Science and Pollution Research*, 28:52724-52743.

Zorzoli, G. B., (2008). Piacenza capitale dell'energia. *Tip.Le.Co*. Capitolo IV a cura di Brega P.

Appendices

Appendix A

Photos of the field visit to the Po River

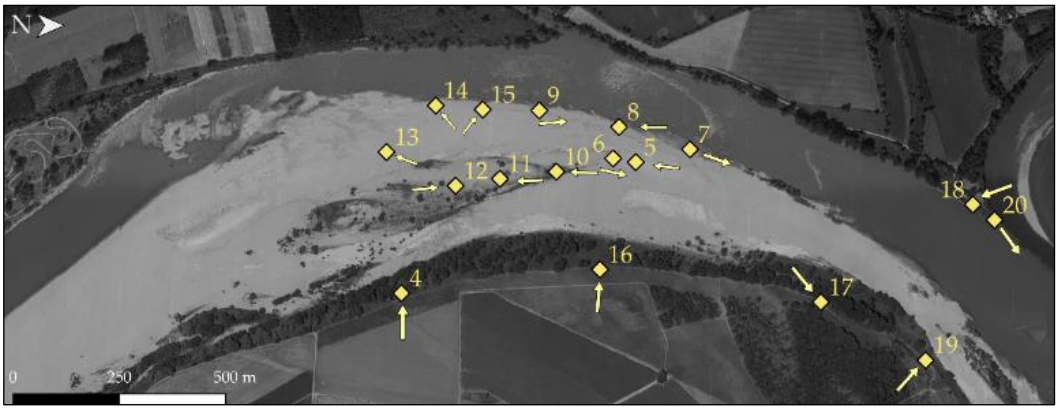

Figure A - 1: Detail of position of pictures (see Figure 33).

Figure A - 2: low water levels along the tailrace and the meander; Photo n°24 on top and Photo n°9 on bottom.

Figure A - 3: Photo n°2 (agricultural field), Photo n°16 and Photo n°17 (hunting ground) showing the riparian belts and land uses internal to Isola Serafini.

Figure A - 4: Top: Photo n°13 showing active erosion of the left bank adjacent to bar 623; Centre and Bottom: Photo n°14 and Photo n°15 depict bank defenses and the remaining riparian belt.

Figure A - 5: Photo n°18 and Photo n°19. Other photos of high vegetation within the incised channel.

Figure A - 6: Photo n°161 and Photo n°163 revealing the longitudinal training walls.

Appendix B

Grid quality properties

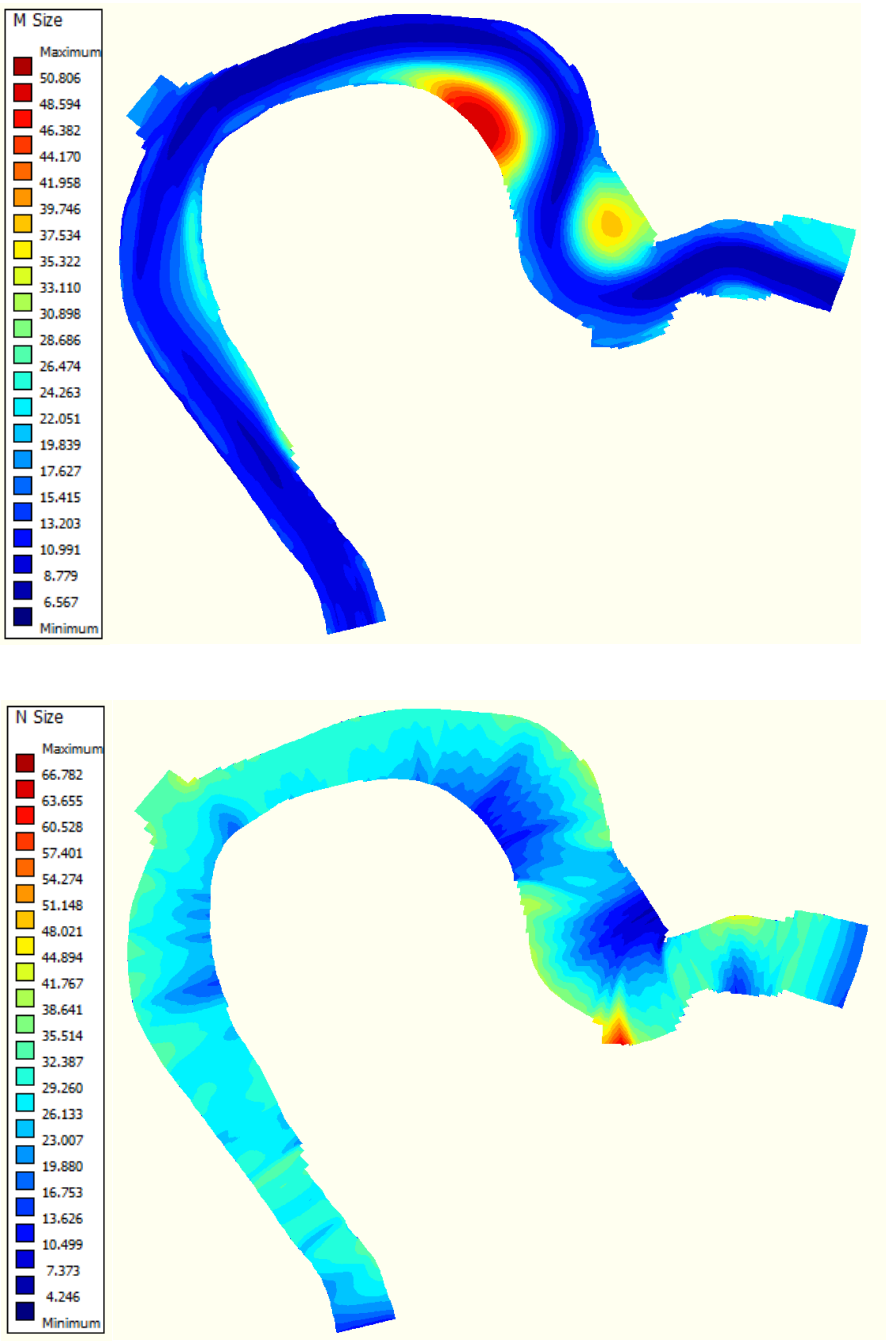

Figure B - 1: Grid maps of M and N Size.

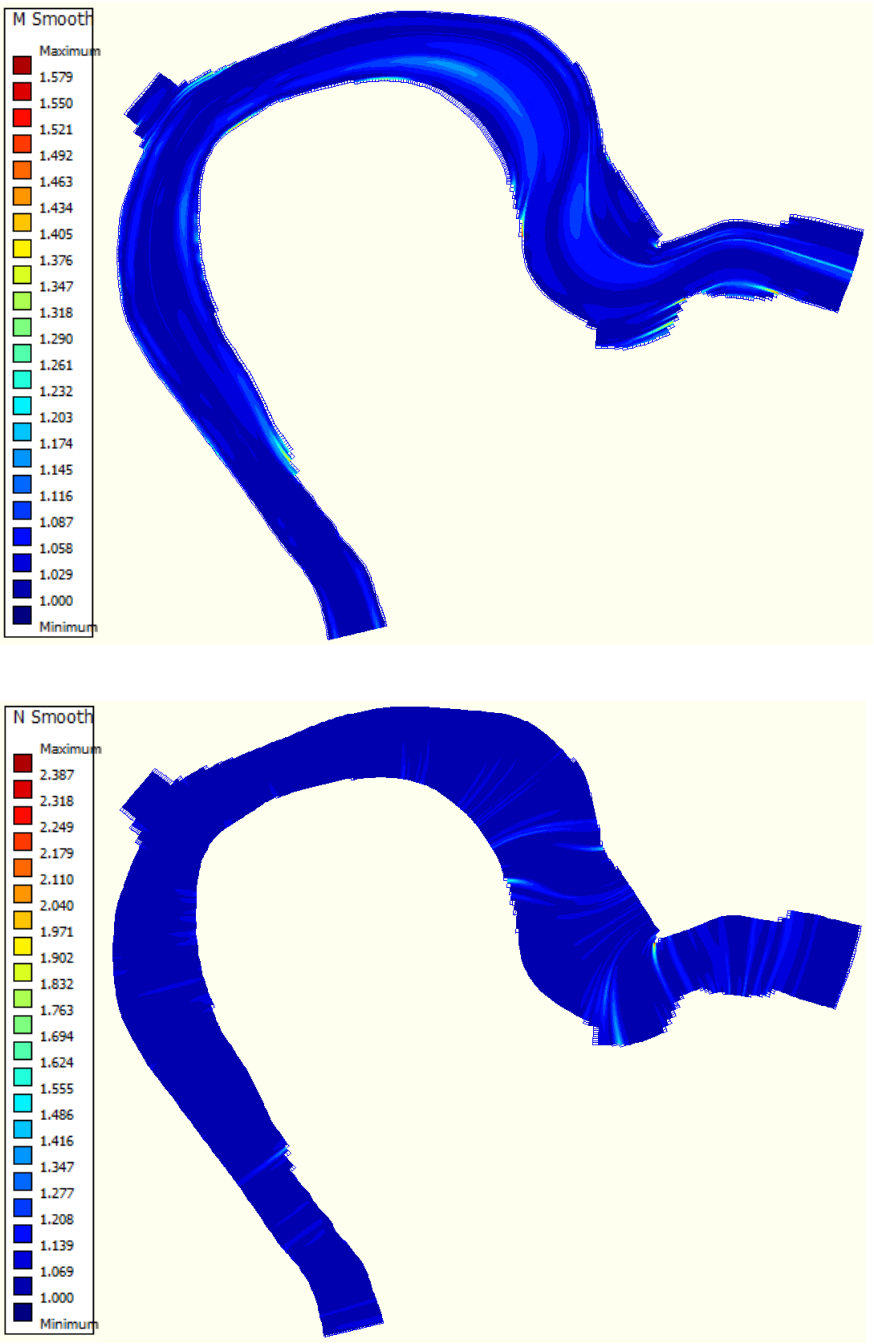

Figure B - 2: Grid property maps of M and N Smoothness.

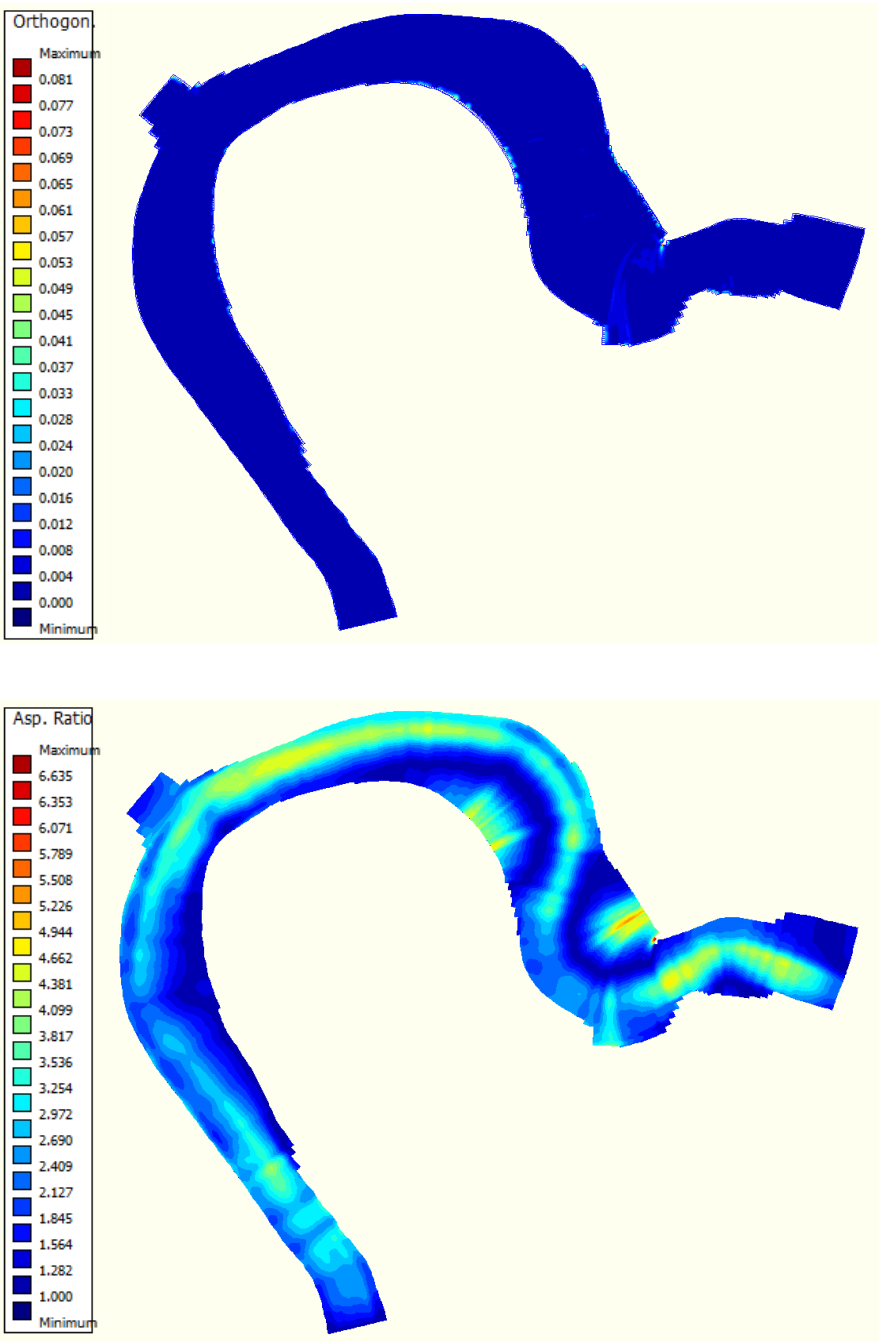

Figure B - 3: Grid property maps of Orthogonality and Aspect Ratio.

Appendix C

Results from the analysis of the degree of nonlinearity of sediment transport

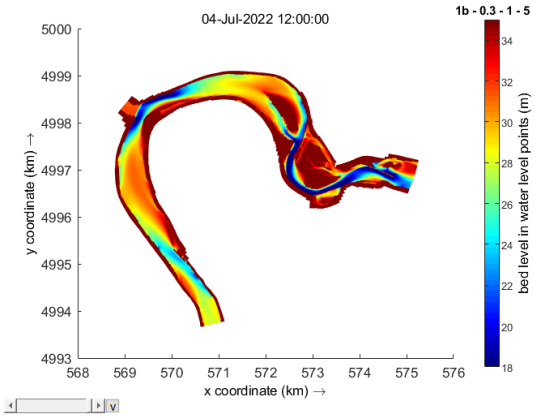

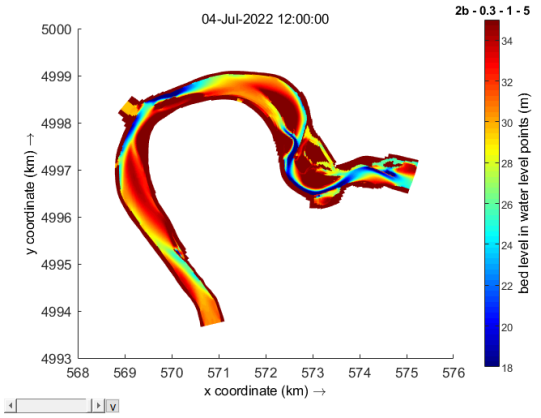

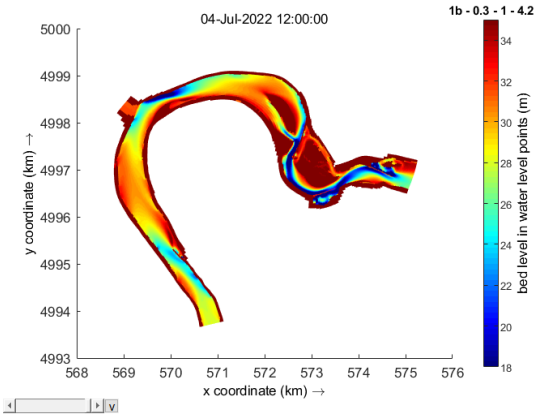

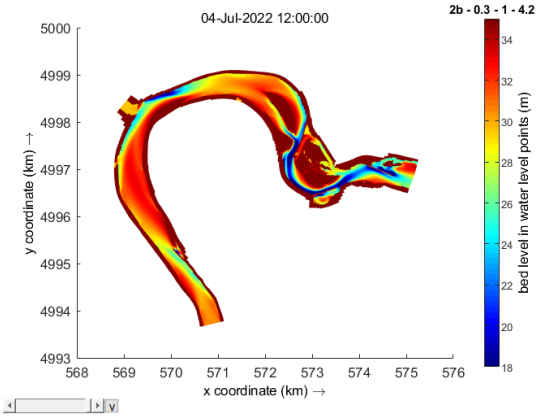

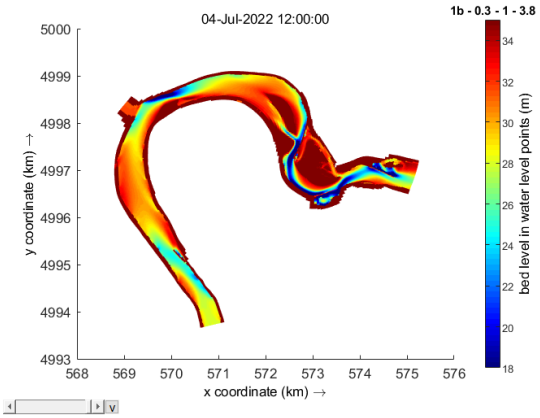

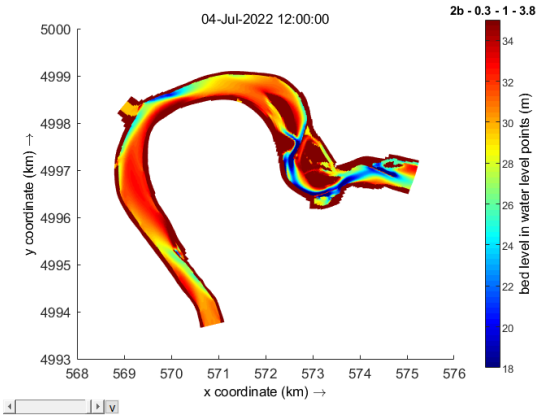

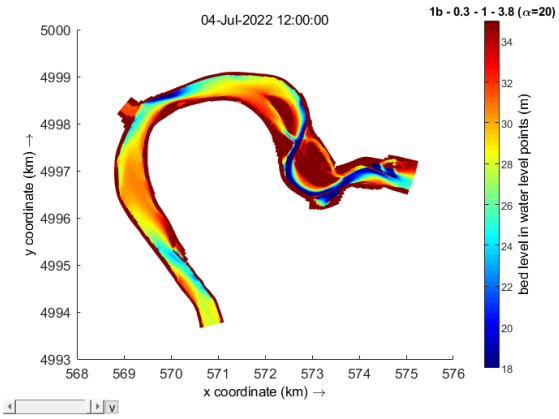
1b - 0.3 - 1 - 3.8 (α=20)
04-Jul-2022 12:00:00
y coordinate (km) →
x coordinate (km) →
bed level in water level points (m)

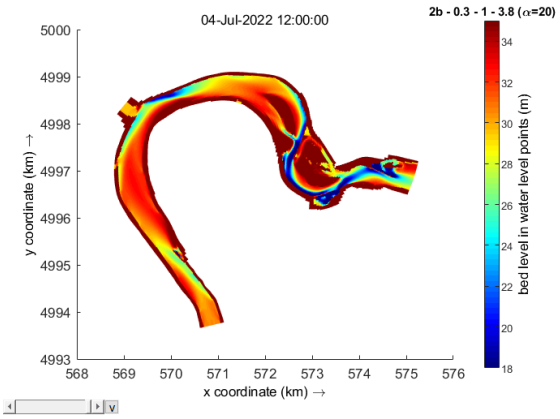
2b - 0.3 - 1 - 3.8 (α=20)
04-Jul-2022 12:00:00
y coordinate (km) →
x coordinate (km) →
bed level in water level points (m)

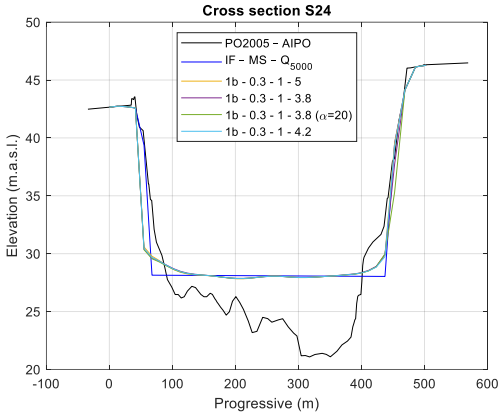
Cross section S24
PO2005 - AIPO
IF - MS - Q5000
1b - 0.3 - 1 - 5
1b - 0.3 - 1 - 3.8
1b - 0.3 - 1 - 3.8 (α=20)
1b - 0.3 - 1 - 4.2
Elevation (m.a.s.l.)
Progressive (m)

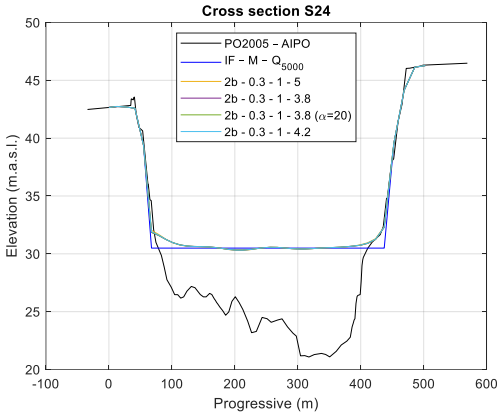
Cross section S24
PO2005 - AIPO
IF - M - Q5000
2b - 0.3 - 1 - 5
2b - 0.3 - 1 - 3.8
2b - 0.3 - 1 - 3.8 (α=20)
2b - 0.3 - 1 - 4.2
Elevation (m.a.s.l.)
Progressive (m)

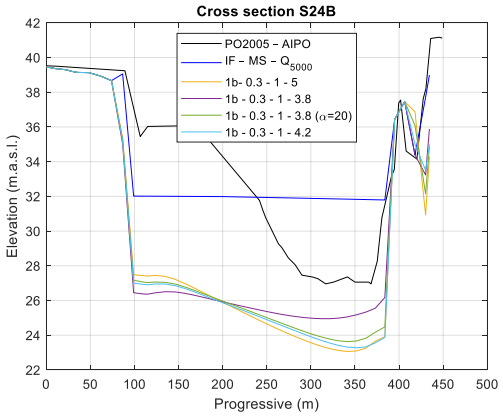
Cross section S24B
PO2005 - AIPO
IF - MS - Q5000
1b- 0.3 - 1 - 5
1b - 0.3 - 1 - 3.8
1b - 0.3 - 1 - 3.8 (α=20)
1b - 0.3 - 1 - 4.2
Elevation (m.a.s.l.)
Progressive (m)

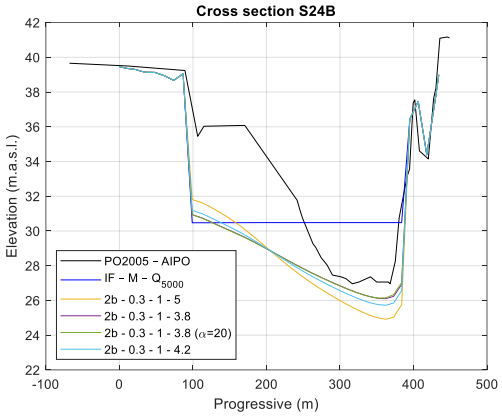
Cross section S24B
PO2005 - AIPO
IF - M - Q5000
2b - 0.3 - 1 - 5
2b - 0.3 - 1 - 3.8
2b - 0.3 - 1 - 3.8 (α=20)
2b - 0.3 - 1 - 4.2
Elevation (m.a.s.l.)
Progressive (m)

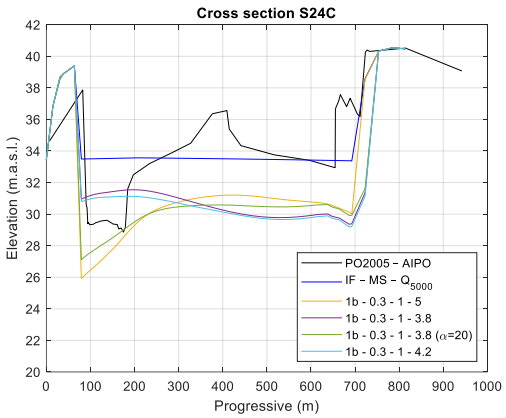
Cross section S24C
PO2005 - AIPO
IF - MS - Q5000
1b - 0.3 - 1 - 5
1b - 0.3 - 1 - 3.8
1b - 0.3 - 1 - 3.8 (α=20)
1b - 0.3 - 1 - 4.2
Elevation (m.a.s.l.)
Progressive (m)

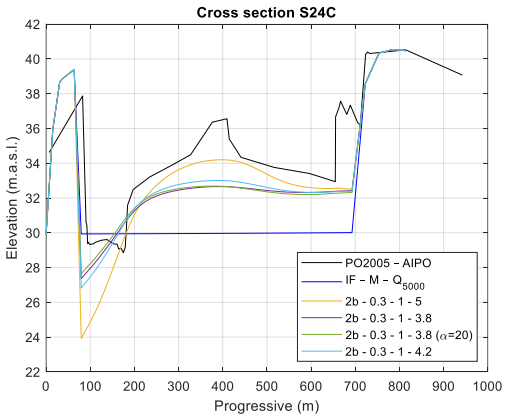
Cross section S24C
PO2005 - AIPO
IF - M - Q5000
2b - 0.3 - 1 - 5
2b - 0.3 - 1 - 3.8
2b - 0.3 - 1 - 3.8 (α=20)
2b - 0.3 - 1 - 4.2
Elevation (m.a.s.l.)
Progressive (m)

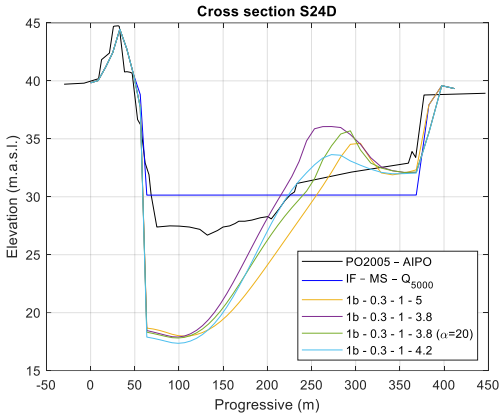
Cross section S24D
Elevation (m.a.s.l.)
Progressive (m)
PO2005 – AIPO
IF – MS – Q5000
1b - 0.3 - 1 - 5
1b - 0.3 - 1 - 3.8
1b - 0.3 - 1 - 3.8 (α=20)
1b - 0.3 - 1 - 4.2

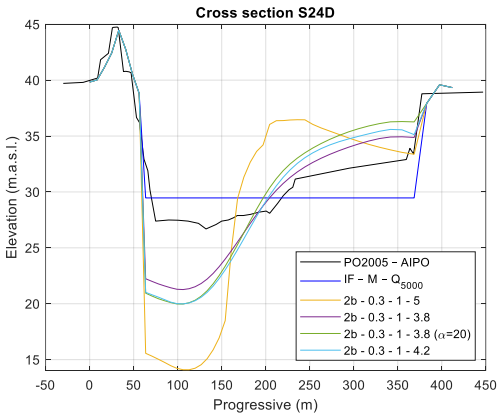
Cross section S24D
Elevation (m.a.s.l.)
Progressive (m)
PO2005 – AIPO
IF – M – Q5000
2b - 0.3 - 1 - 5
2b - 0.3 - 1 - 3.8
2b - 0.3 - 1 - 3.8 (α=20)
2b - 0.3 - 1 - 4.2

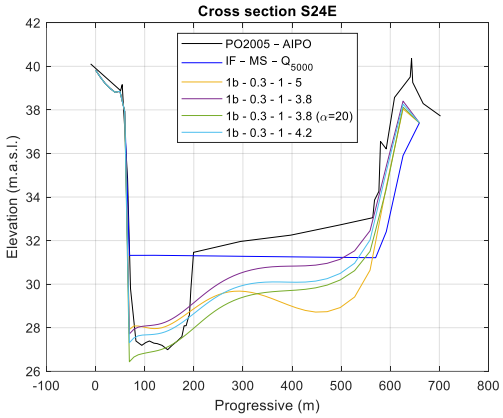
Cross section S24E
Elevation (m.a.s.l.)
Progressive (m)
PO2005 – AIPO
IF – MS – Q5000
1b - 0.3 - 1 - 5
1b - 0.3 - 1 - 3.8
1b - 0.3 - 1 - 3.8 (α=20)
1b - 0.3 - 1 - 4.2

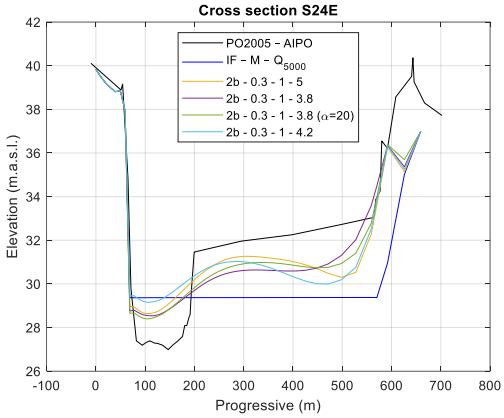
Cross section S24E
Elevation (m.a.s.l.)
Progressive (m)
PO2005 – AIPO
IF – M – Q5000
2b - 0.3 - 1 - 5
2b - 0.3 - 1 - 3.8
2b - 0.3 - 1 - 3.8 (α=20)
2b - 0.3 - 1 - 4.2

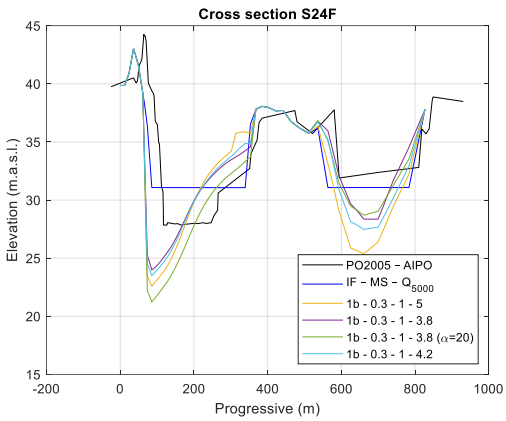
Cross section S24F
Elevation (m.a.s.l.)
Progressive (m)
PO2005 – AIPO
IF – MS – Q5000
1b - 0.3 - 1 - 5
1b - 0.3 - 1 - 3.8
1b - 0.3 - 1 - 3.8 (α=20)
1b - 0.3 - 1 - 4.2

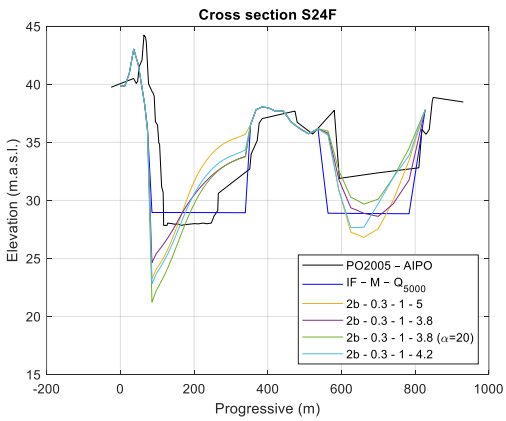
Cross section S24F
Elevation (m.a.s.l.)
Progressive (m)
PO2005 – AIPO
IF – M – Q5000
2b - 0.3 - 1 - 5
2b - 0.3 - 1 - 3.8
2b - 0.3 - 1 - 3.8 (α=20)
2b - 0.3 - 1 - 4.2

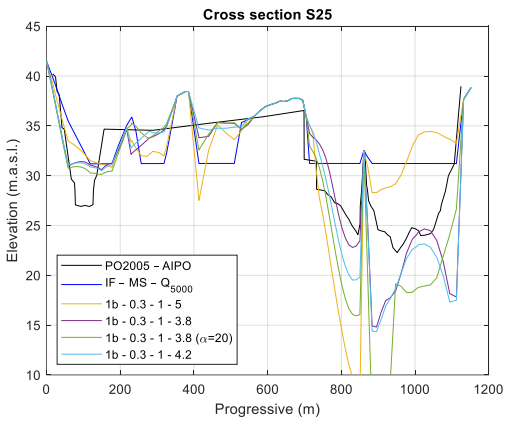
Cross section S25
Elevation (m.a.s.l.)
Progressive (m)
PO2005 – AIPO
IF – MS – Q5000
1b - 0.3 - 1 - 5
1b - 0.3 - 1 - 3.8
1b - 0.3 - 1 - 3.8 (α=20)
1b - 0.3 - 1 - 4.2

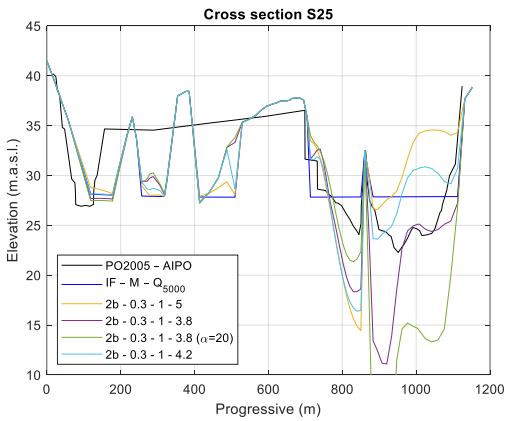
Cross section S25
Elevation (m.a.s.l.)
Progressive (m)
PO2005 – AIPO
IF – M – Q5000
2b - 0.3 - 1 - 5
2b - 0.3 - 1 - 3.8
2b - 0.3 - 1 - 3.8 (α=20)
2b - 0.3 - 1 - 4.2

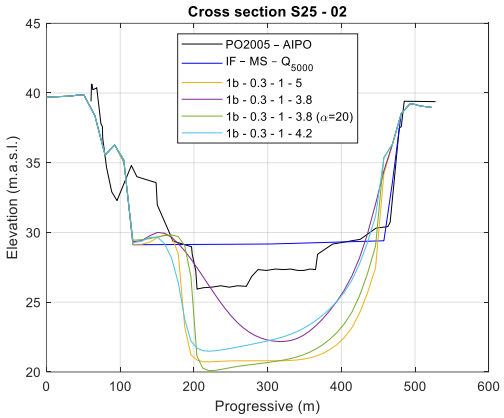
Cross section S25 - 02
PO2005 – AIPO
IF – MS – Q5000
1b - 0.3 - 1 - 5
1b - 0.3 - 1 - 3.8
1b - 0.3 - 1 - 3.8 (α=20)
1b - 0.3 - 1 - 4.2
Elevation (m.a.s.l.)
Progressive (m)

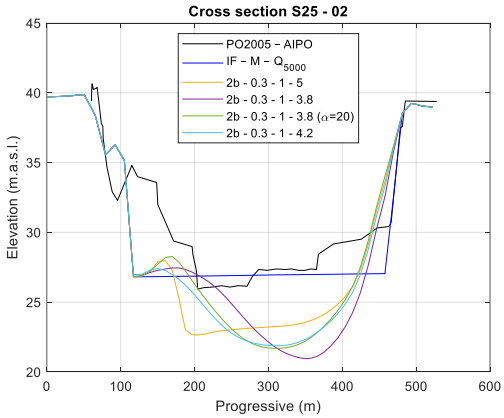
Cross section S25 - 02
PO2005 – AIPO
IF – M – Q5000
2b - 0.3 - 1 - 5
2b - 0.3 - 1 - 3.8
2b - 0.3 - 1 - 3.8 (α=20)
2b - 0.3 - 1 - 4.2
Elevation (m.a.s.l.)
Progressive (m)

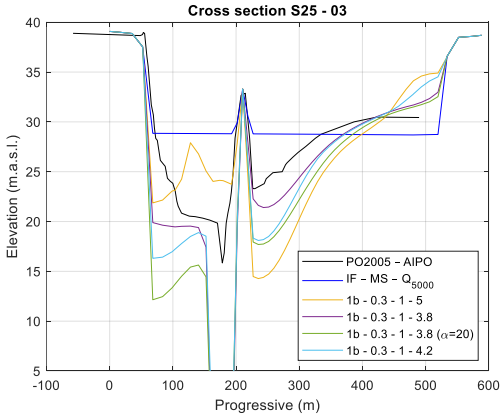
Cross section S25 - 03
PO2005 – AIPO
IF – MS – Q5000
1b - 0.3 - 1 - 5
1b - 0.3 - 1 - 3.8
1b - 0.3 - 1 - 3.8 (α=20)
1b - 0.3 - 1 - 4.2
Elevation (m.a.s.l.)
Progressive (m)

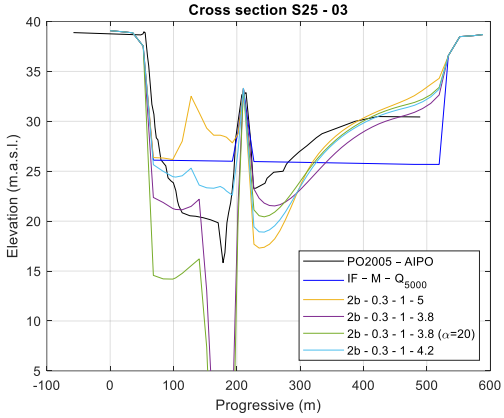
Cross section S25 - 03
PO2005 – AIPO
IF – M – Q5000
2b - 0.3 - 1 - 5
2b - 0.3 - 1 - 3.8
2b - 0.3 - 1 - 3.8 (α=20)
2b - 0.3 - 1 - 4.2
Elevation (m.a.s.l.)
Progressive (m)

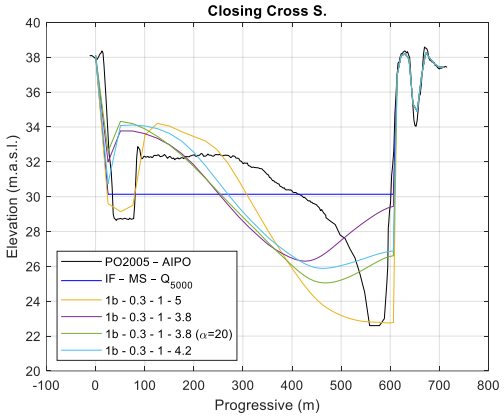
Closing Cross S.
PO2005 – AIPO
IF – MS – Q5000
1b - 0.3 - 1 - 5
1b - 0.3 - 1 - 3.8
1b - 0.3 - 1 - 3.8 (α=20)
1b - 0.3 - 1 - 4.2
Elevation (m.a.s.l.)
Progressive (m)

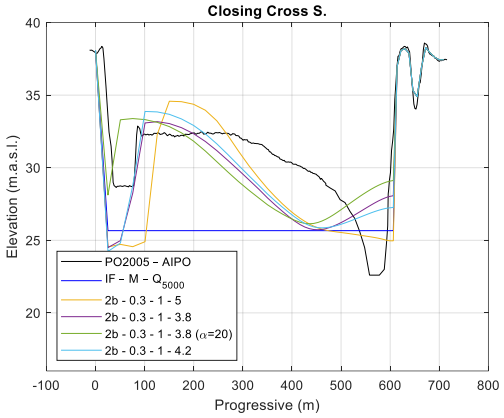
Closing Cross S.
PO2005 – AIPO
IF – M – Q5000
2b - 0.3 - 1 - 5
2b - 0.3 - 1 - 3.8
2b - 0.3 - 1 - 3.8 (α=20)
2b - 0.3 - 1 - 4.2
Elevation (m.a.s.l.)
Progressive (m)

Appendix D

Results from the analysis of the morphological parameters

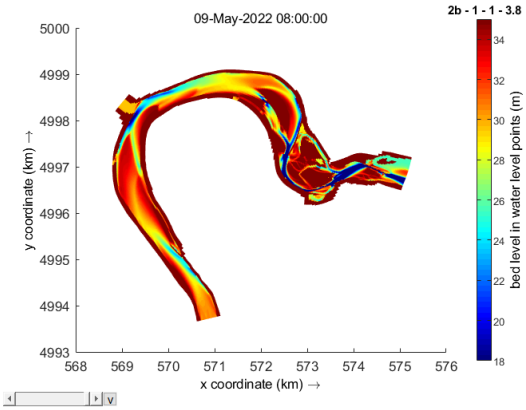

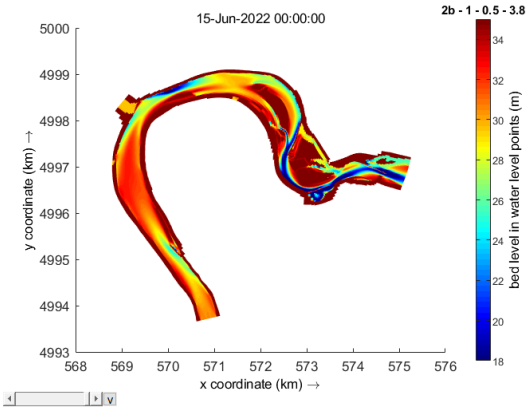

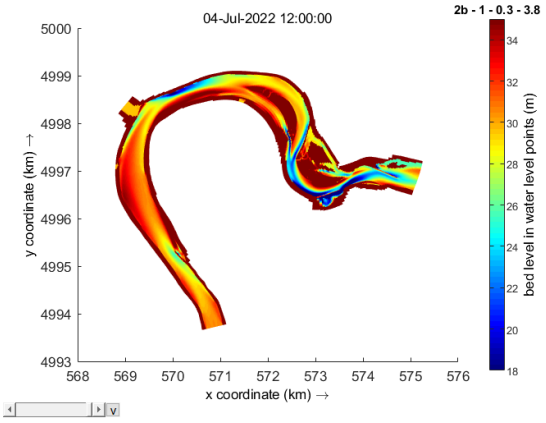

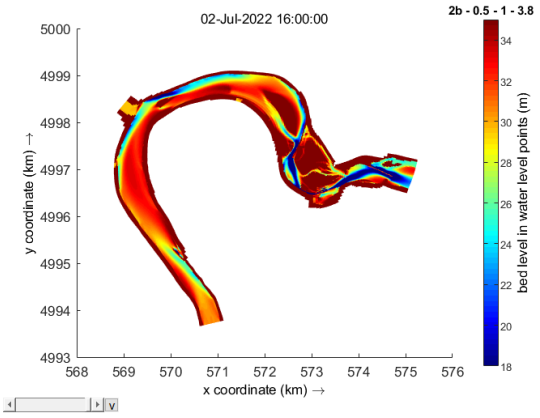

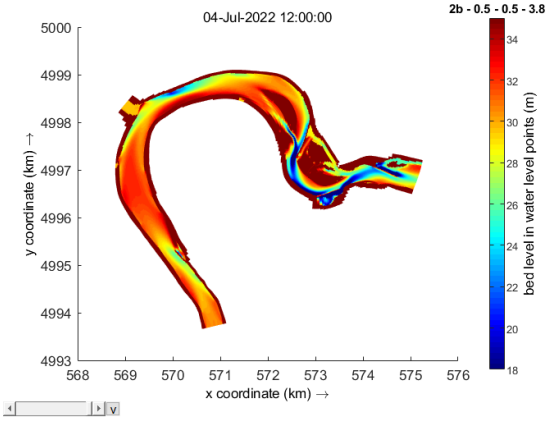

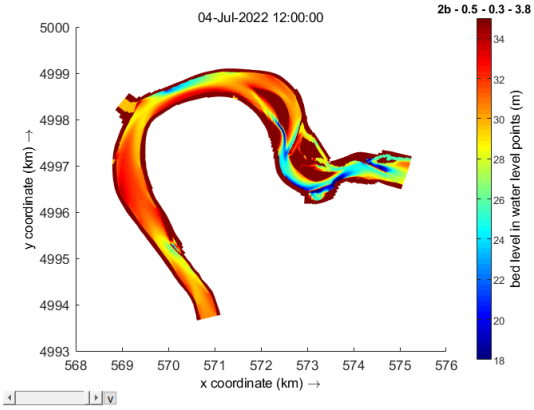

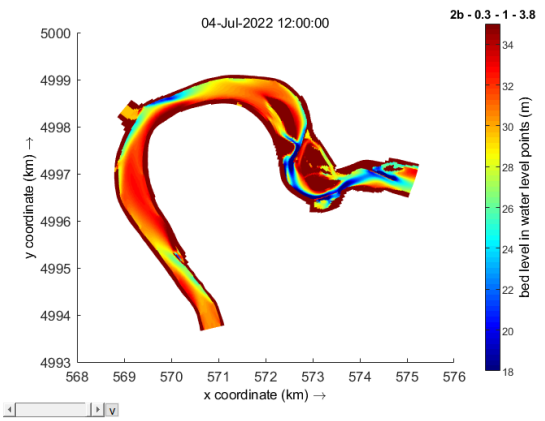
2b - 0.3 - 1 - 3.8
04-Jul-2022 12:00:00
y coordinate (km) →
x coordinate (km) →
bed level in water level points (m)

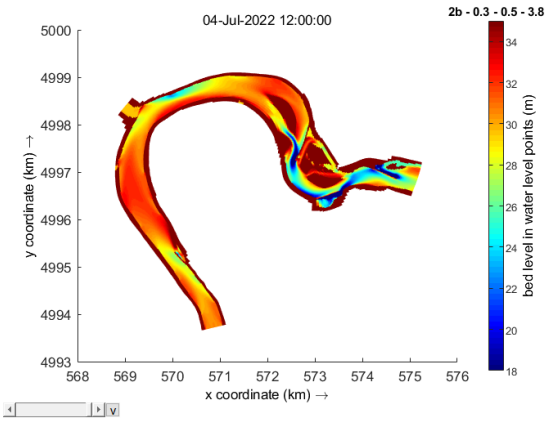
2b - 0.3 - 0.5 - 3.8
04-Jul-2022 12:00:00
y coordinate (km) →
x coordinate (km) →
bed level in water level points (m)

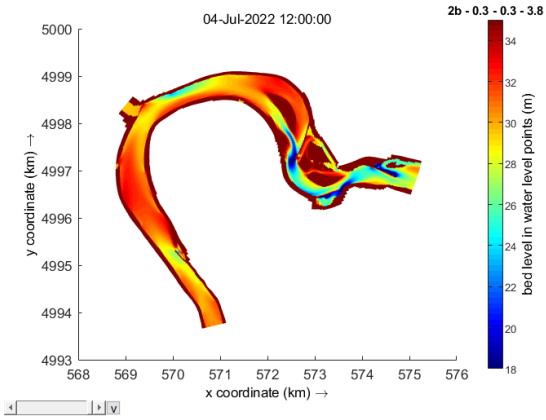
2b - 0.3 - 0.3 - 3.8
04-Jul-2022 12:00:00
y coordinate (km) →
x coordinate (km) →
bed level in water level points (m)

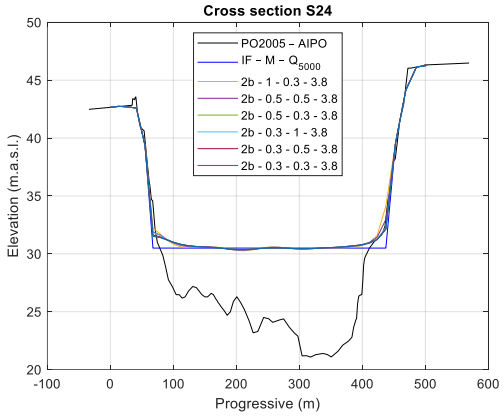
Cross section S24
Elevation (m.a.s.l.)
Progressive (m)
PO2005 - AIPO
IF - M - Q5000
2b - 1 - 0.3 - 3.8
2b - 0.5 - 0.5 - 3.8
2b - 0.5 - 0.3 - 3.8
2b - 0.3 - 1 - 3.8
2b - 0.3 - 0.5 - 3.8
2b - 0.3 - 0.3 - 3.8

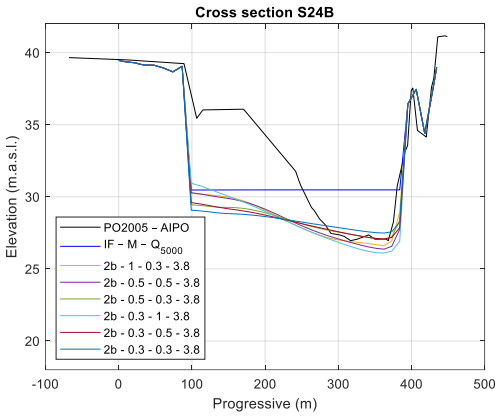
Cross section S24B
Elevation (m.a.s.l.)
Progressive (m)
PO2005 - AIPO
IF - M - Q5000
2b - 1 - 0.3 - 3.8
2b - 0.5 - 0.5 - 3.8
2b - 0.5 - 0.3 - 3.8
2b - 0.3 - 1 - 3.8
2b - 0.3 - 0.5 - 3.8
2b - 0.3 - 0.3 - 3.8

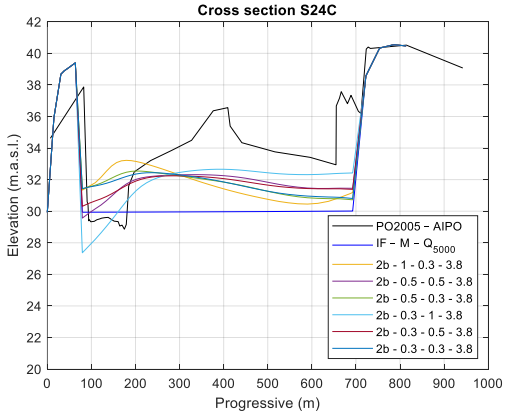
Cross section S24C
Elevation (m.a.s.l.)
Progressive (m)
PO2005 - AIPO
IF - M - Q5000
2b - 1 - 0.3 - 3.8
2b - 0.5 - 0.5 - 3.8
2b - 0.5 - 0.3 - 3.8
2b - 0.3 - 1 - 3.8
2b - 0.3 - 0.5 - 3.8
2b - 0.3 - 0.3 - 3.8

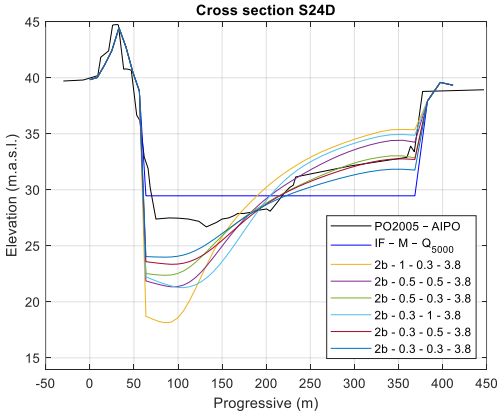
Cross section S24D
Elevation (m.a.s.l.)
Progressive (m)
PO2005 - AIPO
IF - M - Q5000
2b - 1 - 0.3 - 3.8
2b - 0.5 - 0.5 - 3.8
2b - 0.5 - 0.3 - 3.8
2b - 0.3 - 1 - 3.8
2b - 0.3 - 0.5 - 3.8
2b - 0.3 - 0.3 - 3.8

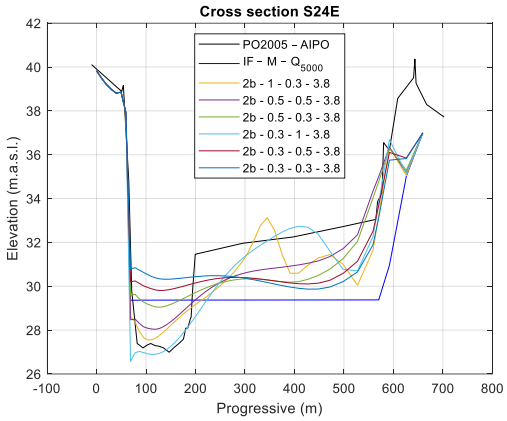
Cross section S24E
PO2005 – AIPO
IF – M – Q5000
2b - 1 - 0.3 - 3.8
2b - 0.5 - 0.5 - 3.8
2b - 0.5 - 0.3 - 3.8
2b - 0.3 - 1 - 3.8
2b - 0.3 - 0.5 - 3.8
2b - 0.3 - 0.3 - 3.8
Elevation (m.a.s.l.)
Progressive (m)

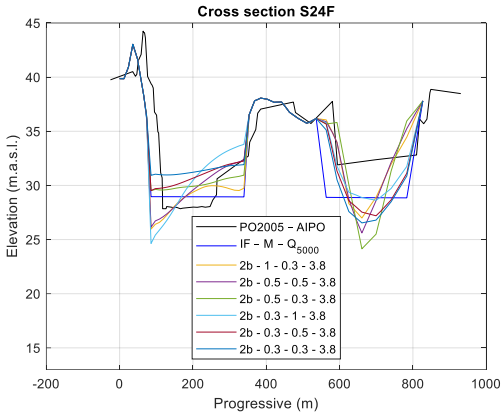
Cross section S24F
PO2005 – AIPO
IF – M – Q5000
2b - 1 - 0.3 - 3.8
2b - 0.5 - 0.5 - 3.8
2b - 0.5 - 0.3 - 3.8
2b - 0.3 - 1 - 3.8
2b - 0.3 - 0.5 - 3.8
2b - 0.3 - 0.3 - 3.8
Elevation (m.a.s.l.)
Progressive (m)

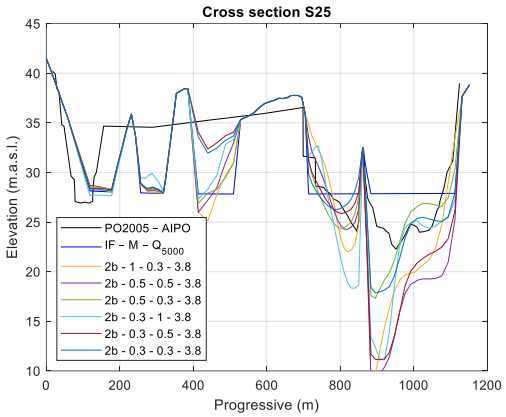
Cross section S25
PO2005 – AIPO
IF – M – Q5000
2b - 1 - 0.3 - 3.8
2b - 0.5 - 0.5 - 3.8
2b - 0.5 - 0.3 - 3.8
2b - 0.3 - 1 - 3.8
2b - 0.3 - 0.5 - 3.8
2b - 0.3 - 0.3 - 3.8
Elevation (m.a.s.l.)
Progressive (m)

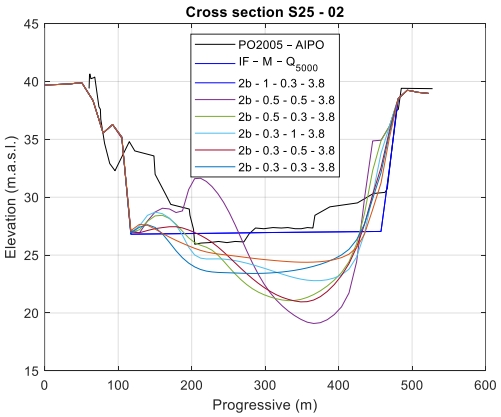
Cross section S25 - 02
PO2005 – AIPO
IF – M – Q5000
2b - 1 - 0.3 - 3.8
2b - 0.5 - 0.5 - 3.8
2b - 0.5 - 0.3 - 3.8
2b - 0.3 - 1 - 3.8
2b - 0.3 - 0.5 - 3.8
2b - 0.3 - 0.3 - 3.8
Elevation (m.a.s.l.)
Progressive (m)

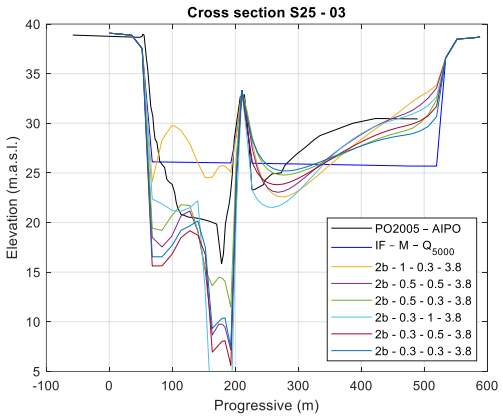
Cross section S25 - 03
PO2005 – AIPO
IF – M – Q5000
2b - 1 - 0.3 - 3.8
2b - 0.5 - 0.5 - 3.8
2b - 0.5 - 0.3 - 3.8
2b - 0.3 - 1 - 3.8
2b - 0.3 - 0.5 - 3.8
2b - 0.3 - 0.3 - 3.8
Elevation (m.a.s.l.)
Progressive (m)

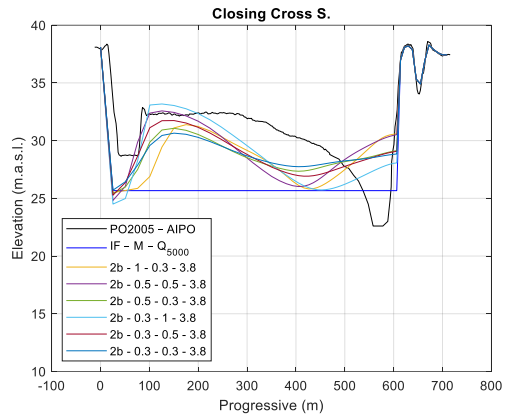
Closing Cross S.
PO2005 – AIPO
IF – M – Q5000
2b - 1 - 0.3 - 3.8
2b - 0.5 - 0.5 - 3.8
2b - 0.5 - 0.3 - 3.8
2b - 0.3 - 1 - 3.8
2b - 0.3 - 0.5 - 3.8
2b - 0.3 - 0.3 - 3.8
Elevation (m.a.s.l.)
Progressive (m)

Appendix E

Results of the analysis of short-term and medium-term effect of asymmetrical inflows

- Short-term effects

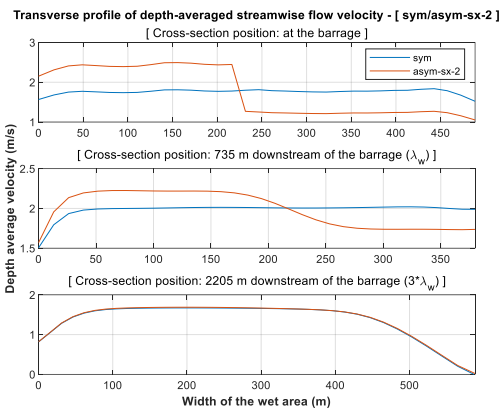

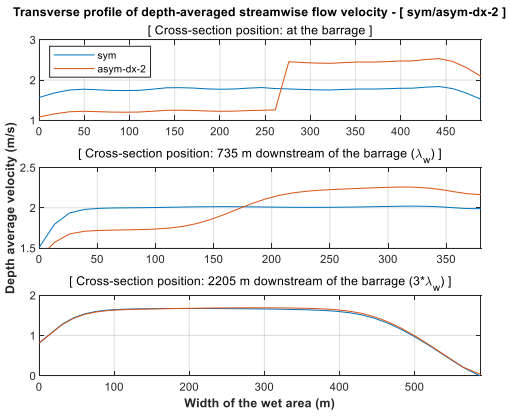

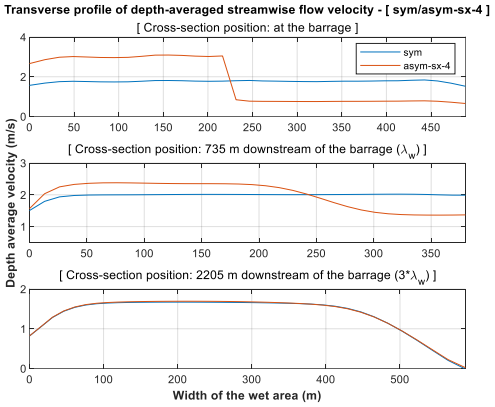

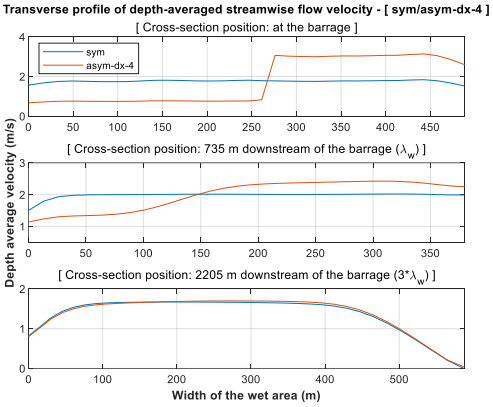

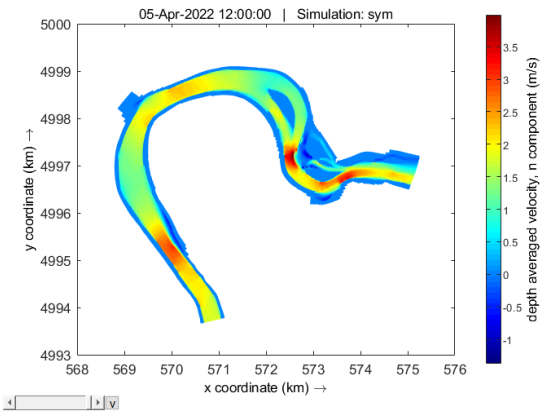

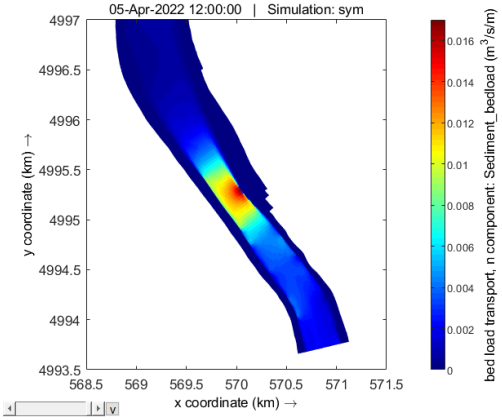

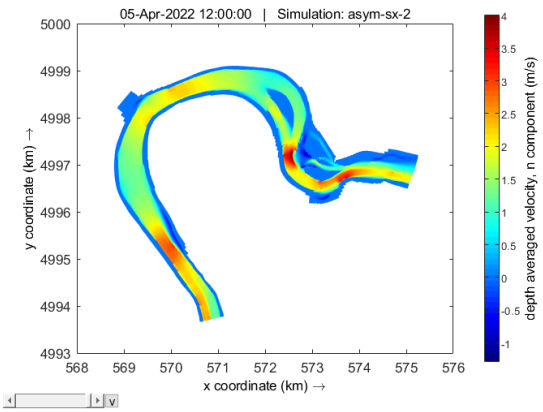
05-Apr-2022 12:00:00 | Simulation: asym-sx-2
y coordinate (km) →
x coordinate (km) →
depth averaged velocity, n component (m/s)

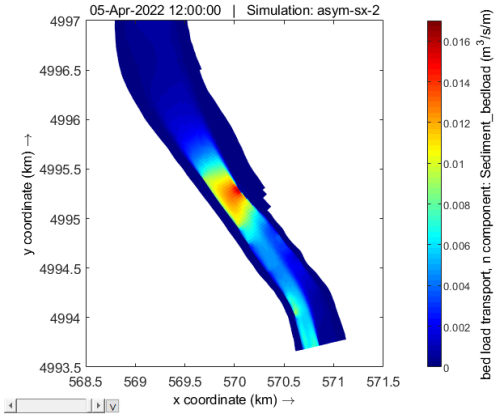
05-Apr-2022 12:00:00 | Simulation: asym-sx-2
y coordinate (km) →
x coordinate (km) →
bed load transport, n component: Sediment_bedload (m³/s/m)

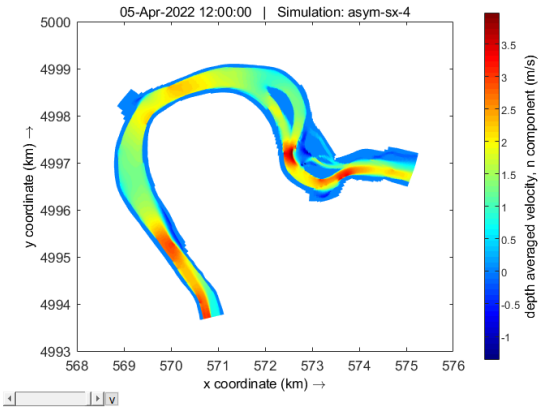
05-Apr-2022 12:00:00 | Simulation: asym-sx-4
y coordinate (km) →
x coordinate (km) →
depth averaged velocity, n component (m/s)

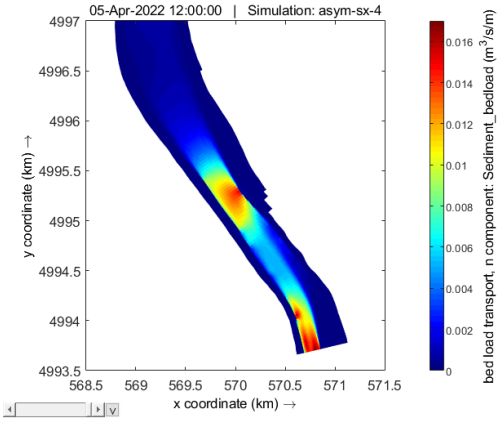
05-Apr-2022 12:00:00 | Simulation: asym-sx-4
y coordinate (km) →
x coordinate (km) →
bed load transport, n component: Sediment_bedload (m³/s/m)

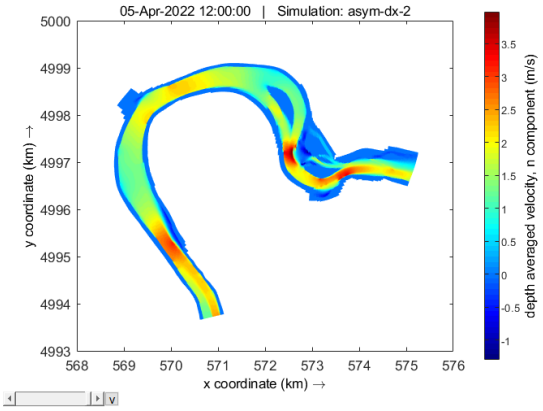
05-Apr-2022 12:00:00 | Simulation: asym-dx-2
y coordinate (km) →
x coordinate (km) →
depth averaged velocity, n component (m/s)

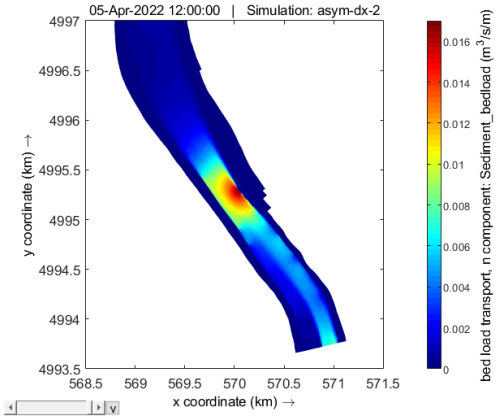
05-Apr-2022 12:00:00 | Simulation: asym-dx-2
y coordinate (km) →
x coordinate (km) →
bed load transport, n component: Sediment_bedload (m³/s/m)

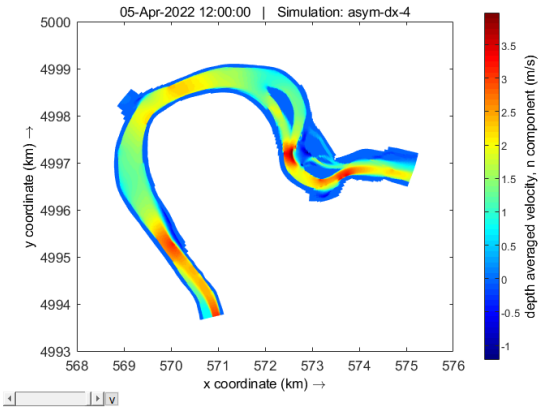
05-Apr-2022 12:00:00 | Simulation: asym-dx-4
y coordinate (km) →
x coordinate (km) →
depth averaged velocity, n component (m/s)

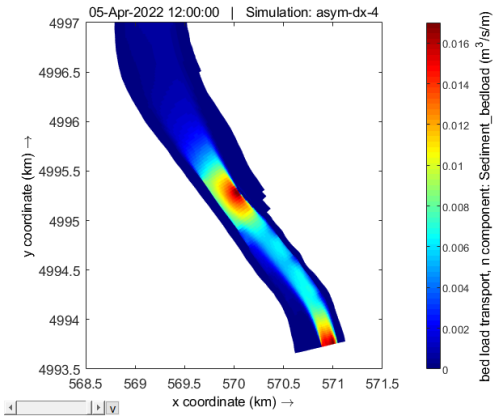
05-Apr-2022 12:00:00 | Simulation: asym-dx-4
y coordinate (km) →
x coordinate (km) →
bed load transport, n component: Sediment_bedload (m³/s/m)

- Medium-term effects

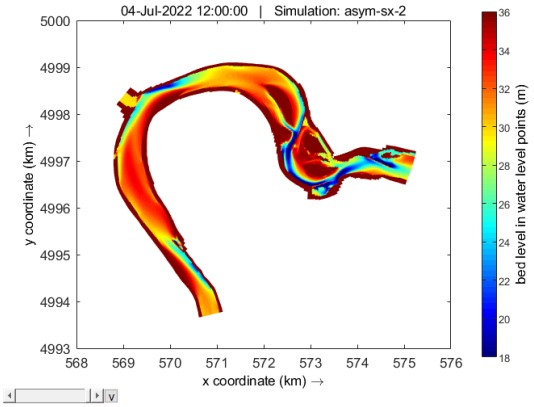

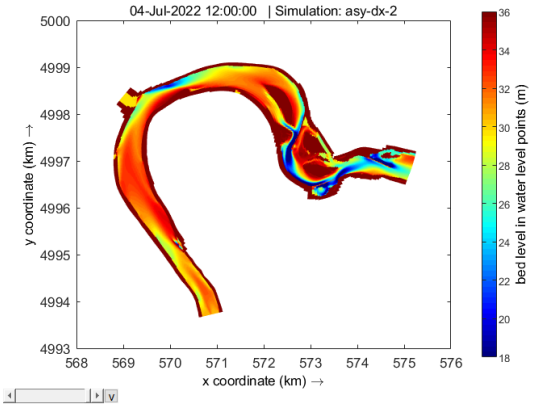

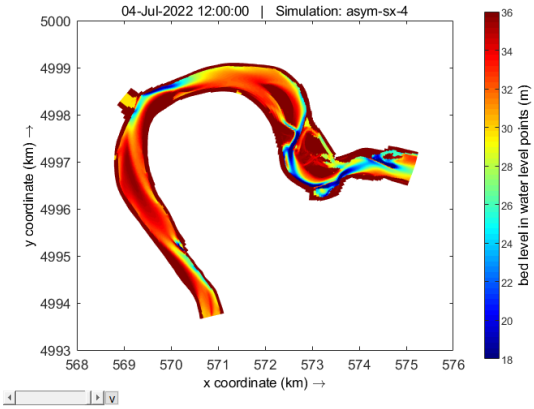

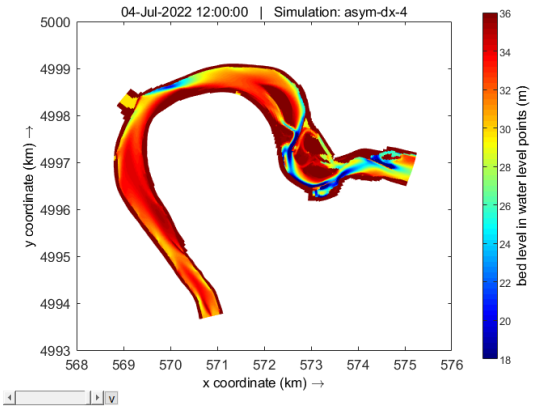

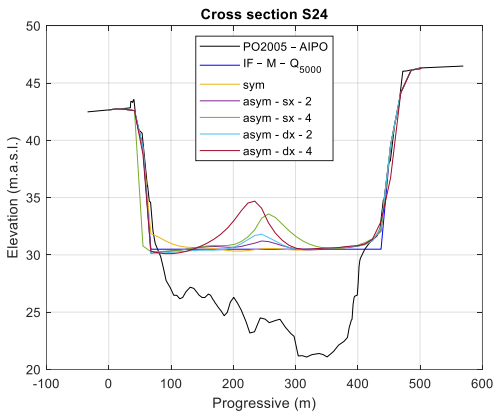

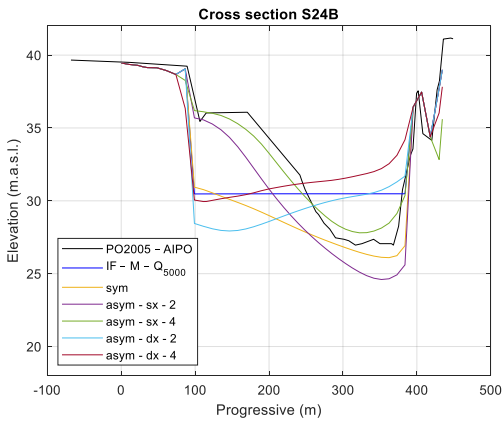

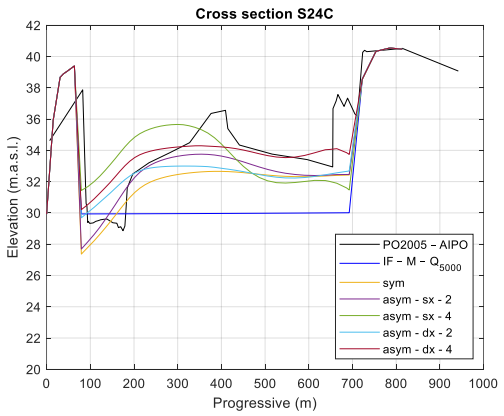

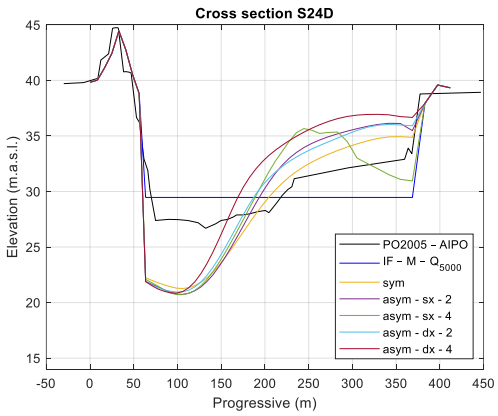

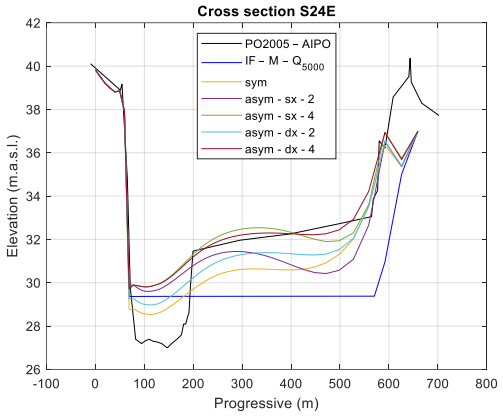
Cross section S24E
PO2005 – AIPO
IF – M – Q5000
sym
asym - sx - 2
asym - sx - 4
asym - dx - 2
asym - dx - 4
Elevation (m.a.s.l.)
Progressive (m)

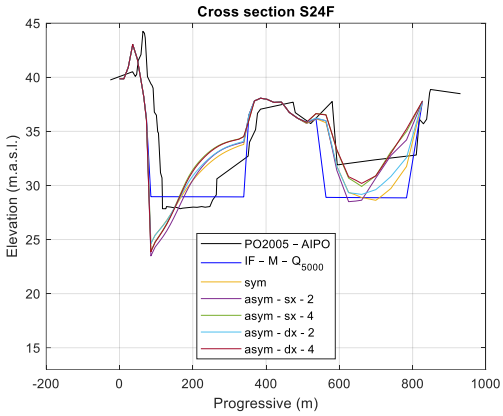
Cross section S24F
PO2005 – AIPO
IF – M – Q5000
sym
asym - sx - 2
asym - sx - 4
asym - dx - 2
asym - dx - 4
Elevation (m.a.s.l.)
Progressive (m)

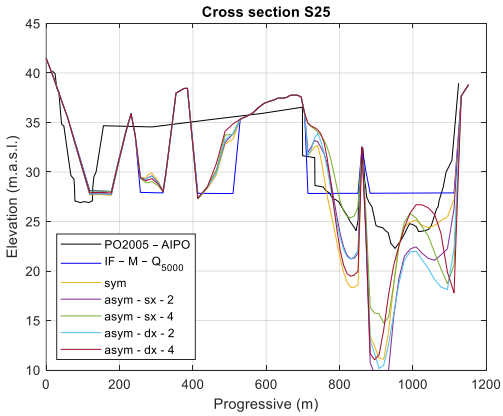
Cross section S25
PO2005 – AIPO
IF – M – Q5000
sym
asym - sx - 2
asym - sx - 4
asym - dx - 2
asym - dx - 4
Elevation (m.a.s.l.)
Progressive (m)

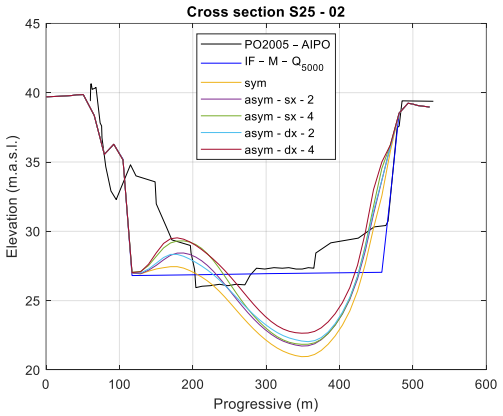
Cross section S25 - 02
PO2005 – AIPO
IF – M – Q5000
sym
asym - sx - 2
asym - sx - 4
asym - dx - 2
asym - dx - 4
Elevation (m.a.s.l.)
Progressive (m)

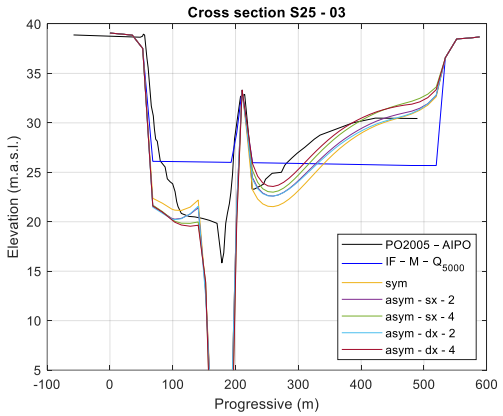
Cross section S25 - 03
PO2005 – AIPO
IF – M – Q5000
sym
asym - sx - 2
asym - sx - 4
asym - dx - 2
asym - dx - 4
Elevation (m.a.s.l.)
Progressive (m)

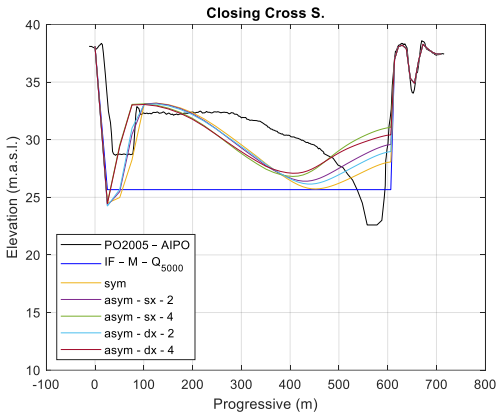
Closing Cross S.
PO2005 – AIPO
IF – M – Q5000
sym
asym - sx - 2
asym - sx - 4
asym - dx - 2
asym - dx - 4
Elevation (m.a.s.l.)
Progressive (m)